KTH Engineering Sciences

The Effective Convectivity Model for Simulation and Analysis of Melt Pool Heat Transfer in a Light Water Reactor Pressure Vessel Lower Head

CHI THANH TRAN

Doctoral Thesis in Energy Technology

Stockholm, Sweden 2009

THE EFFECTIVE CONVECTIVITY MODEL

FOR SIMULATION AND ANALYSIS OF MELT POOL HEAT TRANSFER

IN A LIGHT WATER REACTOR PRESSURE VESSEL LOWER HEAD

Doctoral Thesis

by

Chi Thanh TRAN

School of Engineering Sciences
Department of Physics
Division of Nuclear Power Safety

STOCKHOLM, 2009

KUNGLIGA TEKNISKA HÖGSKOLAN

Royal Institute of Technology

Ecole Royale Polytechnique

Kgl. Technische Hochschule

Avdelningen för Kärnkraftsäkerhet

Division of Nuclear Power Safety

Post Address:	AlbaNova University Center Roslagstullsbacken 21, D5
	STOCKHOLM 10691, Sweden
Telephone:	(46) 8 - 55378826
Fax:	(46) 8 - 55378830
URL:	http://www.safety.sci.kth.se
E-mail:	*thanh@safety.sci.kth.se*

Defense of dissertation: **10:00 AM - September 02, 2009**

FA32, AlbaNova University Center

Roslagstullsbacken 21, STOCKHOLM 10691

To the memory of my father

Abstract

Severe accidents in a Light Water Reactor (LWR) have been a subject of intense research for the last three decades. The research in this area aims to reach understanding of the inherent physical phenomena and reduce the uncertainties in their quantification, with the ultimate goal of developing models that can be applied to safety analysis of nuclear reactors, and to evaluation of the proposed accident management schemes for mitigating the consequences of severe accidents.

In a hypothetical severe accident there is likelihood that the core materials will be relocated to the lower plenum and form a decay-heated debris bed (debris cake) or a melt pool. Interactions of core debris or melt with the reactor structures depend to a large extent on the debris bed or melt pool thermal hydraulics. In case of inadequate cooling, the excessive heat would drive the structures' overheating and ablation, and hence govern the vessel failure mode and timing. In turn, threats to containment integrity associated with potential ex-vessel steam explosions and ex-vessel debris uncoolability depend on the composition, superheat, and amount of molten corium available for discharge upon the vessel failure. That is why predictions of transient melt pool heat transfer in the reactor lower head, subsequent vessel failure modes and melt characteristics upon the discharge are of paramount importance for plant safety assessment.

The main purpose of the present study is to develop a method for reliable prediction of melt pool thermal hydraulics, namely to establish a computational platform for cost-effective, sufficiently-accurate numerical simulations and analyses of core Melt-Structure-Water Interactions in the LWR lower head during a postulated severe core-melting accident. To achieve the goal, an approach to efficient use of Computational Fluid Dynamics (CFD) has been proposed to guide and support the development of models suitable for accident analysis.

The CFD method, on the one hand, is indispensable for scrutinizing flow physics, on the other hand, the validated CFD method can be used to generate necessary data for validation of the accident analysis models. Given the insights gained from the CFD study, physics-based models and computationally-efficient tools are developed for multi-dimensional simulations of transient thermal-hydraulic phenomena in the lower plenum of a LWR during the late phase of an in-vessel core melt progression. To describe natural convection heat transfer in an internally heated volume, and molten metal layer heated from below and cooled from the top (and side) walls, the Effective Convectivity Models (ECM) are developed and implemented in a commercial CFD code. The ECM uses directional heat transfer characteristic velocities to transport the heat to cooled boundaries. The heat transport and interactions are represented through an energy-conservation formulation. The ECM then enables 3D heat transfer simulations of a homogeneous (and stratified) melt pool formed in the LWR lower head.

In order to describe phase-change heat transfer associated with core debris or binary mixture (e.g. in a molten metal layer), a temperature-based enthalpy

formulation is employed in the Phase-change ECM (so called the PECM). The PECM is capable to represent natural convection heat transfer in a mushy zone. Simple formulation of the PECM method allows implementing different models of mushy zone heat transfer for non-eutectic mixtures. For a non-eutectic binary mixture, compositional convection associated with concentration gradients can be taken into account. The developed models are validated against both existing experimental data and the CFD-generated data. ECM and PECM simulations show a superior computational efficiency compared to the CFD simulation method.

The ECM and PECM methods are applied to predict thermal loads imposed on the vessel wall and Control Rod Guide Tubes (CRGTs) during core debris heatup and melting in a Boiling Water Reactor (BWR) lower plenum. It is found that during the accident progression, the CRGT cooling plays a very important role in reducing the thermal loads on the reactor vessel wall. Results of the ECM and PECM simulations suggest a high potential of the CRGT cooling to be an effective measure for severe accident management in BWRs.

Keywords: *light water reactor, hypothetical severe accident, accident progression, accident scenario, core melt pool, heat transfer, turbulent natural convection, heat transfer coefficient, phase change, mushy zone, crust, lower plenum, analytical model, effective convectivity model, CFD simulation.*

Acknowledgement

First of all, I would like to express great thanks to Professor Nam Dinh, for his supervision, for his whole-hearted, excellent guiding and helping me from the first step when the thesis project was formulated through all the steps of my graduate study.

I am specially grateful to Professor Tomas Lefvert, who steps in to take over the supervision role after Professor Nam Dinh left to his new appointment with the Idaho National Laboratory. Professor Tomas Lefvert's support in this stage is gratefully acknowledged.

I am very thankful to Dr. Pavel Kudinov for his always taking time to listen, to answer questions, to discuss, for careful reading of my manuscripts and giving me fruitful comments.

My special thanks to Professor Bal Raj Sehgal and Dr. Weimin Ma for their helps, useful comments and discussions.

Thanks to Kajsa and Jenny for all the support during the whole period of my study.

I would like to thank all my colleagues Aram, Roberta, Sean, Tomasz, Francesco, Andrei, Viet-Anh, Joanna, Hua, Shengjie, Andreas, Liangxing, Ivan as well as all the other people at the Nuclear Power Safety Division for their assistance, for making a friendly and supportive working environment.

My warmest gratitude goes to my wife Le Hong Hoa, my daughter Tran Le Hong Lien and my son Tran Duc Anh for their love, encouragement and endless support.

This research was supported in the framework of MSWI-APRI project by the Swedish Nuclear Safety Radiation Authority (SSM, the former SKI), Swedish Power Companies, Swiss Federal Nuclear Safety Inspectorate (ENSI, the former HSK), Nordic Nuclear Safety Research (NKS), and by European Commission in the framework of SARNET project.

List of publication

PEER REVIEW PUBLICATIONS

[1] C.T. TRAN, T.N. DINH, “Analysis of Melt Pool Heat Transfer in a BWR Lower Head”, Transactions of ANS Winter Meeting, Albuquerque, NM, USA, November 12-18, Vol. 95, pp. 629-631, 2006.

[2] C.T. TRAN, T.N. DINH, “An Effective Convectivity Model for Simulation of In-Vessel Core Melt Progression in Boiling Water Reactor”, 2007 International Congress on Advances in Nuclear Power Plants (ICAPP'07), Nice Acropolis, France, May 13-18, 2007.

[3] C.T. TRAN and T.N. DINH, “Simulation of Core Melt Pool Formation in a Reactor Pressure Vessel Lower Head Using an Effective Convectivity Model”, International Topical Meeting on Nuclear Reactor Thermal Hydraulics – NURETH-12, Pittsburgh, Pennsylvania, USA, September 30 – October 04, 2007.

(Selected for publication in the International Journal of Nuclear Engineering and Technology - NET, in press)

[4] C.T. TRAN and T.N. DINH, "Application of the Phase-change Effective Convectivity Model to Analysis of Core Melt Pool Formation and Heat Transfer in a BWR Lower Head", Transactions of ANS 2008 Annual Meeting, Anaheim, California, USA, June 8-12, Vol. 98, pp. 617-618, 2008.

[5] C.T. TRAN, P. KUDINOV and T.N. DINH, "An Approach to Numerical Simulation and Analysis of Molten Corium Coolability in a BWR Lower Head", Experimental and CFD Code Applications to Nuclear Reactor Safety (XCFD4NRS) Meeting, Grenoble, France, September 10-12, 2008.

(Accepted for publication in special issue of Nuclear Engineering and Design Journal)

[6] M. BUCK, M. BURGER, A. MIASSOEDOV, X. GAUS-LIU, A. PALAGIN, L. GODIN-JACQMIN, C.T. TRAN, W.M. MA, V. CHUDANOV, "The LIVE Program: Test and Analyses on In-Vessel Severe Accident Progression", Proceedings of The 3rd European Review Meeting on Severe Accident Research (ERMSAR-2008), Nesseber, Bulgaria, September 23-25, 2008.

(Selected for publication in Progress in Nuclear Energy Journal, under review)

[7] C.T. TRAN, P. KUDINOV, "The Effective Convectivity Model for Simulation of Molten Metal Layer Heat Transfer in a Boiling Water Reactor Lower Head", 2009 International Congress on Advances in Nuclear Power Plants (ICAPP'09), Shinjuku Tokyo, Japan, May 10-14, 2009.

[8] C.T. TRAN and T.N. DINH, "The Effective Convectivity Model for Simulations of Melt Pool Heat Transfer in a Light Water Reactor Pressure

Vessel Lower Head. Part I: Physical Processes, Modeling and Model Implementation", *Accepted for publication in Journal of Progress in Nuclear Energy.*

[9] C.T. TRAN and T.N. DINH, "The Effective Convectivity Model for Simulation of Melt Pool Heat Transfer in a Light Water Reactor Pressure Vessel Lower Head. Part II: Model Assessment and Application", *Accepted for publication in Journal of Progress in Nuclear Energy.*

TECHNICAL REPORTS

[1] T.N. Dinh, W.M. Ma, A. Karbojian, P. Kudinov, C.T. Tran, “Melt-Structure-Water Interactions During Postulated Severe Accidents in LWRs”, HSK Research Project Report, Royal Institute of Technology (KTH), Division of Nuclear Power Safety, Stockholm, Sweden, February 2007.

[2] T.N. Dinh, W.M. Ma, A. Karbojian, P. Kudinov and C.T. Tran, “APRI-6: Study on Steam Explosion and Corium Coolability in Ex-Vessel Severe Accident Scenarios”, Project Report 2006, SKI 2006/631/200607008 NPS/APRI-0703-01, Division of Nuclear Power Safety, Royal Institute of Technology (KTH), Stockholm, March 2007.

[3] T.N. Dinh, W.M. Ma, A. Karbojian, P. Kudinov, C.T. Tran and R.C. Hansson, “Ex-Vessel Corium Coolability and Steam Explosion Energetics in Nordic Light Water Reactors”, NKS Research Report – NPS-SARAM071001, Division of Nuclear Power Safety, Department of Physics, School of Engineering Sciences, Royal Institute of Technology (KTH), Stockholm, Sweden, October 2007.

[4] W.M. Ma, P. Kudinov, A. Karbojian, C.T. Tran, R.C. Hansson, T.N. Dinh, "Project Melt-Structure-Water Interactions During Postulated Severe Accidents in LWRs", HSK Research Report 2008, January 25, 2009.

[5] T.N. Dinh, W. Ma, P. Kudinov, A. Karbojian. C.T. Tran, R. Hansson, "KTH Research on Severe Accidents: Contribution to the Sixth Accident Phenomena of Risk Importance (APRI-6) Final Report", January 2009.

LIST OF PRESENTATIONS

[1] Thanh Tran and Nam Dinh, “Control Rod Drive Cooling in BWR as Severe Accident Mitigation Measure: Steps toward Assessment of Efficiency and Vulnerability (INCO Project)”, Proceedings of the 22nd Meeting of Advisory Group for Research Project “Melt-Structure-Water Interactions (MSWI) during Severe Accidents”, AlbaNova University Center, Stockholm, May 17, 2006.

[2] Thanh Tran, “ECM - The Effective Convectivity Model: Implementation in Fluent Code and Validation”, Proceedings of the 23rd Meeting of Advisory

Group for Research Project “Melt-Structure-Water Interactions (MSWI) during Severe Accidents”, AlbaNova University Center, Stockholm, November 15, 2006.

[3] Thanh Tran and Nam Dinh, “CRGT Cooling in BWR as a Severe Accident Mitigation Measure: Modeling, Validation and Applications”, Proceedings of the 24th Meeting of Advisory Group for Research Project “Melt-Structure-Water Interactions (MSWI) during Severe Accidents”, AlbaNova University Center, Stockholm, June 20, 2007.

[4] Chi Thanh TRAN, "Development, Validation and Application of an Effective Convectivity Model for Simulation of Melt Pool Heat Transfer in Light Water Reactor Lower Head", Licentiate Thesis, AlbaNova, University Center, Stockholm, December 11, 2007.

[5] Chi Thanh TRAN, "Analysis of Boiling Water Reactor Severe Accident Scenarios", Proceedings of the 26th Meeting of Advisory Group for Research Project “Melt-Structure-Water Interactions (MSWI) during Severe Accidents”, AlbaNova University Center, Stockholm, June 18, 2008.

[6] Chi Thanh TRAN, "The Effective Convectivity Model for Simulations of Melt Pool Heat Transfer in a BWR Lower Head", Proceedings of the 27th Meeting of Advisory Group for Research Project “Melt-Structure-Water Interactions (MSWI) during Severe Accidents”, AlbaNova University Center, Stockholm, December 17, 2008.

[7] Chi Thanh TRAN, "In-Vessel Coolability and Retention", The Sixth Accident Phenomena of Risk Importance (APRI-6) Meeting, Lejondals Slott, Stockholm, January 22-23, 2009.

Table of contents

Nomenclature

Arabic

C_p	Specific heat capacity, J/(kg.K)
F_{LIQ}	Liquid fraction
g	Gravitational acceleration, m/s^2
G	Flow rate, kg/(m^2.s)
H	Enthalpy, J/kg
H, H_{pool}	Height of a volume or melt pool or fluid layer, m
h	Sensible heat, J/kg
k	Conductivity, W/(m.K)
L	Length (m), or latent heat of the phase change, J/kg
m	Mass, kg
Nu	Nusselt number, $Nu = \dfrac{qH_{pool}}{k\Delta T}$
P	Power, W
Pr	Prandtl number, $\mathrm{Pr} = \nu / \alpha$
q	Heat flux, W/m^2
Q_v	Volumetric heat source, W/m^3
R	Radius of the pool, m
Ra'	Rayleigh number (internal), $Ra' = \dfrac{g\beta Q_v H_{pool}^5}{k\nu\alpha}$
Ra	External Rayleigh number, $Ra = Gr \times \mathrm{Pr}$
Ra_y	Local Rayleigh number, $Ra_y = \dfrac{g\beta\Delta T y^3}{\nu\alpha}$
r_C	Rejectability coefficient
S	Area, m^2
S_c	Source term, W/m^3
t	Time, s
T	Temperature, K
u,v	Fluid velocity, m/s
U	Characteristic velocity, m/s
W	Width of a volume, m
y	Local vertical coordinate, m

Greek

α	Thermal diffusivity, m^2/s, $\alpha = \dfrac{k}{\rho.C_p}$
β	Thermal expansion coefficient, 1/K
ΔC	Concentration difference
ΔH	Latent heat, J/kg
ΔT	Temperature difference, K

ρ	Density, kg/m^3
v	Kinematics viscosity, m^2/s
μ	Dynamic viscosity, Pa.s
η	Kolmogorov scale

Subscripts and superscripts

anl	Annulus
ave	Average
BC	Boundary Condition
chem	Chemical
CM	Core materials
CRGT	Control Rod Guide Tube
crit	Critical
CRW	Core region water
cond	Conduction
decay	Decay
down	Downward
eff	Effective
f	Function of
G	Gas
he	Heated equivalent
i, j	Index
inlet	Inlet
int	Internal
L	Liquid
LG	Liquid gas
LIQ	Liquidus
local	Local
M	Mushy
max	Maximum
MELT	Melting
pool	Pool
out	Outside
side	Sideward
SOL	Solidus
subcool	Subcool
tube	Tube
up	Upward
vessel	To vessel
x	Steam quality
x, y, z	Coordinate axis directions

List of acronyms

ADS	Automatic Depressurization System
AMR	Adaptive Mesh Refinement
APRI	Accident Phenomena of Risk Importance
BWR	Boiling Water Reactor
CFD	Computational Fluid Dynamics
CHF	Critical Heat Flux
CRGT	Control Rod Guide Tube
CSAU	Code Scaling, Applicability and Uncertainty
DB	Debris Bed
DEFOR	Debris Bed Formation
DNS	Direct Numerical Simulation
PWR	Pressurized Water Reactor
LWR	Light Water Reactor
ECCM	Effective Convectivity Conductivity Model
ECM	Effective Convectivity Model
EXCO	Ex-Vessel Coolability
HT	Heat Transfer
IGT	Instrumentation Guide Tube
ILES	Implicit Large Eddy Simulation
INCO	In-Vessel Coolability
IVR	In-Vessel Retention
KTH	Royal Institute of Technology
LES	Large Eddy Simulation
LP	Lower Plenum
LWR	Light Water Reactor
MILES	Monotonically Integrated LES
NPS	Nuclear Power Safety
PECM	Phase-Change ECM
PIRT	Phenomena Identification and Ranking Table
PSA	Probabilistic Safety Assessment
RPV	Reactor Pressure Vessel
SAM	Severe Accident Management
SARNET	Severe Accident Research Network of Excellence
SARP	Severe Accident Research Priorities (or Program)
SBO	Station Blackout
SEE	Steam Explosion Energetics
SE	Steam Explosion
SGS	Sub-Grid Scale

Chapter 1: Introduction

1.1. Context of the thesis work

During the past three decades, extensive experimental and analytical researches have been performed on Accident Phenomena of Risk Importance (APRI) in Light Water Reactor (LWR) plants. A comprehensive list of 1016 severe accident phenomena was composed as a basis for the Establishing Phenomena Identification and Ranking Tables (PIRT). Among these 1016 severe accident phenomena, 162 in-vessel phenomena were identified, and in-vessel core melt pool heat transfer is one of the important issues (high ranked) of the Severe Accident Research Network of Excellence (SARNET) program (Trambauer and Schwinges, 2007).

An important contribution to state-of-the-art in the area of in-vessel core melt pool heat transfer has been made at the Royal Institute of Technology, Nuclear Power Safety Division (KTH-NPS). A substantial knowledge base was developed, and it has being consolidated, distilled and distributed under SARNET Severe Accident Research Priorities (SARP) activities. Several large-scale research projects in EU Framework Programs FP4 and FP5 have been mutually leveraged on the Swedish APRI research program, which support severe accident research at KTH-NPS over the past 16 years (1993-2008). APRI program at KTH-NPS includes both analytical (e.g. scaling, modeling, simulation and assessment) and experimental activities.

Under APRI-6, the following tasks (Figure 1.1) were identified, involving analytical and modeling works as well as experimental programs (Dinh, 2006):

- Accident scenarios and core melt relocation;
- Debris formation (corium melt fragmentation);
- Coolability of debris bed, dry-out heat flux;
- Debris bed (core melt pool) structures interactions (heat transfer, Control Rod Guide Tube (CRGT) cooling, vessel ablation etc.);
- Corium explosivity (Steam Explosion Energetics);
- Ex-vessel debris bed formation;
- Ex-vessel coolability.

In this context, the “Debris bed (core melt pool) structures interactions” is one of the most important APRI program tasks considered during the years 2006-2008. The main objective of the “Debris bed (core melt pool) structures interactions” task is to develop models and capabilities to enable evaluation of the merit of additional Severe Accident Management (SAM) measures aimed to enhance the in-vessel coolability. The CRGT cooling is considered as a potential SAM measure for Boiling Water Reactors (BWRs).

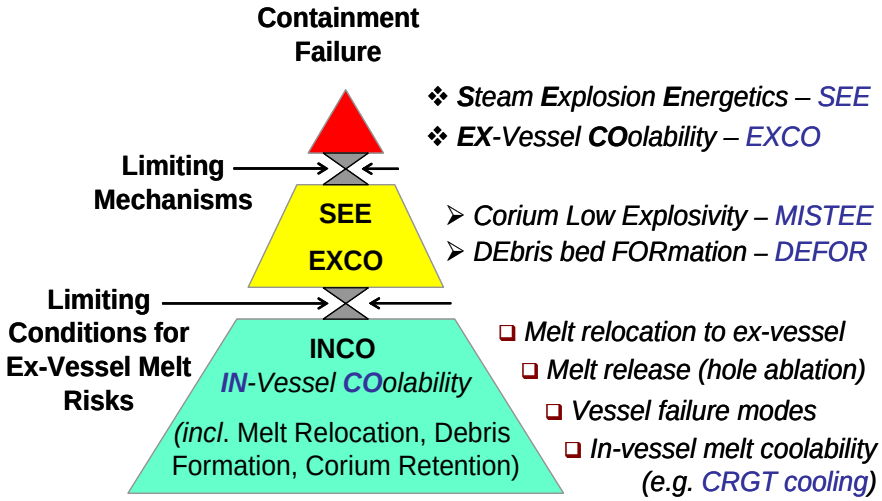

Figure 1.1: Accident progression phenomena and research tasks in APRI-6 (INCO – In-Vessel Coolability Project; MISTEE – Micro Interaction of Steam Explosion Experiment; DEFOR – Debris Formation Project; SEE – Steam Explosion Energetics; EXCO – Ex-Vessel Coolability).

1.2. Severe accident progression in a BWR

1.2.1. BWR design specifics

From safety point of view the following differences of the BWR configuration from a Pressurized Water Reactor (PWR) are of importance: larger reactor vessel diameter, bigger total mass of the reactor internal metallic components and the presence of a forest of penetrated CRGTs in the lower plenum.

Due to both boiling and steam separation processes occurring inside the Reactor Pressure Vessel (RPV), the BWR vessel height and diameter are typically larger than that those of a PWR. The diameter of a BWR vessel is of about 6-7m, while the diameter of a PWR vessel is about 4-5m. The BWR vessel contains steam separators and dryers, and other equipment such as core spray system, core support structures, fuel assemble channels and bypass, claddings, barrels, CRGTs, Instrumentation Guide Tubes (IGTs) and shroud etc. All these equipment and internal structures result in a bigger total mass of metallic components, available in a BWR compared with those of a PWR.

Most importantly, the BWR lower plenum compared to that of a PWR includes a large number of CRGTs and IGTs. The CRGT number and arrangement in the lower plenum vary for different designs. In the present study two ABB-Atom reactor configurations are referred. The reference reactors have the thermal power of 2500 MWt and 3900 MWt, contain 121 CRGT and 169 CRGTs respectively. During normal operation, a small water flow rate (62.5 g/sec equivalent to 15 kg/m^2.sec) is provided for purging of CRGTs. It was proposed that the coolant flow in CRGTs can be adapted as an avenue to enhance coolability of debris and core melt pool formed in the lower plenum (Sehgal, 2006). The consideration is due to three folds: i) possible modification is

minimal with adding a water supply and control system; ii) the forest of CRGTs provides large area for heat transfer from corium to coolant; iii) the flowrate of the CRGT cooling (nominal 15 kg/m^2.sec ~ 10 kg/s in total) is so small that can be provided by a battery-driven pump.

1.2.2. In-vessel accident progression

As the accident has been initiated, the core uncovery will lead to melting of the core materials due to the decay heat and possible chemical heat released during oxidation of Zirconium. Here the core materials are referred as the materials in the core and equipment placed above/below the reactor core (steam separators, steam dryers and reactor internal structures). We start the analysis of in-vessel accident progression in a BWR with calculations of core materials melting based on the time-dependent decay power function implemented in the MELCOR code (Gauntt, 2005), with taking into account the oxidation heat and possible CRGT cooling water flow rate injected to the reactor.

In the presence of Zirconium oxidation and CRGT flow, the molten fraction of core materials (F_{LIQ}^{CM}) in a BWR can be calculated as follows:

$$F_{LIQ}^{CM} = \frac{\int_{t_1}^{t} \left(P_{decay} + P_{chem} - G_{CRGT} \cdot S_{CRGT} \cdot h_{LG} \right) dt}{\sum_{i=1}^{3} m_i \left[C_{pi} \left(T_{MELTi} - T_{0i} \right) + L_i \right]} \qquad (1.1)$$

where:

t	time after reactor shutdown, sec;
P_{decay}	decay power, W;
P_{chem}	power released by oxidation of Zr;
G_{CRGT}	CRGT mass flow rate, kg/(m^2.sec);
S_{CRGT}	cross section areas, m^2;
h_{LG}	latent heat of evaporation, J/kg;
m_i	mass of i-component (core materials), kg;
T_{0i}	initial temperature of i-material, K;
T_{MELTi}	melting temperature of i-material, K;
C_{pi} and L_i	respective specific heat and latent heat of phase change of i-component;

Time t_1 is the time counted from the accident start (reactor shutdown) to the moment when the core region is fully uncovered, and defined as:

$$\int_0^{t_1} (P_{decay} + P_{chem} - G_{CRGT} \cdot S_{CRGT} \cdot h_{LG}) dt - m_{CRW} \cdot h_{LG} = 0 \quad (1.2)$$

Where m_{CRW} is the amount of water remained in the core region after instantaneous evaporation of water due to pressure drop, as the Automatic Depressurization System (ADS) has been activated. The input parameters used for calculations of molten fraction are taken from a reference ABB-Atom reactor, the thermal power of which is 3900 MWt. Estimation of total chemical reaction heat is based on total Zr mass of 52680 kg, heat generation is 6500 kJ/kg Zr. It is assumed that oxidation starts in one hour after the start of accident, and lasts for one hour in all scenarios with different fraction of oxidized Zr.

Calculations using Eqs.(1.1) and (1.2) show that the fraction of Zr involved in oxidation is an important parameter affecting the amount of melted core materials (Figure 1.2). However, it is seen that the CRGT cooling started from the beginning is efficient, and capable of slowing and terminating core materials melting, if the CRGT injected water can be efficiently used. Results of MELCOR Station Blackout (SBO) calculation also show that the nominal CRGT water flow is sufficient for cooling the debris relocated into the lower plenum, thus avoiding the vessel failure.

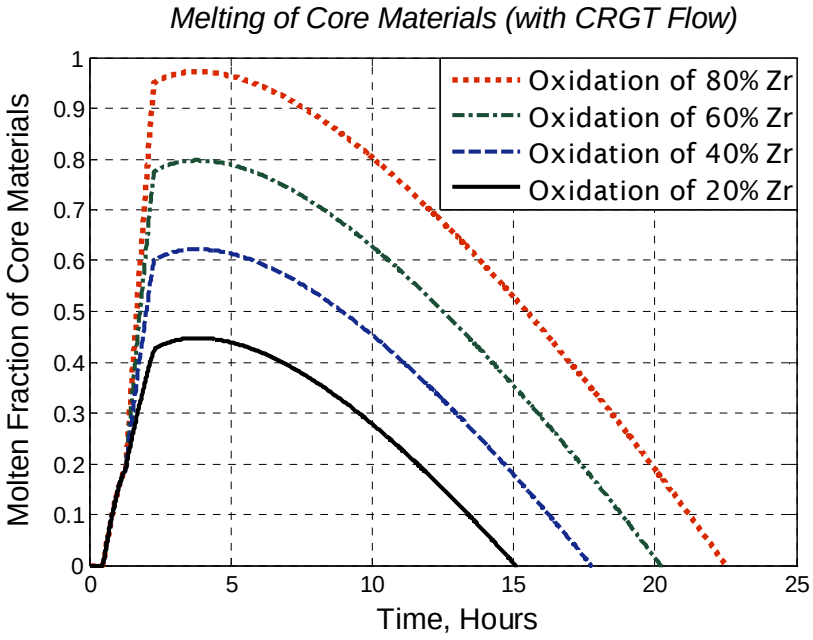

Figure 1.2: Molten fraction of core materials in a reference BWR with different mass of Zr oxidized. CRGT cooling flow rate is 15 kg/(m^2.sec) activated from the accident start.

Other calculations with different rates of CRGT cooling flow show that increase of the CRGT cooling flow rate can significantly reduce the amount of melted materials in the reactor (Figure 1.3). Without CRGT cooling water flow, even with a small amount of Zr oxidized (20%), the molten fraction of core materials in the reactor is rapidly increased, reaching 100% only after about 2 hours into accident initiation.

Note that significant (accident progression) scenario and phenomenological uncertainties exist in predicting the amount of Zr undergone oxidation in the core region under CRGT cooling. Oxidation may take place in the debris bed (melt pool) formed in the lower plenum with suboxidized materials. Oxidation rate of Zr in the lower plenum depends on heating process and diffusion of oxygen in the formed debris bed. Experiments showed that oxidation can be a fast process (order of tens of minutes) (Asmolov et al., 2004).

The molten materials in the core region (or on the core support plates and the crust crucible) will be eventually relocated into the lower plenum region. It is clear that the corium melt progression in the lower head region depends on the melt amount, temperature, morphology, relocation path of accident progression in the core region, and conditions of the lower head structures.

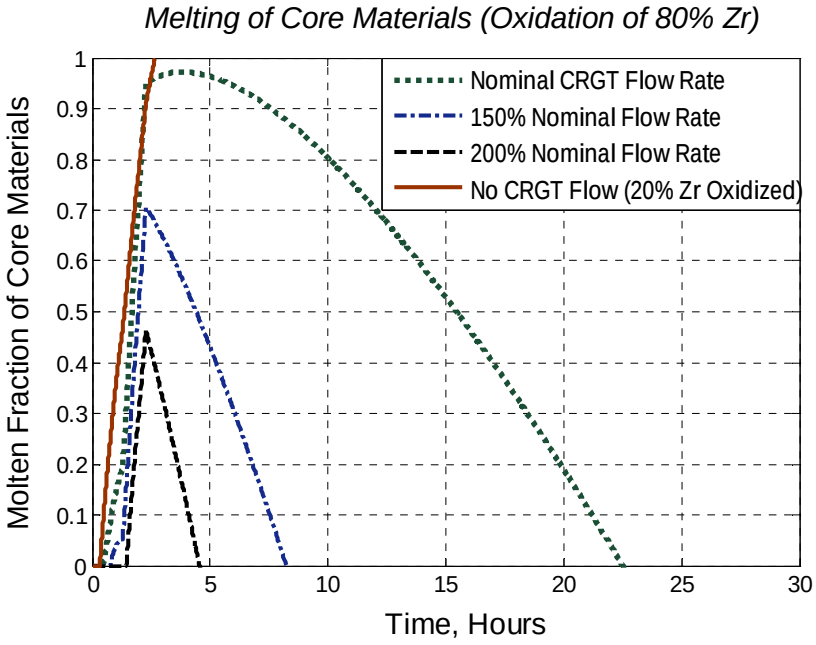

Figure 1.3: Molten fraction of core materials in a reference BWR under different CRGT water flow rates.

There are three mechanisms for core material relocation from the original core boundary into the lower plenum: candling, sideward relocation along the peripheral regions of the core as it was observed in the TMI-2 accident (Tolman et al., 1988), and/or downward relocation through the failure of the core plate or the penetration tube. Basically, relocation modes can be grouped into 3 types: candling mode, small jets modes and big jet mode (Figure 1.4). Conditions of the lower plenum may be wet (filled by water - A, B) or dry (without water - C, D), and the lower plenum may contain fragmented debris (B, D). The in-vessel accident scenarios can be defined as combination of different relocation modes with different configurations of the lower plenum. Different accident phenomena are then identified and presented in Table I.1.

In the presence of CRGT cooling, it is assumed that water is available in the lower plenum. The water level in the lower plenum can be decreased only with either intensive evaporation caused by the hot materials relocated in the lower plenum, or leakage through the failed penetrations. Therefore the probability of configuration C (Figure 1.4) is evaluated extremely small. In the presence of deep water in the lower plenum, the relocating molten core materials will be fragmented into small particles and solidified (Karbojian et al., 2009). A debris bed is formed in the lower plenum.

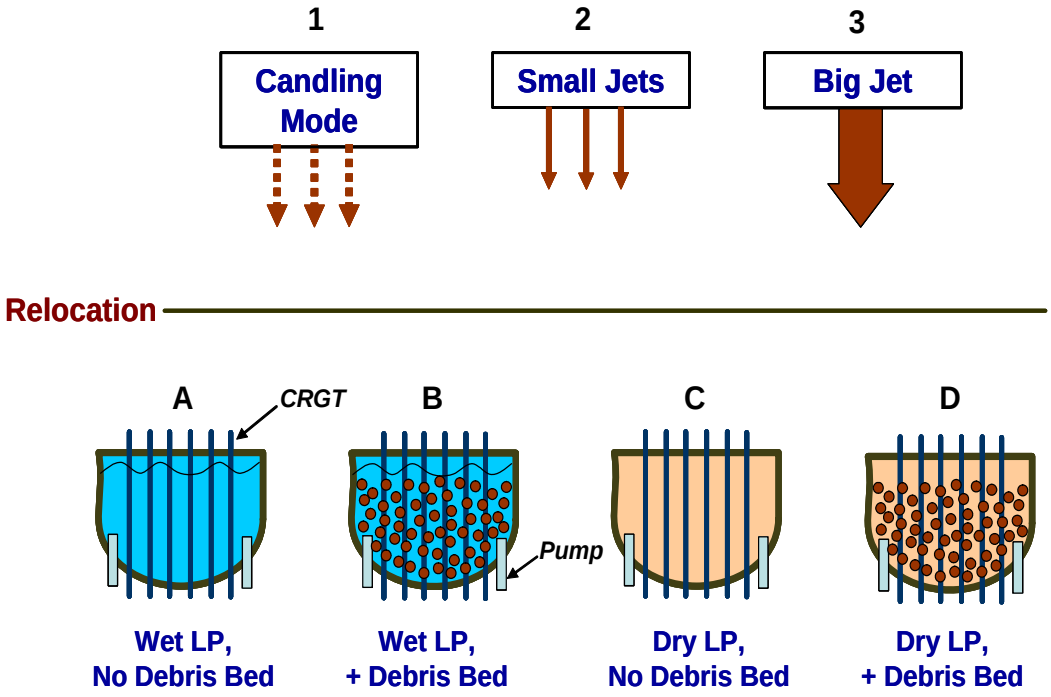

Figure 1.4: Relocation modes and possible configurations in a BWR lower plenum.

The other possible scenario is formation of a debris cake. Due to gradual candling or small jets relocation mode, a certain amount of debris is relocated into the lower plenum prior to extensive relocation (configuration B and D, Figure 1.4). The next relocations into the formed configuration will fill the pores of debris bed. A debris cake (or melt pool) is formed in the lower plenum.

In the presence of CRGT water flow to the reactor, configuration D is evaluated as low probability. Therefore, in the present work, we consider two configurations: debris bed and debris cake (melt pool) in the lower plenum. The other accident scenarios which are related to penetration failure identified in Table I.1 are not considered.

Without an adequate cooling, the debris bed (cake) continues to heatup and then will be remelted, leading to formation of a melt pool in the lower plenum (Figure 1.5). Two cooling measures can be considered for heat removal from the debris bed, or debris cake (melt pool): the first is the cooling by water flows in CRGTs (CRGT cooling), and the second is the cooling by water on top of the melt pool. External vessel cooling by

water which is pumped into the reactor cavity is a part of accident management, but it can not be provided on the early stage of core melt relocation. Whether or not the decay-heated corium will be kept within the lower plenum depends on SAM activated and cooling capability. In any case, the heat transfer regime of a melt pool will determine timing and failure mode of the reactor vessel.

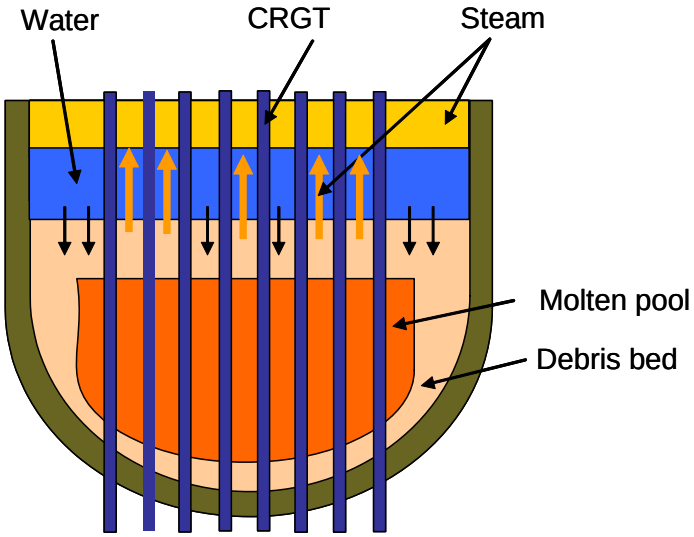

Figure 1.5: Melt pool formation in a BWR lower plenum.

Table I.1: Combination of relocation modes and lower plenum conditions (Figure 1.4)

Lower Plenum conditions	**Relocation mode 1** (Figure 1.4)	**Relocation mode 2** (Figure 1.4)	**Relocation mode 3** (Figure 1.4)
A	- Leads to B, D	- Leads to B, D - IGT failure	- Jet fragmentation - Impingement on IGTs - IGT failure
B	- Leads to B, D	- Jet fragmentation - Impingement on IGTs - IGT failure - IGT ejection	- Formation of debris bed - Formation of debris cake - Impingement on IGTs, pumps - IGT failure - IGT or pump ejection
C	- Formation of debris cake or melt pool	- Impingement on penetrations and vessel wall - Formation of debris cake or	- Impingement on penetrations and vessel wall with subsequent instantaneous melt-through

		melt pool	
D	- Formation of debris cake - IGT failure - IGT ejection	- Formation of debris cake - Impingement on IGTs - IGT failure - IGT ejection	- Formation of debris cake - Impingement on IGTs, pumps - IGT failure - IGT ejection - Internal pump ejection

1.2.3. Melt pool in a lower plenum

A melt pool formed in a lower plenum is characterized by multi-component and multi-phase materials under high temperature and complex flows. In the case of molten pool formation in the lower plenum, complicated chemical reactions are occurring at the prevailing high temperatures (> 2200^{o}C), in a mixture containing U, O, Zr, Fe, Ni, Cr and control rod materials. The important factors are:

(i) Possibility of a miscibility gap which could lead to melt layers stratifications;

(ii) The composition and properties (e.g. liquidus/solidus temperature, thermal conductivity, viscosity) of the oxidic pool and metal layer.

The melt pool chemistry can significantly affect the melt pool composition and layer configuration, which in turn may change the heat flux distribution on the vessel wall (Seiler et al, 2007). However, the knowledge base in this area is still under development (Seiler et al., 2003).

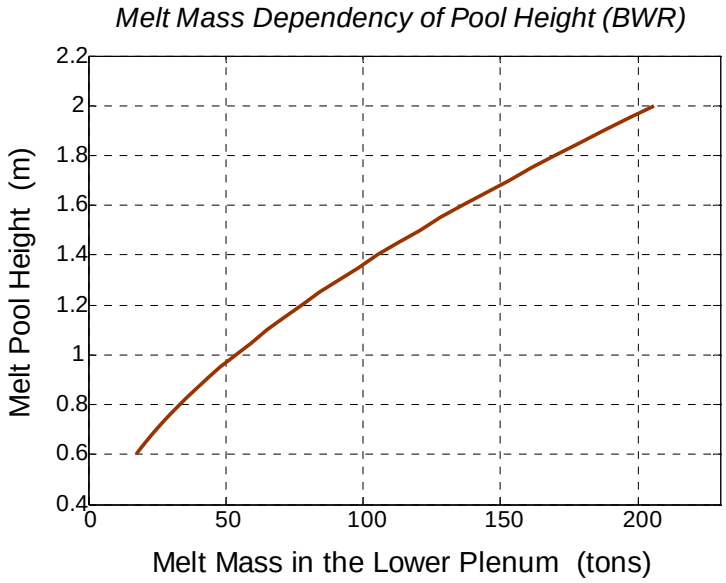

Figure 1.6: Dependency of pool height on amount of melt in the lower plenum.

In the case of formation of a homogeneous melt pool in the lower plenum, heat transfer in the pool is governed by turbulent natural convection, which is characterized by internal Rayleigh number (*Ra'*). Rayleigh number of a decay-heated melt pool is a function of melt property, internal heat generation and the pool's height. The height of the formed melt pool depends on the melt mass relocated into the lower plenum. For the reference reactor, the melt mass dependency of the pool height is delineated in Figure 1.6. Different melt pool height values will be referred in remained part of the thesis work.

1.2.4. Melt pool stratification

Under a certain scenario, it is possible that a stratified melt pool is formed in the lower plenum, i.e. with a metal layer atop. The lower part of stratified pool contains either oxidic components of corium (a mixture of ZrO_2 and UO_2 in liquid phase), or solid oxidic components and liquid metals. The upper metal layer consists of light components of molten metals. Under certain thermal conditions, crusts of solid materials may be formed along the vessel wall, the cooled CRGTs and the top surface of the lower pool containing corium mixture.

Heat generation in the metallic layer is insignificant (depends on fission product re-distribution), and the main heat source to the metallic layer is coming from the oxidic pool from below. Two ways of removing the heat from a metal layer are radiation heat transfer (or boiling heat transfer) from the top surface and conduction to the vessel wall and CRGTs laterally. The high conductivity of the metal and the effective heat transfer from the top and CRGT wall surfaces (Figure 1.7) probably reduce significantly temperature of the metallic layer. This reduction in temperature results in formation of a crust on the top of oxidic melt pool. In the case of effective cooling by the CRGTs, crust layers surrounded CRGTs are expected to appear in the oxidic pool region and in the metal layer region.

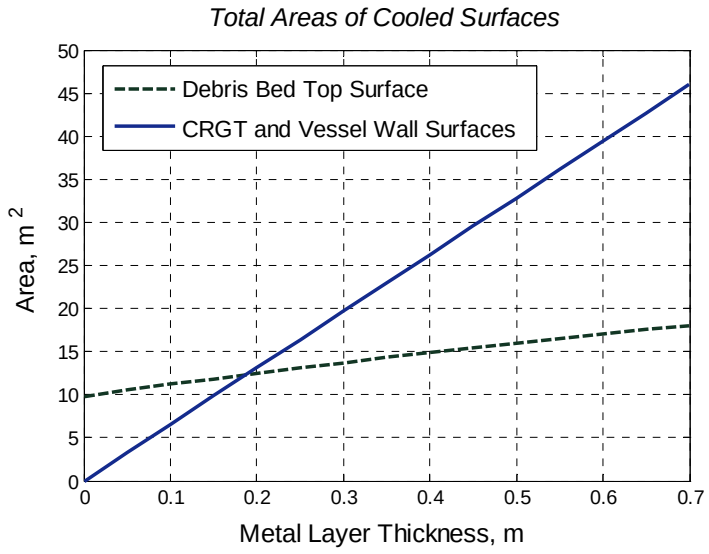

Figure 1.7: Total areas of cooled surfaces connected to the metal layer atop of 0.7 m deep pool of oxidic melt in a BWR lower head.

The presence of such a metallic layer raises some concerns for the vessel integrity, since a large fraction of the heat removed from the top of the oxidic melt pool, could be focused to the side of the metallic layer and threaten the vessel wall or CRGTs at that location. Physically, heat transfer inside such a layer is governed by a mixture of Rayleigh-Benard convection and the boundary layer development along available inclined walls, so called mixed natural convection, which has been studied on separate-effect basis both analytically (Theofanous et al., 1994) and experimentally (Globe and Dropkin, 1959; Churchill and Chu, 1975, Dinh et al., 2004). In the case of mixed natural convection in the metallic layer, the heat transfer coefficient is a function of the external Rayleigh number (*Ra*) and Prandtl number (*Pr*).

1.3. Significance of the thesis work

In case of melt pool formation in a BWR lower plenum, it is of paramount importance for the plant safety analysis that we are able to predict with a sufficient level of accuracy the timing and mode of the vessel failure, and melt characteristics (e.g. mass, composition, temperature) upon the vessel failure. The vessel failure mode and melt characteristics are governing parameters of ex-vessel melt risks associated with fuel-coolant interaction and debris bed formation/coolability in the Swedish nuclear power plants (Kudinov et al, 2008).

Clearly it is hard to study experimentally melt pool heat transfer, due to its multi-physics nature, presence of phase changes, chemical reactions and material interactions (Bechta et al., 2008b). Simulation of melt pool heat transfer still remains a big challenge due to high Rayleigh numbers, long transient of accident progression, and the presence of phase changes. The difficulty is further increased in a BWR whose lower plenum contain a forest of penetrations (CRGTs, IGTs) which significantly complicates the lower plenum geometry, heat transfer, and fluid flow patterns induced by cooled CRGTs.

Several methods for analysis of the lower plenum processes have been developed and employed. In the existing methods, the heat transfer correlations are used to describe turbulent natural convection, so they are referred as correlation-based methods. However, due to their specific limitations, these methods are not straightforwardly applicable for the task at hand. The Computational Fluid Dynamics (CFD) methods have also been employed to study turbulent natural convection in volumetrically heated liquid pools and fluid layers (e.g., Dinh and Nourgaliev, 1997; Nourgaliev and Dinh, 1997). However, the CFD simulations at high Rayleigh numbers are computationally expensive. No CFD simulations of large and decay-heated melt pool formation were found in the literature, largely due to the added burden in computations associated with moving phase-change boundary and long transients.

Therefore it is important for reliable safety analysis to have a method which is sufficiently-accurate and computationally-efficient for simulation of melt pool heat transfer. The method should incorporate the advantages of the modern CFD method and the available correlation-based methods.

1.4. Problem formulation and study subject

It is clear that predictions of the melt pool characteristics and thermal loads on the vessel wall and reactor internal structures, as well as evaluations of the cooling measure effectiveness are essential for safety analysis. In order to perform such a safety assessment, reliable and effective tools are needed for simulations of heat transfer of a melt pool with high-fidelity prediction results.

The main purpose of the present thesis work is to develop a method for prediction of thermal loads imposed on the Boiling Water Reactor (BWR) internal structures and vessel wall during a postulated severe core-melting accident, to enable reliable assessment of efficiency of different SAM measures.

The objectives of the present thesis work are as follows:

- Development of approach for efficient use of modern CFD methods and combination of experimental and CFD-generated data for development and validation of accident analysis heat transfer simulation methods which can reliably predict phenomena driven by both integral and locally distributed parameters;
- Development and validation of adequate and computationally affordable tools for simulation of melt pool heat transfer during the late phase of a core-melting severe accident in a BWR lower head;
- To apply the developed method and models (codes) for assessment of CRGT cooling efficacy as a SAM measure in the proposed novel scheme for mitigation of severe accident consequences.

In the present thesis work, the analytical models based on the average heat transfer correlations are developed for some specific geometry of a BWR melt pool. Analytical models provide average heat fluxes, i.e. the first approximation of energy splitting, which can be used for comparison with the results obtained by the other methods.

The structure of the thesis work is organized as follows. In the remained part of this Chapter, the main achievements of the thesis work are introduced. Literature review of the existing methods and melt pool heat transfer modeling is presented in Chapter 2. Chapter 3 is describing the approach proposed for reactor safety analysis and the CFD method. That is the central methodology (approach) which aims to efficient use of the CFD in supporting development of the accident analysis models for solution of BWR melt pool heat transfer and assessment of thermal loads in the lower plenum. Chapter 4 describes the models developed in the present work: the Effective Convectivity Model (ECM), the Phase-change ECM (PECM), and the metal layer ECM/PECM. Chapter 5 presents validation of the developed ECM, PECM and metal layer ECM/PECM. In Chapter 6, applications of the PECM and metal layer PECM are presented with discussion of key findings and evaluation of CRGT cooling efficiency. A summary of the thesis work is given in Chapter 7. Descriptions of the method and models, their validation results and applications are referred to and supplemented in Appendices A-F.

1.5. The main achievements

1.5.1. Development of an approach to efficient use of the modern CFD method for BWR severe accident safety analysis

The CFD methods are indispensable for investigating complex fluid physics, can be used to perform "numerical experiments" and obtain useful data which could not be acquired experimentally. However, reliable CFD simulations are very expensive, thus the methods are not directly applicable to simulation of accident progression hypothetically happened in a nuclear reactor. Meanwhile the accident analysis models (e.g. correlation-based methods) which are more effective and powerful are not capable for revealing and quantifying the potential heat transfer local effects.

The question raised is how to synergistically leverage on the advantages of both the CFD methods and the accident analysis methods into solution of the proposed safety issues. In the present work, an approach to efficient use of the CFD method is developed, aiming to the safety analysis of BWR in the accident progression.

The developed approach consists of five steps. Based on the analysis of governing physical phenomena involved in a severe accident, the CFD method is used to perform heat transfer simulations in specific geometries of BWR lower plenum, getting the insights into flow physics. The validated CFD method is then used to produce necessary data for validation purpose. Based on the understanding and insights obtained from CFD study, the accident analysis models (ECM, PECM for internally heated volume and metal layer ECM/PECM in the present thesis work) are developed and validated. Validation of the accident analysis models is performed with the dual approach, i.e. against the existing experimental data and against the CFD generated data where experimental data are not covered. Validated accident analysis models are directly used for simulations of melt pool heat transfer in a BWR lower plenum.

In the present work, the selected CFD method is the Implicit Large Eddy Simulation (ILES). The ILES method was validated against various experiments. The CFD ILES simulations in specific BWR lower plenum geometries revealed the local heat transfer effect. That is, the downward heat flux from a melt pool to the vessel wall is locally enhanced, in the vicinity of CRGT which is cooled by water flow from the inside. The enhanced heat flux is 5-7 times higher than that of the peripheral areas. This effect is related to boundary layer flow development along the CRGT and flow impingement on the bottom wall. CFD study confirmed that the effect is attributed for corium fluid which is characterized by low Prandtl number (low fluid Prandtl number effect).

The low fluid Prandtl number effect was quantified with CFD simulations and implemented in the accident analysis model (PECM). The influence of the low Pr number effect on vessel wall temperature evolution is then quantified with the PECM. It was found that the local heat transfer effect caused by low fluid Prandtl number leads to an additional heatup of the BWR vessel wall during a severe accident, and consequently may threaten the vessel integrity.

1.5.2. Development of accident analysis models

In the present thesis work, the following models were developed:

- Effective Convectivity Model (ECM) for simulation of an enveloped melt pool heat transfer;
- The Phase-change ECM (PECM) for simulation of melt pool formation heat transfer;
- The metal layer ECM which is used for heat transfer simulation of Rayleigh-Benard convection or mixed natural convection (i.e. Rayleigh-Benard convection in the presence of side cooling) in a molten metal layer;
- Metal layer PECM for simulation of metal layer heat transfer in the presence of transient phase change (eutectic and non-eutectic mixtures).

The ECM was built on the concept of effective convectivity implemented in the Effective Convectivity Conductivity Model (ECCM) developed by Bui and Dinh (1996). In contrast with the ECCM where effective convectivity model describes heat transfer in the vertical direction and effective conductivity model is used for the horizontal direction, in the ECM, only the effective convectivity model is used. The main idea of the ECM is to use the directional heat transfer characteristic velocities (or simply characteristic velocities) to transport the heat in an internally heated volume to it cooled boundaries. Solving the energy conservation equation, the ECM uses the characteristic velocities instead of instantaneous fluid velocities, thus the need of solving Navier-Stokes equations is eliminated. The characteristic velocities which were derived using energy balance equations are determined using the heat transfer coefficients (Nusselt number). In the ECM, the directional Steinberner-Reineke heat transfer correlations are used, thus the ECM is a correlation-based method. The ECM was implemented in the **Fluent** code (FLUENT Inc., 2006), using the User Defined Function (UDF). The characteristic velocities are implemented in the code through the heat source term.

For simulation of melt pool formation heat transfer, the ECM was extended to phase-change problems (PECM). The PECM employs the enthalpy formulation based on a fixed grid for solution of solidification/melting of eutectic and non-eutectic mixtures. In the PECM, mushy zone convection heat transfer is described by mushy zone heat transfer characteristic velocities (or simply named mushy characteristic velocities) which are reduced characteristic velocities. Different models of mushy zone heat transfer can be described in the PECM platform using different relations for dependency of mushy characteristic velocities on the liquid fraction.

The ECM method was extended to simulation of convection heat transfer in a molten metal layer. In contrast with the developed ECM and PECM for a decay-heated pool, natural convection in a molten metal layer is caused by temperature differences between the lower heated wall and top (and side) cooled walls. Development of metal layer ECM and PECM was guided by the approach developed in the present thesis work. Characteristic velocities directed vertically and horizontally are used to transfer the heat

from the bottom heated wall to the cooled walls atop and laterally. The Globe-Dropkin and Churchill-Chu correlations are used to determine the corresponding characteristic velocities. To describe natural convection in a mushy zone, the metal layer PECM uses the mushy zone characteristic velocities which are functions of the characteristic velocity in the bulk fluid, and liquid fraction. The characteristic velocity in the bulk fluid is determined using the combined external Rayleigh number, which is a function of the fluid property, fluid layer thickness, temperature gradient, and compositional gradient. Compositional gradient which depends on the mushy zone (assumed to have dendrite structure) characteristics, fluid property, intensity of the bulk fluid convection, direction and rate of cooling, is determined using the rejectability coefficient. The metal layer ECM and PECM was implemented in the **Fluent** code, through the heat source term. Note that the metal layer does not contain any heat source, the heat source term is used only for description of the convective terms with characteristic velocities.

1.5.3. Validation of the CFD method and developed models

Validation is necessary for the CFD method and accident analysis models developed in the present work, namely the ECM, PECM and metal layer ECM/PECM.

As the main tool for studying fluid flow physics, the used CFD method should be reliable and capable of predicting turbulent natural convection heat transfer with sufficient accuracy. The selected CFD method (LIES) employed in the present work was validated against several existing heat transfer experiments for both integral and local effects. Results of CFD ILES simulations show that the method is capable of predicting turbulent heat transfer coefficients with acceptable deviation, i.e. less than experimental.

For validation of the accident analysis models developed in the present thesis work, the dual approach is used. Validation of the ECM, PECM and metal layer ECM/PECM was extensively performed against both available experimental data and CFD generated data.

Validation of the ECM and PECM covered the whole spectrum of governing physical phenomena involved in decay-heated melt pool heat transfer, in a wide range of internal Rayleigh number for various types of geometry of interest (fluid layer, rectangular cavity, BWR unit volume, semicircular cavity, torospherical cavity, and hemispherical pool). The ECM and PECM were validated not only steady state experiments, but also the transient heat transfer experiments. Results of ECM and PECM validation show that the ECM and PECM are capable to predict melt pool energy splitting, temperature profiles (superheat), heat flux profiles, and crust thickness with sufficient accuracy. Performance of the ECM and PECM showed that the developed tools are capable of predicting long transients of a severe accident in a BWR.

Validation of the metal layer ECM and PECM was also performed extensively against various experiments and CFD ILES generated data, including all the governing physical phenomena of metal layer heat transfer, that is, Rayleigh-Benard convection, mixed natural convection, boundary layer heat transfer, and transient phase change. Validation of the metal layer PECM against various non-eutectic binary melt heat transfer

experiments showed that with appropriate models of mushy characteristic velocity and compositional convection, the PECM is capable of predicting crust evolution and mushy zone thickness evolution of transient solidification.

1.5.4. Practical application of the method

The ECM, PECM and metal layer ECM/PECM were applied to simulation and analysis of melt pool heat transfer in a BWR lower plenum during a severe reactor accident. Both homogeneous and stratified melt pools, with different pool's heights were simulated, in the specific geometries of BWR. The simulations were made on the assumption that the IGTs are plugged during the accident progression, and have no affect on the melt pool heat transfer. The key findings are as follows:

- In case of formation of a debris bed (cake) with a thick (height, or depth) < 0.7 m in the BWR lower plenum, the CRGT cooling at nominal water flow rate, i.e. 62.5 g/sec or equivalent to 15 kg/(m^2.sec) for the reference reactor, is sufficient to remove the decay heat generated in the debris bed (or cake and melt pool later on), and protect the vessel wall from thermal attack; In the case of higher debris bed (cake), the CRGT cooling is insufficient, the vessel wall is predicted to fail in the section connected to the uppermost region of the debris bed (melt pool); Additional cooling measure (e.g. external cooling) is needed for protection of the vessel from failure;
- Taking into account the corium Prandtl number effect, the PECM simulation shows that the local effect of heat transfer (i.e. the enhancement of the downward heat flux to the vessel wall) results in additional heatup of the vessel wall during an accident; There is possibility that the vessel wall failure takes place in the vicinity of the peripheral CRGTs due to thermal creep; Even vessel failure may not be avoided, the CRGT cooling significantly delays the process of vessel wall heatup and failure;
- Results of the metal layer PECM simulation of a stratified melt pool formed in the BWR lower plenum show that in the presence of CRGT cooling, the decay heat transferred from an oxidic melt pool (debris pool) to the metal layer atop is efficiently removed by the cooled CRGTs, no focusing effect is predicted;
- However, in the case of stratified melt pool formation in the lower plenum, the metal layer PECM simulation shows that the CRGT cooling at the nominal water flow rate is insufficient to remove the high transient heat flux imposed on CRGTs from the metal layer; An increase of CRGT water flow rate (e.g. to 30 kg/m^2.sec) is requires to ensure no failure of CRGT due to dryout.

The ECM/PECM simulation results and key findings suggest that CRGT cooling possesses a high potential as an effective and reliable mechanism to remove the decay heat from a melt pool formed in the BWR lower plenum. Thus, CRGT cooling presents a credible candidate for implementation as a SAM measure in BWRs.

Chapter 2: Literature review

2.1. Existing methods for solution of problems

In this Chapter, a review of the existing methods for prediction of melt pool energy splitting and thermal loading on the reactor vessel wall and structures is provided. These methods can be divided into two main groups: lumped-parameter methods and distributed-parameter methods (including the CFD methods). All the existing methods were developed based on the natural convection heat transfer correlations. A huge number of experiments were performed and different experimental correlations were established for both internally heated volume and fluid layer heated from below and cooled from the top. However, the applicability of a specific correlation to reactor melt pool conditions may remain questionable, due to specific (non-prototypical) conditions under which the correlation was obtained. Meanwhile, the CFD methods become widely used for research purposes and may become an efficient tool for scrutinizing flow physics. Therefore, in this chapter the numerical and experimental works related to heat transfer of an internally heated volume and fluid layer are also reviewed in brief.

2.1.1. Lumped-parameter methods

The lumped-parameter method was broadly used for prediction of thermal loads from an enveloped decay-heated melt pool to its boundaries. The method is based on energy balance equation and heat transfer correlations describing turbulent natural convection in a molten corium volume, or mixed natural convection (Rayleigh-Benard convection in presence of side wall cooling) in a molten metal fluid layer. The lumped-parameter method was implemented in several works, including Park and Dhir (1992), Theofanous et al. (1994), and in the system codes as MELCOR (Gauntt et al., 2005), MAAP (Henry and Landgren, 2003). More detailed information of the lumped-parameter methods is presented in Appendix B.

Limitation of the lumped-parameter methods is that the method is based on pre-defined configurations of an enveloped volume. The methods are not capable for resolving phase change problems, thus it is not applicable for prediction of spatio-temporal dynamics of melt pool formation in complex 3D geometry.

2.1.2. Distributed-parameter methods

The effective diffusivity method which is classified in the group of distributed-parameter methods was pioneered by Cheung et al. (1992). The main idea of the effective convectivity method is using the modified effective conductivity to describe turbulent natural convection in a heated fluid layer with different initial and boundary conditions imposed to the top and lower boundaries. The effective diffusivity model was implemented in several later works including the Effective Convectivity Conductivity Model (ECCM) (Bui and Dinh, 1996), Dombrovskii et al. (1998), SCDAP code (SCDAP/RELAP-3D, 2003), and Willschuetz et al. (2006).

Detailed information of these methods can be found in Appendix B. The limitations of these methods are related to the effective diffusivity (conductivity) which may lead to distortion in temperature distributions, which in turn can cause errors in the predicted thermal loads imposed on the pool boundaries. In addition, the effective diffusivity may significantly affect the mushy zone evolution, thus the distributed-parameter methods are not appropriate for simulations of melt pool formation heat transfer.

A summary of in-vessel phenomenological modeling and heat transfer correlations used in the system codes is provided in Table II.1.

Table II.1: Lower plenum modeling employed in the severe accident codes

Phenomena	SCDAP/RELAP	MELCOR 1.8.6	MAAP4
Debris Bed (DB) *			
Formation of solid particles and porosity	Considered, single porosity for mixture (oxide and metal)	Considered, different values for oxide and metal	Considered, single porosity for mixture (oxide and metal)
Formation of molten pool	Considered (Natural convection)	Considered (Natural convection)	Considered (natural convection)
Crust growth and shrinkage	Considered	Considered	Considered
Stratification	Not considered	Considered (natural convection)	Considered (natural convection)
Gap formation between debris bed and vessel wall	Not considered	Not considered	Considered
Heat Transfer (HT) *			
HT between DB	2D model (axial and radial directions)	1D model, correlations based on temperature differences	1D model (bed to bed)
Molten pool HT - Molten pool temperature - HT coefficient to boundaries	- Uniform temperature field of the pool (high conductivity) - Mayinger upward HT correlations; Jahn-Reineke	- Uniform temperature field of the pool - Bonnet correlation to upper surface; ACOPO correlation to radial surface	- Uniform temperature field of the pool (high conductivity) - Mayinger upward HT coefficients; Park-Dhir local

	correlation for angle effect		downward correlation
Gap cooling HT	Not considered (Specified gap HT coefficient by user)	Not considered (Specified gap HT coefficient by the users)	Monde correlations, heat removal from both of lateral crust and RPV wall
Metallic layer HT	Not considered	ACOPO correlations to upper and radial surfaces; Globe-Dropkin correlation to lower surface	Mixed natural convection (Globe-Dropkin correlation)
RPV lower plenum temperature distribution	2D heat conduction model	2D heat conduction model	2D heat conduction model

**) DB - Debris Bed; HT - Heat Transfer.*

2.1.3. CFD study

a) Simulation of fluid flows

With the extraordinary increase of capability and availability of computing resources, the CFD method has become widely used in both fluid physics research and engineering practice.

The Direct Numerical Simulation (DNS) method is used in the fundamental research to study the mechanisms in certain flows. DNS is also used for the determination of turbulence statistics to develop special features of statistical turbulence models. The first direct simulations were those by Orszag and Patterson (1972) for decaying isothermal isotropic turbulence, those by Lipps (1976) for weakly turbulent, those by Grotzbach (1982) for fully turbulent Rayleigh-Benard convection of air, those by Grotzbach (1987) for internally heated fluid layer natural convection, and those by Kim (1988) for forced convection in channels with heat transfer. The DNS method was successfully used for investigation of turbulence characteristics of natural convection in an internally heated fluid layer (Nougaliev and Dinh, 1997), for examining Prandtl number dependence of Nusselt number in a Rayleigh-Benard convection fluid layer (Verzicco and Camussi, 1999; Kerr and Herring, 2000). Recently, based on DNS data an analysis of turbulent diffusion and turbulent heat flux of both internally heated fluid layers and Rayleigh-Benard convection has been performed (Chandra and Grotzbach, 2008).

The Large Eddy Simulation (LES) method is also a good tool to access high Reynolds or high Rayleigh number flows. In the nuclear field, full advantage of LES can

be taken by applying it intensively to the thermal fluid-structure interaction problems (Grotzbach and Worner, 1999). However, applicability of the DNS and LES is limited due to their computational expensiveness. Mostly the DNS is used for simple or small-scale geometries.

b) Phase-change modeling

In the numerical method, modeling of phase-change convection widely employs a formulation based on the enthalpy conservation equation. The main advantage of this method is that the latent heat can be treated using a fixed grid. The mushy models treat the mushy region relationship between the liquid mass fraction and temperature in an arbitrary manner (Voller and Prakash, 1987). In a non-eutectic binary system, the relationship between the liquid fraction and temperature, however, is a function of local solute concentration. During solidification, the change of solute concentration causes a change in density, in some cases leads to compositional convection in addition to thermal convection, i.e. double diffusive convection in a mushy zone (Huppert and Turner, 1981; Worster, 1997).

Due to redistribution of solute concentration, a comprehensive model is required for describing solute transport equation along with the Navier-Stokes and energy equations. Such a model was developed by Bennon and Incropera (1987a, 1987b) using the principles of classical mixture theory to obtain a set of continuum conservation equations for binary, solid-liquid phase-change systems. The other models based on volume-averaged transport equations were proposed by Beckermann and Viskanta (1988), Voller et al. (1989), Ni and Beckermann (1991), for prediction of macro-segregation during binary melt solidification.

In order to describe dendrite growing during solidification of a binary system, there is a need to track the evolution of the solid-liquid interface. A wide range of methods have been proposed in literature. Generally, the methods which use standard numerical discretizations for the governing equations can be divided into two classes: front tracking methods and order parameter methods. The tracking methods can use deforming grids (Sullivan and Lynch, 1987), or modifications of the finite different (or finite element) approximations in the vicinity of the interface, or through the distribution of the interface heat source (Udaykumar et al., 2003; Zhao et al., 2003; Juric and Tryggvason, 1996). Order parameter methods class includes the level set methods (Chen et al., 1997; Kim et al., 2000), phase-field methods (Beckermann et al., 1999; Beckermann, 2006) and enthalpy methods (Chatterjee and Chakraborty, 2006; Voller, 2008). Note that, required scale for resolution of the solid-liquid interface in the mushy zone is several orders of magnitude smaller than the typical cell size used in a discrete numerical solution of the governing macroscopic transport equations (Pardeshi et al., 2008). Tracking the evolution of the solid-liquid interface is still computationally challenging.

2.2. Experimental works and heat transfer correlations

2.2.1. Simulant and real corium tests in an internally heated volume

a) Internally heated pool with isothermal boundary conditions

During the years of 1970s, a number of experimental and analytical studies were focused on obtaining the heat transfer correlations for natural convection of internally heated fluid in different kinds of geometry, e.g. fluid layer, rectangular, semi-circular and elliptical "slice-type" (torospherical) cavity, cylindrical and hemispherical pools. A number of correlations were produced from the experiments of Fiedler and Wille (cited by in Kulacki and Emara, 1977), Kulacki and Goldstein (1972), Jahn and Reineke (1974), Mayinger et al. (1976), Kulacki and Emara (1977), Steinberner-Reineke (1978), Gabor et al. (1980) etc. These correlations which were developed mostly experimentally (a few was developed computationally or analytically) are describing the dependency of the average Nusselt number at the cooled surfaces. It is seen that the dependencies $Nu_{up}(Ra)$ at the upper surface are quite similar in trend and values for different geometries (e.g. fluid layer, rectangular, semi-circular and elliptical cavities). More interestingly, the heat transfer correlations $Nu = f(Ra)$, at all cooled boundaries, are applicable in the entire range of Rayleigh number (10^6-10^{16}). This allows us to assume that there is a similarity in the physical mechanism governing natural convection flows and heat transfer in an internally heated pool in the laminar and turbulent regimes.

The fluid mostly used in the simulant experiments were water and Freon. The range of Prandtl number for water (Pr = 2.5-7) and Freon (Pr = 8-11) is one order magnitude greater than the prototypic Pr of the core melt (Pr = 0.1-0.6). So the question arisen is whether the heat transfer correlations obtained in the simulant material experiments are applicable to the predictions of melt pool behavior in a severe accident. Some later computational analyses showed that the effect of Pr number on heat transfer coefficients is insignificant. However, the small-scale experiments using joule-heating of molten uranium oxide at Argonne Natural Laboratory (ANL) showed higher downward heat fluxes than those predicted on the basis of simulant material experiment data. The effect of the fluid's low Prandtl number on its heat transfer characteristics in internally heated liquid pools was numerically studied by Nourgaliev et al. (1997a). The effects of Pr number on Nu number at the bottom surface are found to be significant and they become larger with increasing of Ra number.

In the late 1990s, the natural convection heat transfer in internally heated liquid pools was studied to determine the consequences of severe (meltdown) accidents in light water reactors and to devise accident management schemes. The In-Vessel Retention (IVR) concept was an important accident management strategy applied to VVER (Loviisa Nuclear Power Plant) and AP-600 (Theofanous et al, 1994, Rempe et al., 2008). It was noted that the fluid layer data obtained from 1970s experiments may not be relevant to the large-scale geometry of the reactor vessel (elliptical-formed or hemi-spherical pools) and the boundary conditions of an isothermally downward curved surface. In this context, new experimental programs were pursued to obtain necessary data, and support extrapolation of existing correlations to the prototypic conditions. The experimental

programs which were performed with isothermal boundary conditions are COPO-I experiment (Kymalainen et al., 1994), mini-ACOPO (Theofanous et al., 1994), hemispherical pool (called bell jar) heat transfer experiments (Asfia et al., 1996), and ACOPO experiment (Theofanous et al., 1997).

The heat flux on the COPO-I side wall (vertical wall) was essentially uniform and predicted well with the Steinberner-Reineke sideward correlation. However, the COPO-I upward heat flux was slightly higher than those predicted by the Steinberner-Reineke correlation. The mini-ACOPO experiment test section has a diameter of 0.4m (1/8 reactor scale). This experiment confirmed the idea that the cool-down would be arrested and natural convection would be investigated during a transient cool-down. The ACOPO experiment simulates natural convection heat transfer from volumetrically heated pools, at half-scale reactor lower head geometry (hemi-spherical). The results are in substantial agreement with those of the mini-ACOPO experiment. Results of the ACOPO experiment strongly supported the analytical results based on the Steinberner-Reineke and Mayinger et al. correlations.

b) Experiments with phase changes

The early experiments of melt pool convection were conducted with isothermal boundary conditions without phase change, starting from 1970s and were lasting until the middle of 1990s. Phase-change heat transfer experiments have been started in the late 1990s, some of the experiments were performed with the real corium: RASPLAV, MASCA, METCOR (Strizhov and Asmolov, 2000; Asmolov et al., 2004; Bechta et al., 2008a, 2008b), the others were performed using salt: RASPLAV-SALT, SIMECO, LIVE (Strizhov and Asmolov, 2000; Sehgal et al., 1998; Miassoedov et al., 2007), or water as the corium simulant: COPO-II, BALI (Helle et al., 1998; Bernaz et al., 1998).

The main objective of the RASPLAV Project was to provide data on the behavior of molten core materials on the RPV lower head under severe accident conditions, and to access the possible physicochemical interactions between molten corium and the vessel wall. Data were also obtained to confirm heat transfer modeling for a large convective corium pool within the lower plenum. During the first phase of the RASPLAV project (1994-1997), the large-scale experiments demonstrated clearly that behavior of corium melts differed from that of simulant materials. Under certain conditions, the corium would separate into layers that were enriched in zirconium and uranium. The second phase of the project (started from 1997) concentrated on exploring the physical and chemical phenomena occurring in a convective molten pool. The effect of different corium compositions, the potential for and effects of material stratification and the influence of various boundary conditions were investigated. It demonstrated that the homogeneous corium melt behaved comparably to simulant materials in natural circulation, therefore previous evaluations based on simulant material data could be scaled to prototypic reactor conditions. It was shown that such a behavior can be expected if molten pool contained oxidic materials. The heat transfer correlations established in the simulant materials tests can be used for the convection of a homogenous corium melt pool at equivalent *Ra* numbers (Asmolov et al., 2001).

However, two of the four large-scale RASPLAV tests conducted with sub-oxidized corium exhibited an unexpected behavior. Post-test examinations showed that the melt pool, initially of a homogenous composition and density, stratified into two layers of unequal density. The lower layer of a denser material was richer in uranium while the upper lighter layer was richer in metallic Zr (Strizhov and Asmolov, 2000). Although further investigations showed that the main reason was in small carbon content in the melt, in light of these results the interest was to obtain more data with respect to prototypic core materials behavior at high temperatures. In the framework of an OECD Project, the MASCA experiments were performed (Asmolov et al., 2004). Successful MASCA-1 experiments were performed and new remarkable results were obtained. It was found that under the inert atmosphere, the Zr in the melt actively stole oxygen from UO_2 which prompted some steel to combine with uranium to form a heavy alloy which sank to the bottom of the pool. The last few experiments in MASCA-2 started with a corium mixture containing UO_2, ZrO_2, Zr and steel heated under an inert atmosphere. The expected alloy formation between uranium and steel occurred and a metal layer was formed at the bottom of the pool. There was also a metal layer at the top of the pool, i.e. a three layer pool. However, when steam is added to the test section, the uranium is converting to UO_2 and releasing the steel, which being lighter joined back the layer at the top of the pool. The UO_2 and ZrO_2 formed joined the oxidic pool and the two layer configuration was obtained again. The MASCA experiments were focusing on stratifications, chemical interactions of metals and oxygen, therefore no significant conclusion on the pool heat transfer has been made.

The materials interaction behavior has been studied in the medium-scale experiments with a prototypic corium within the METCOR project (Bechta et al, 2008b). The completed studies of VVER vessel steel corrosion caused by its interaction with molten UO_{2+X}-ZrO_2-FeO_Y corium in the oxidizing above-melt atmosphere have shown that corrosion rates in air and steam are close. At a relatively low temperature the diffusion of Fe^{2+} ions into the solid oxidic layer on the steel surface, which controls corrosion kinetics, is characterized by activation energy values similar to that of simple steel oxidation in air. But if the steel surface temperature exceeds the level of 1050 °C, the corrosion intensifies, which is explained by formation of a liquid phase in the interaction zone.

The SIMECO experiments were performed to investigate the effect of boundary crusts and mushy layers on natural convection heat transfer (Sehgal et al., 1998). Binary salt mixtures were employed as a melt simulant. Both eutectic and non-eutectic mixtures of sodium-potassium nitrates $NaNO_3$-KNO_3 were used in the experiments. The experiment concluded that the upward Nusselt number is close to that determined from the Steinberner-Reineke correlation.

The COPO-II and BALI experiments (Helle et al., 1998; Bernaz et al., 1998) were performed in large 2D slice geometry to study the thermal-hydraulic of a corium pool; water was used as the simulant. The boundaries of the pool were cooled till freezing so truly isothermal boundaries were established. The measured values of the COPO-II showed that upward Nusselt numbers are consistent with BALI results. However, they are slightly higher than those predicted by the widely used correlation of Steinberner and

Reineke, and also higher than those measured in 3D ACOPO experiments which did not have crusts at the boundaries.

In the last 4 years, the LIVE program has been performed at Forschungszentrum Karlsruhe (Miassoedov et al., 2007). The main focus of the LIVE experimental program is to address remaining uncertainties in melt pool heat transfer with phase change. The LIVE L1 test was performed in 2006, the experimental technique used was similar to that of SIMECO, but in 3D pool geometry. The LIVE experimental program is in its active phase and analysis of the LIVE data is in progress.

Experimental studies have shown that large uncertainty still remains in corium chemistry which defines physicochemical interactions between the core materials and RPV that may result in a significant change in melt pool heat transfer and the accident progression. Nevertheless, the experimental heat transfer correlations built on the data from the simulant fluid experiments under isothermal boundary conditions are applicable to a corium melt pool with phase change.

2.2.2. Fluid layer heated from below and cooled from the top and side walls

While a large number of works have been performed for different fluids to investigate turbulent natural convection in a fluid layer heated from below and cooled from the top (e.g. Kek and Muller, 1993; Cioni et al., 1996), only a few numbers of experiments were performed in the presence of side cooling (Churchill and Chu, 1975; Kirkpatrick and Bohn, 1986; Theofanous et al., 1994).

The research work has been focused on establishing Rayleigh number dependence of Nusselt number, and Prandtl number dependence of Nusselt number between the heated and cooled walls (Globe and Dropkin, 1959; O'Toole and Silveston, 1961; Threlfall, 1975; Viskanta et al., 1986; Cioni et al., 1997; Roche et al, 2002). Generally the relationship between Nusselt number and Rayleigh number depends on geometry and fluid properties. A summary of important experiments can be found in Chavanne et al. (2001).

A large number of experiments with phase change were performed with different fluids for both eutectic and non-eutectic mixtures, to investigate natural convection due to thermal and concentration gradients in a mushy zone. Aqueous ammonium chloride (NH_4Cl-H_2O) was widely used to study dendrite growth and compositional convection (double diffusive convection) during solidification of binary melt (Beckermann and Viskanta, 1988; Christenson and Incropera, 1989; Cao and Poulikakos, 1990; Kumar et al, 2003; Peppin et al., 2008). It was shown that during solidification of a non-eutectic binary mixture, due to rejection of one solute from the solid-liquid interface, the salt-depleted residual fluid is driving buoyancy-driven convection and development of chimneys in the mushy zone takes place (Peppin et al., 2008). As a result the composition in the bulk fluid is changed with time (Wettlaufer et al., 1997). This phenomenon was also observed in another experiment with Al-Cu alloy (Trivedi et al., 2001). The change in solute concentration of bulk fluid leads to feasible compositional convection.

2.2.3. Heat transfer correlations

a) Internally heated volume

A number of heat transfer correlations were developed from the experiments performed with isothermal boundary conditions (Rempe et al, 2008). The results of several experiments with phase change for both the core melt and the simulant materials verified the applicability of the upward, sideward and downward heat transfer coefficients of isothermal boundary condition experiments. It is worth to mention some of the heat transfer coefficients which are widely used in practical applications and important (i.e. further use and reference) in the present work. The list of correlations also gives an idea for a further selection of heat transfer coefficients to be used in the developed models of the present work. For an internally heated volume, representative heat transfer coefficients are listed as follows.

Kulacki-Goldstein correlations (1972) for a fluid layer cooled from the top and bottom wall:

$$Nu_{up} = 0.436\, Ra'^{0.228},\ 4\times10^{4} \le Ra' \le 10^{7},\ 5.76 \le \mathrm{Pr} \le 6.09 \qquad (2.1)$$

$$Nu_{down} = 1.503\, Ra'^{0.095} \qquad (2.2)$$

Jahn-Reineke experiment (1974) for a semi-circular segment with all walls being cooled:

$$Nu_{down} = 0.54\, Ra'^{0.18}\left(\frac{H}{R}\right)^{0.26},\ 10^{7} \le Ra' \le 5\times10^{10},\ \mathrm{Pr} = 7 \qquad (2.3)$$

where H is the height of the pool and R is the radius of the semi-circular segment.

Mayinger et al. correlations (1976) for a semi-circular segment with all walls being cooled:

$$Nu_{down} = 0.55\, Ra'^{0.2},\ 7\times10^{6} \le Ra' \le 5\times10^{15} \text{ and } \mathrm{Pr} = 7 \qquad (2.4)$$

Kulacki-Emara experiment (1977) for a fluid layer cooled from the top:

$$Nu_{up} = 0.389\, Ra'^{0.228},\ 2\times10^{3} \le Ra' \le 2\times10^{12},\ 6 \le \mathrm{Pr} \le 7 \qquad (2.5)$$

Steinberner-Reineke correlations (1978) for a rectangular cavity when all walls are cooled:

$$Nu_{up} = 0.345\, Ra'^{0.233},\ 5\times10^{12} \le Ra' \le 3\times10^{13},\ \mathrm{Pr} \approx 7 \qquad (2.6)$$

for the upward heat transfer coefficient. Laminar flow regime sideward heat transfer is described as:

$$Nu_{side} = 0.65\, Ra'^{0.19} \tag{2.7}$$

Turbulent flow regime sideward heat transfer is described as:

$$Nu_{side} = 0.85\, Ra'^{0.19} \tag{2.8}$$

For downward heat transfer, the correlation is:

$$Nu_{down} = 1.389\, Ra'^{0.095} \tag{2.9}$$

Asfia et al. correlation (1996) for downward heat transfer coefficient (hemispherical pools):

$$Nu_{down} = 0.54\, Ra'^{0.2},\ 1\times 10^{10} \le Ra' \le 1.1\times 10^{14} \tag{2.10}$$

Theofanous et al. correlations (1997) for the upward and downward Nusselt number in a hemispherical pool (ACOPO experiment):

$$Nu_{up} = 1.95 \cdot Ra'^{0.18},\ 10^{12} \le Ra' \le \times 10^{16},\ 1.7 < \mathrm{Pr} < 8.6 \tag{2.11}$$

$$Nu_{down} = 0.3 \cdot Ra'^{0.22} \tag{2.12}$$

b) Rayleigh-Benard convection and mixed natural convection

A large number of experimental and analytical works have been devoted to relationship between Nusselt number and Rayleigh number. In the early works, the scaling law ($Nu \sim Ra^{\gamma}$) was established: $\gamma = 1/4$ (Davis, 1922), $\gamma = 1/3$ (Malkus, 1954), and $\gamma = 2/7$ (University of Chicago, late 1980s). While Rayleigh number is the control parameter of heat transfer, the fluid Prandtl number also causes a significant effect. Experimental exponent of Ra seems to increase with increase of Prandtl number: that is 0.26 in mercury with $Pr = 0.02$; 0.28-0.29 for $Pr = 1$, and 0.33 was obtained for high Pr (Goldstein, 1990). Nevertheless, very weak dependence of the Nusselt number on Pr number is observed in the range of $0.7 < Pr < 21$ (Roche et al., 2002). In a later study, Verzicco and Camussi (1999) suggested that depending on Pr number, there are two distinct flow regimes: in the first ($Pr < 0.35$) the flow is dominated by large-scale recirculation cell that is the most important "engine" for heat transfer; in the second regime, the large-scale flow plays a negligible role in heat transfer which is mainly transported by the thermal plumes. Kerr (1996), Kerr and Herring (2000) analyzing the DNS data concluded that the trends in boundary length scale are consistent with $Nu \sim Ra^{\beta}$ where $2/7 < \beta < 0.309$. This conclusion is consistent with Castaing et al. (1989),

Shraiman and Siggia (1990), Cioni (1997), and Grossmann and Lohse (2000) that for small *Pr* number fluid $Nu \sim Pr^{2/7}$.

For a fluid layer with external heating, i.e. heated from below and cooled from the top, heat transfer coefficients through the layer can be determined as follows.

The Globe-Dropkin (1959) correlation for a fluid layer heated from below and cooled from the top:

$$Nu = 0.069 \cdot Ra^{0.333} \mathrm{Pr}^{0.074} \qquad (2.13)$$
$$3\text{x}10^5 < Ra < 7\text{x}10^9; \qquad 0.02 < Pr < 8750$$

The O'Toole-Silveston (1961) correlation for a fluid layer with high *Ra* number:

$$Nu = 0.104\ Ra^{0.305}\ \mathrm{Pr}^{0.084} \qquad (2.14)$$

Cioni correlation (1997):

$$Nu = 0.25 \cdot (Ra\ \mathrm{Pr})^{2/7} \qquad (2.15)$$
$$\text{For } 10^6 < Ra < 10^9; \quad Pr < 0.3$$

For an isothermal vertical plate, the Churchill-Chu (1975) correlation for any *Pr* and *Ra* number less than 10^{12}:

$$Nu_{side}^{1/2} = 0.825 + \frac{0.387\ Ra^{1/6}}{\left[1 + (0.492 / \mathrm{Pr})^{9/16}\right]^{8/27}} \qquad (2.16)$$

Eckert-type correlation (1950) for boundary layer model heat transfer along an inclined cooled surface:

$$Nu_{side}^{local} = 0.508\ \mathrm{Pr}^{1/4}\left(\frac{20}{21} + \mathrm{Pr}\right)^{-1/4} Ra_y^{1/4} \qquad (2.17)$$

It should be noted that most of the correlations describe surface average heat transfer coefficients. The profile of heat transfer coefficient through a boundary layer developed along an inclined cooled wall can be described by expression (2.17).

2.3. Formulation of tasks of the thesis work

Based on the objectives given in Section 1.4 and findings from the literature review summarized above, the following tasks are formulated for the thesis work:

- Development of an approach to efficient use of the CFD methods for the plant safety analysis during the severe accident progression in a Swedish BWR;
- Performing CFD simulations of melt pool heat transfer in specific geometry of BWR lower plenum to obtain insights in to flow physics, and necessary data of melt pool heat transfer for validation purpose;
- Based on the insights gained from CFD study, to develop an accident analysis model for prediction of both integral and locally distributed thermal loads of a homogeneous melt pool form in a BWR lower plenum with sufficient accuracy; Extension of the accident analysis model to simulation of phase change problem for both eutectic and non-eutectic mixtures; Performing validation of the developed accident analysis models;
- Development and validation of an accident analysis model for simulation of metal layer heat transfer, Extension of the model to simulation of transient phase change for both eutectic and non-eutectic binary mixtures;
- Application of the developed and validated accident analysis models to simulations of melt pool heat transfer (homogeneous and stratified melt pools), determination of thermal loads on the reactor internal structures (CRGTs) and the vessel wall;
- Evaluation of CRGT cooling efficiency under steady state and transient thermal loads from a homogeneous melt pool, or a stratified melt pool.

Chapter 3: Computational fluid dynamics for nuclear reactor safety

3.1. An approach to efficient use of CFD for reactor safety analysis

The high-resolution CFD method is a uniquely capable tool to gain the insights into flow physics and to reveal and examine local fluid flow and heat transfer effects. However, the CFD method is not feasible for solution of a majority of nuclear reactor safety tasks, such as accident analysis. In contrast, simplified models which are more suitable for analysis of long transient processes often lack the capability to details, including local heat transfer effects. Consequently, the use of the simplified models limits the predictive capability of safety analysis tools, and as a rule necessitates application of large (and largely unquantified) safety margins to compensate for the impact of modeling assumptions in simplified models.

In the present work, an approach proposed and adopted aimed at the efficient use of the modern CFD tools for the plant safety analysis is demonstrated in the context of a severe accident progression in a BWR lower head. The developed approach which is described in Figure 3.1 consists of five steps:

(i) Analysis and decomposition of a severe accident problem into a set of separate-effect phenomena;

(ii) Validation of the CFD models on relevant separate-effect experiments for the reactor prototypical ranges of governing parameters;

(iii) Development of effective models and closures on the base of physical insights gained from relevant experiments and CFD simulations;

(iv) Using data from the integral experiments and CFD simulations performed under reactor prototypic conditions for validation of the effective model with quantification of uncertainty in the prediction results;

(v) Application of the computationally-effective model to simulate and analyze the severe accident transient under consideration, including sensitivity and uncertainty analysis.

In the first step (Step I), based on the experience in analysis of melt pool heat transfer, the governing physical phenomena are identified. An analysis is performed with the aim to recognizing the potential heat transfer local effects which may affect significantly on melt pool heat transfer and thermal loadings. The potential effects are then examined by a validated CFD method (the next section). For a BWR with CRGT cooling, in case of melt pool formation in the lower plenum, the potential important effects can be:

- Heat transfer along the CRGT cooled walls;
- Flow impingement on the vessel wall in the vicinity of CRGTs and localized enhancement of heat transfer due to corium *Pr* number;

- Crust formation on the vessel and CRGT walls.

In the second step (Step II), an appropriate CFD method is selected. In the present work, the Implicit LES (ILES) is used (the ILES is introduced in the next section). The ILES is validated against experimental data, for both averaged and distributed experimental data. The validated CFD method is used for simulations of melt pool heat transfer, in specific BWR geometries of interest. The unit volume which is a rectangular cavity full of corium surrounded a CRGT is selected as specific geometry for the BWR lower plenum. The height of a unit volume is varying depending on the melt pool height. The CFD generated data for the unit volume are used for validation of accident analysis models afterward.

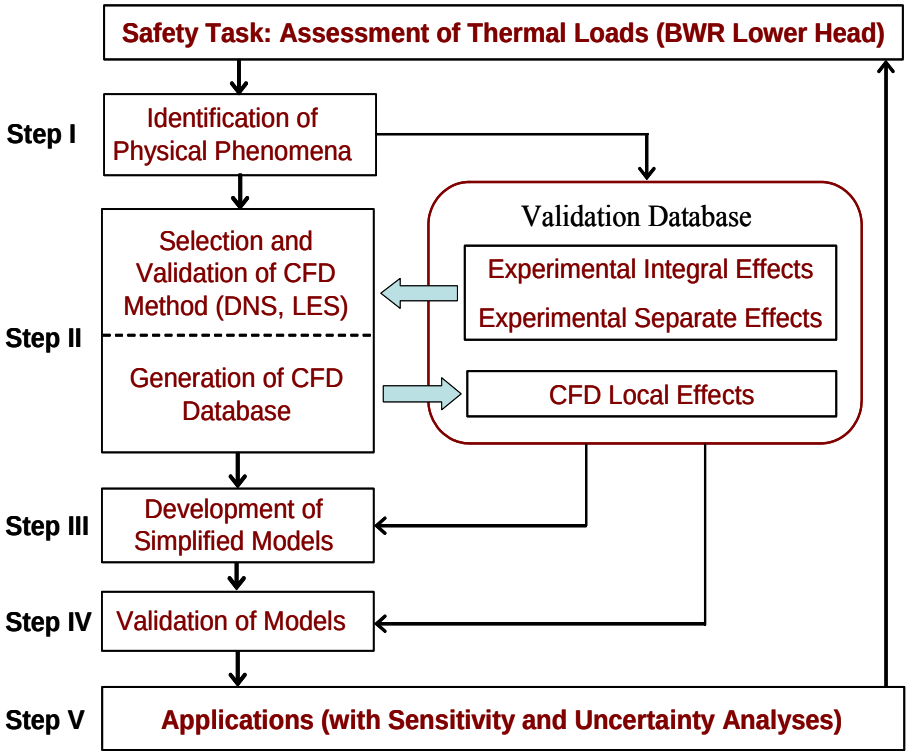

Figure 3.1: A framework for development, validation and application of analysis methods for core melt pool heat transfer in a BWR lower head.

In the third step (Step III), the accident analysis effective models are developed based on the insights gained from the CFD study. The accident analysis models are the Effective Convectivity Model (ECM) and the Phase-change ECM (PECM). Detailed descriptions of the ECM and PECM are available in Chapter 4.

The ECM and PECM are validated using a dual-tier approach, i.e. validated against both experimental data and the CFD generated data, for the whole spectrum of governing physical phenomena involved in melt pool heat transfer, with a wide range of geometries. Validation of the ECM/PECM is the fourth step (Step IV) of the method (Figure 3.1) and presented in Chapter 5.

In the final step (Step V), the ECM and PECM are applied to reactor scale simulations. The local heat transfer effects which were revealed and quantified by CFD simulations are implemented in the PECM, and the influence of the local effects on the thermal loads to the vessel wall and CRGTs is quantified based on uncertainty and sensitivity analyses. Applications of the ECM/PECM are presented in Chapter 6.

3.2. CFD study of heat transfer progresses in a LWR lower head

3.2.1. The CFD method

Computational fluid dynamics (CFD) is one of the branches of fluid mechanics that uses numerical methods and algorithms to solve and analyze problems that involve fluid flows. The fluid flow generally can be described by continuity equation, momentum equation (Navier-Stokes equations) and energy equation.

The problems rise when dealing with turbulent characteristics of the flow. The turbulent flow produces fluid interaction over a large range of length scales. This problem means that it is required that for the turbulent flow regime calculations must attempt to take this into account by modifying the Navier-Stokes equations and using turbulence models to model the Reynolds stress tensor $\rho\overline{u_i u_j}$. The most popular turbulence models are k-ε and k-ω models. However, in many cases, for instance, the flow of an internally heated volume in large geometry, these models fail to predict heat transfer characteristics of the turbulent natural convection flow (Dinh and Nourgaliev, 1997).

The direct numerical simulation (DNS) is a method in computational fluid dynamics in which the Navier-Stokes equations are numerically solved without any turbulence model. This means that the whole range of spatial and temporal scales of the turbulence must be resolved. All the spatial scales of the turbulence must be resolved in the computational mesh, from the smallest dissipative scales (Kolmogorov microscales), up to the integral scale L, associated with the motions containing most of the kinetic energy. DNS captures all of the relevant scales of turbulent motion, so no model is needed for the smallest scales. However, this approach is extremely expensive, if not intractable, for complex problems on modern computing machines. Hence there is a need for models to represent the smallest scales of fluid motion.

Large Eddy Simulation (LES) is a technique in which the smaller eddies are filtered and are modeled using a sub-grid scale model, while the larger energy-carrying eddies are resolved. Thus, in LES the large scale motions of the flow are calculated, while the effect of the smaller universal scales (the so called sub-grid scales) are modeled using a Sub-Grid Scale (SGS) model. This method generally requires a more refined mesh than a Reynolds-Averaged Navier-Stokes Equations (RANS) model, but a far coarser mesh than a DNS solution.

One of the LES methods is called Implicit LES (ILES), or “no model” LES, which is a method for modeling high Reynolds’ number flows that combine computational efficiency and ease of implementation with predictive calculations and flexible

application (Margolin et al., 2006). ILES involves solving the Navier-Stokes equations using high-resolution algorithms, where the time solution does not have maximum and minimum values. In ILES, the SGS flow physics is provided by intrinsic, nonlinear, high-frequency filters built into the discretization and implicit SGS models. The main idea in ILES is that the numerical diffusion in an appropriately constructed numerical scheme plays the role of sub-grid scale mixing, so that no additional sub-grid scale treatment is required. An analysis of past works as well as a review of recent advances in turbulence modeling and simulation revealed that an empirical selection of numerical schemes of ILES method for turbulent natural convection in internally-heated liquid pools has a root in Monotonically Integrated LES (or MILES) method (Boris et al, 1992).

Numerical simulations for different unstably stratified thermal flows using the ILES method showed that the method works quite well in predicting mixing and heat transfer of natural convection in volumetrically heated liquid pools and for transient cool-down liquid pools (Nourgaliev et al., 1997b). Applications of the ILES to simulation of turbulent natural convection heat transfer in an internally heated volume with different Rayleigh numbers show that with increasing of grid resolution, the predicted heat transfer coefficient is increased and reaches its stable value at a certain fine-enough grid cell size. Further increase of the grid cell size does not significantly affect the predicted heat transfer coefficient (Figure 3.2).

The ILES method is validated against experimental data. The predicted by ILES heat transfer coefficients are compared with the experimental data, for both averaged value and spatial distribution (the local heat transfer coefficient). Validation of the ILES method is presented in the next subsection.

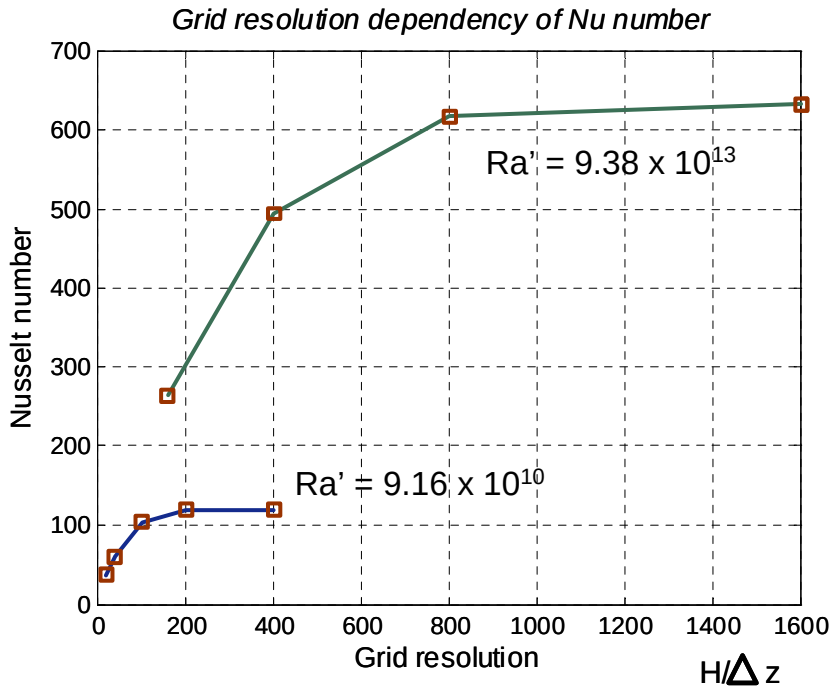

Figure 3.2: Grid resolution dependence of heat transfer coefficients.

3.2.2. Validation of the CFD method

CFD ILES method is validated against heat transfer experiments with natural convection in an internally heated volume, and with Rayleigh-Benard convection in a fluid layer heated from below and cooled from the top. Table III.1 summaries the experiments used for CFD method validation. Predicted by the CFD ILES average and local heat transfer coefficients were compared with experimental data.

Table III.1: Validation matrix for the CFD ILES method

Fluid type	**Experimental data**	**Rayleigh number**	**Predicted parameters**
Internally heated fluid volume (turbulent natural convection)	Kulacki-Emara correlation (1977)	10^8 - 10^{14} (internal)	Average upward Nusselt number (Appendix A)
	Steinberner-Reineke experiment (1978)	3.52×10^{13} (internal)	Energy splitting (average upward, sideward and downward heat transfer coefficients)
			Local sideward Nusselt number (along vertical walls)
Metal layer (Rayleigh-Benard convection)	MELAD B1 experiment (Theofanous et al., 1994)	1.5×10^9 (external)	Average upward heat transfer coefficient
	Transient Gau-Viskanta experiment (1985)	$< 1.2 \times 10^6$ (external)	Crust thickness evolution (Appendix E)

a) Internally heated volume

CFD ILES upward heat transfer coefficients (*Ra'* in the range of 10^8-10^{14}) against Kulacki-Emara correlation are presented in Appendix A. The CFD predicted heat transfer coefficients are well fitted in 15% margins of the Kulacki-Emara correlation.

The CFD ILES method was also used to predict Steinberner-Reineke heat transfer experiment (1978). Steinberner and Reineke experiment was performed in a rectangular cavity with sizes of (0.8m x 0.8m x 0.035m). The test fluid was water in which the volumetric heat sources were simulated by Joulean heating. A set of heat transfer coefficient correlations was produced and the local heat transfer coefficient along the vertical wall was reported.

Table III.2 reports the CFD predicted upward, sideward and downward heat fluxes compared with those of the analytical model based on the Steinberner-Reineke directional correlations. The upward and sideward heat fluxes are well agreed, the downward heat fluxes are in the acceptable range, although they are slightly deviated. The CFD method not only well predicts the average heat fluxes, the method is also capable of predicting

the sideward heat transfer coefficient distribution along the vertical cooled wall (Figure 3.3).

Table III.2: CFD predicted and experimental heat transfer coefficients in rectangular cavity with all walls cooled ($Ra' = 3.52x10^{13}$) (Tran and Dinh, 2007a)

Prediction methods	q_{up}, **W/m^2**	q_{side}, **W/m^2**	q_{down}, **W/m^2**
CFD simulation	1045	599	41
Analytical model based on Steinberner-Reineke correlations (1978)	1026	659	55

Results of CFD simulations show that the CFD ILES method well predicts heat transfer coefficients, both average value and spatial distribution profile. The deviation associated with the CFD method predictability (< 15%) can be evaluated less than experimental errors. Thus the CFD ILES method can be used for examining turbulent natural convection and gaining insights into flow physics.

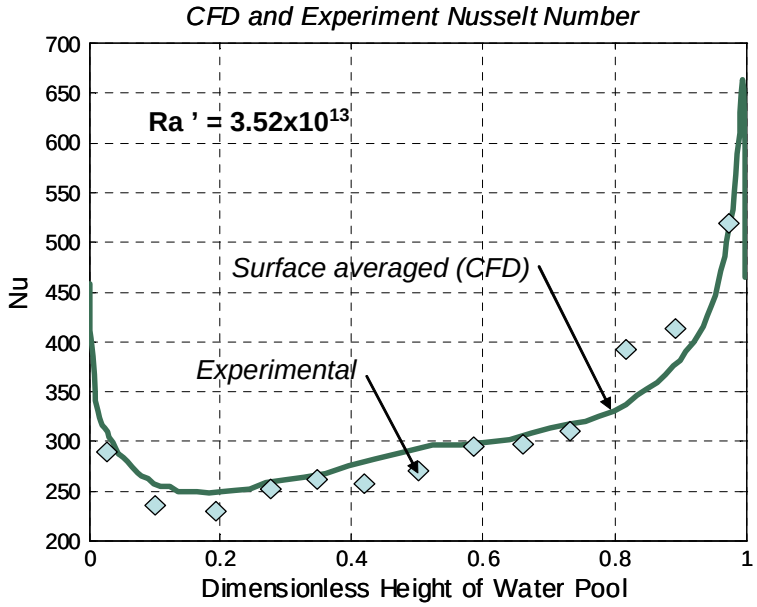

Figure 3.3: CFD predictions and Steinberner-Reineke experimental heat transfer coefficients.

b) Molten metal layer heat transfer

One experiment with Rayleigh-Benard convection has been selected for validation of CFD ILES method. That is MELAD B1 experiment (Theofanous et al., 1994). In MELAD B1 experiment, a rectangular cavity with sizes of (50 cm x 10 cm x 10 cm) was filled by water. The lower boundary of the cavity was imposed a heat flux of 8.58 kW/m^2, while the upper boundary was kept under constant temperature (3.9 ^{o}C). Temperatures of

the lower plate and bulk fluid were measured at a steady-state condition, and the upward heat transfer coefficient was calculated.

Table III.3: CFD simulation and MELAD B1 experiment data

Methods	Bottom plate temperature (^{o}C)	Bulk temperature (^{o}C)	Upward heat transfer coefficient
MELAD B1 experiment	31.9	21.8	46.2
CFD ILES	36.4	20.7	40.2

The CFD ILES is used to simulate MELAD B1 experiment. For Rayleigh-Benard convection in a molten fluid layer, the CFD ILES is capable of predicting the heat transfer coefficient (Table III.3).

3.2.3. CFD study of the effect of molten corium Prandtl number

As described in Figure 3.1, the CFD study belongs to the second step of the proposed approach. The ILES method is applied to simulation of melt pool heat transfer in a unit volume with different heights. The fluid property is chosen to be similar to the property of molten corium, and the heat generation rate in the unit volume is selected as the decay heat rate in few hours into accident initiation (about 1 MW/m^3). In this subsection, we present results of the CFD simulations and the insights obtained from the CFD study.

CFD simulations of melt pool heat transfer in unit volume geometry bounded by the top, CRGT and bottom cooled walls (isothermal boundary conditions), for different pool heights show that predicted upward and sideward heat fluxes are well agreed with those of the analytical model (Figure 3.4). The analytical model is a correlation-based method for calculation of energy splitting in an enveloped volume cooled at boundaries (Appendix B). The CFD simulation results also show that the profile of sideward heat flux is consistent with the boundary layer model (Appendix A, Appendix B). However, as it is shown in the figure, the CFD predicted downward heat flux is significantly higher than that of the analytical model. A detailed analysis of the downward heat flux profile shows that the increase in the averaged downward heat flux is related to the local enhancement of heat flux in the vicinity of CRGT. This local enhancement is a result of impingement of the descending flow along the cooled CRGT wall. Additional CFD simulations for fluids with different Prandtl number confirm that the observed phenomenon is attributed for the corium melt which is characterized by low Prandtl number (Figure 3.5). This low fluid Prandtl number effect was previously studied by Nourgaliev et al. (1997b). For a higher *Pr* number fluid (e.g. *Pr* = 7), the effect is diminished.

It is worth noting that the heat flux is locally enhanced in the vicinity of the CRGT. In the peripheral area, the CFD predicted heat flux value is much lower, and consistent with that of the analytical model (see Appendix B). For a higher *Pr* number fluid (e.g. *Pr* = 7), the average CFD predicted heat flux value is slightly lower than analytical (Figure 3.5).

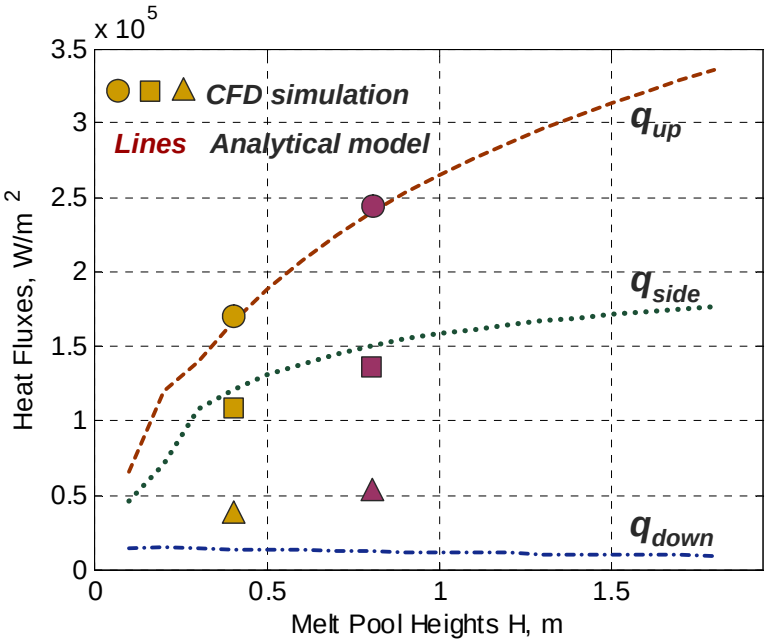

Figure 3.4: Analytical model and CFD simulation energy splitting.

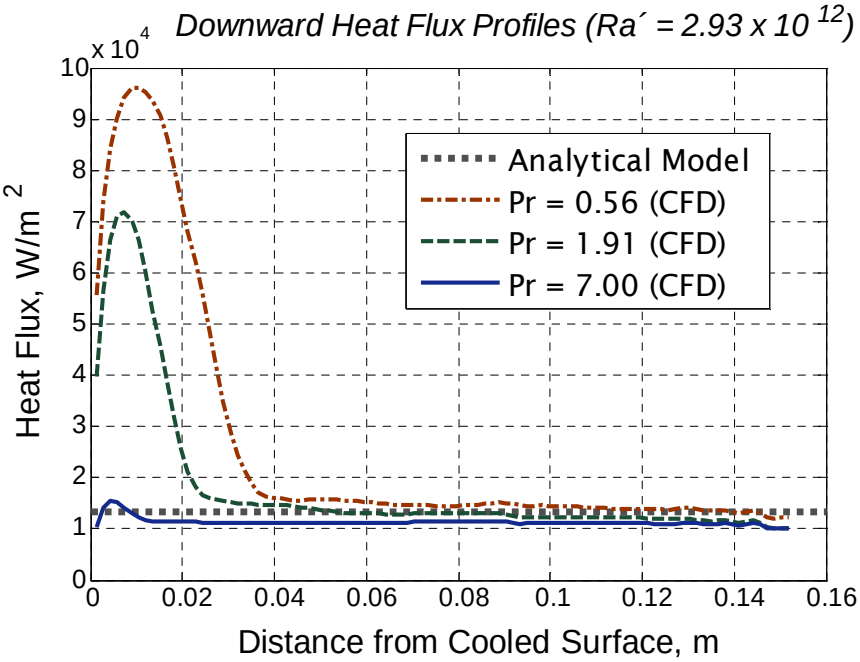

Figure 3.5: CFD predicted downward heat flux profiles for different Prandtl number.

3.3. Uncertainty and sensitivity analysis

The governing phenomena of the late phase melt progression involving a porous debris bed, molten pool and cavity formation still have many uncertainties and are not fully understood due to high temperatures, thermal and chemical interactions of multi-component and multi-phase materials, melting and freezing processes with different geometrical configurations. Moreover, the properties of molten core materials formed in the core region as well as the types and thermal states of the core structures involved, may influence the extent and timing of core melting and the melt progression in the core region, determining the amount and relocation paths of the melt that may be released into the reactor lower plenum. Finally, the arrival conditions of the core material at the lower plenum are also affected by thermal behavior of the molten core material when it passes through the core support plates. Uncertainty of the in-vessel melt progression eventually results in property and mass of the relocated materials in the lower plenum.

Generally, the assessment of uncertainty in simulation results follows the best practice guidelines proposed in NEA/CSNI/R(2007)5 report (Mahaffy et al., 2007). The scenario and phenomenological uncertainty/sensitivity analysis is based on the Code Scaling, Applicability and Uncertainty (CSAU) evaluation methodology (Boyack et al., 1990; Wilson et al., 1990; Wulff et al., 1990). The uncertainty and sensitivity analysis performed in the present work is focused on the melt pool height, and the corium melt property, namely Prandtl number of the homogeneous corium melt.

During the process of melt pool formation, the height of a formed melt pool is changed. It is therefore important to quantify the effect of low *Pr* number fluid on the downward heat flux for different pool's heights. CFD simulations performed for three different values of the pool height (0.3 m; 0.4 m and 0.6 m) show that the enhancement of the downward heat flux is less sensitive to the pool height, and consequently to Rayleigh number (Figure 3.6).

Prandtl number is the control parameter in the heat flux enhancement phenomenon. Clearly, dependent on the accident scenario, the homogeneous corium melt may have different fraction of metallic components. As a consequence, the corium *Pr* number is changed, largely is due to different thermal conductivities of the metallic components and oxidic melt. Calculations of corium *Pr* number based on different fraction of metallic components indicate that corium *Pr* number may vary from the lower bound value of 0.1 to the higher bound value of 0.6. To quantify the effect of low *Pr* number fluid on the downward heat flux, CFD simulations are performed for three different *Pr* number in the range of interest.

Three profiles of the downward heat flux obtained from CFD simulations are presented in Figure 3.7. As it is seen, the local peaked heat flux is lower for the lower bound value of Prandtl number, however, the heat flux is enhanced in a broader region. In the vicinity of the CRGT, the peaked heat flux is about seven times higher than that in the peripheral area for $Pr = 0.56$, while for $Pr = 0.12$, the peaked heat flux is about five times higher than that in the peripheral area. As previously noted the heat flux value in the peripheral area remains unchanged and consistent with that of the analytical model.

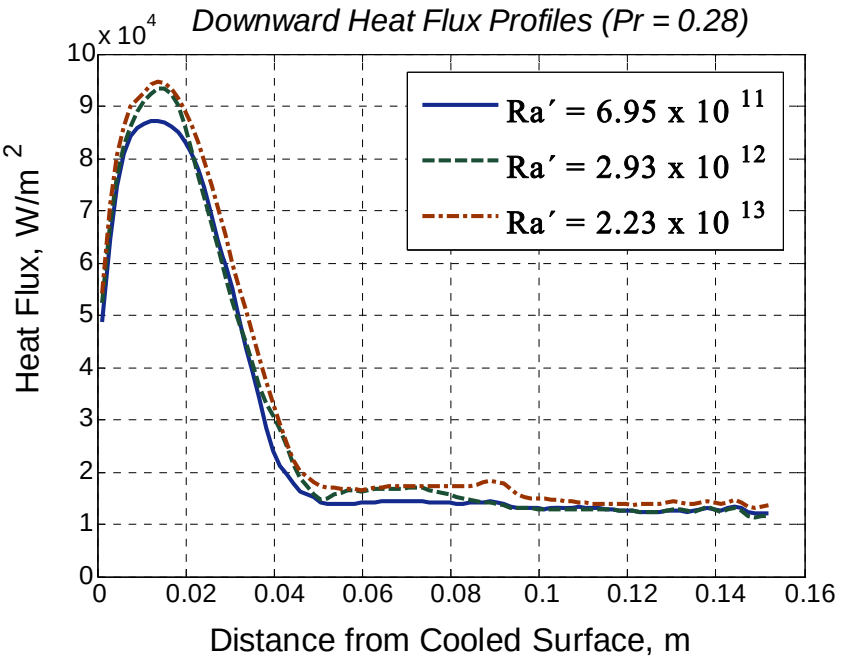

Figure 3.6: CFD predicted downward heat flux profiles for different molten pool heights.

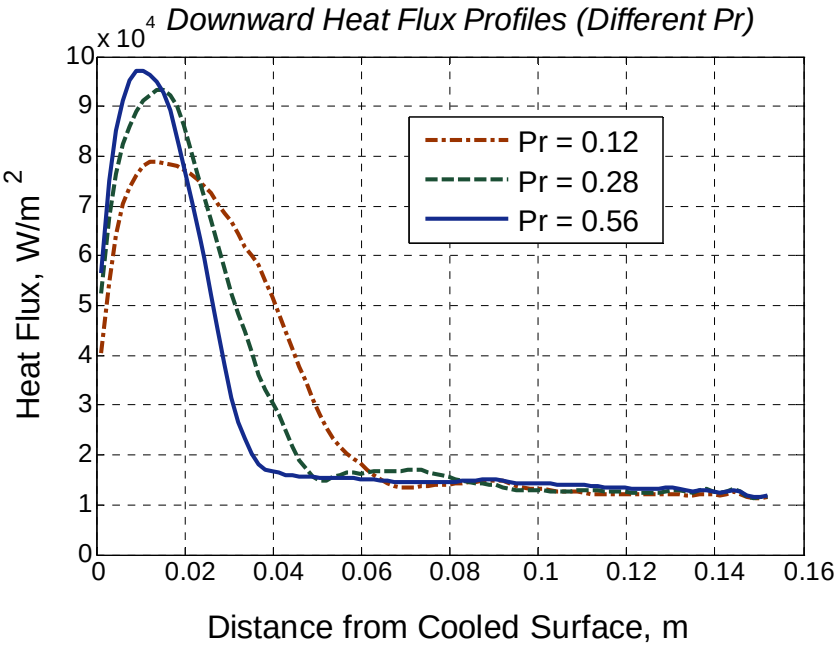

Figure 3.7: Downward heat flux profiles for three different Prandtl number in the range of (0.1 - 0.6).

The two bounding peaked values of the downward heat flux are implemented in the accident analysis model (PECM) and their influence on the transient thermal loads to the BWR vessel walls is quantified using the PECM (Chapter 6).

Chapter 4: The effective convectivity model method

4.1. Development of accident analysis models

The accident analysis models developed in the present work are the Effective Convectivity Model (ECM) and Phase-change ECM (PECM) for both internally heated volumes and molten metal layers (Figure 4.1).

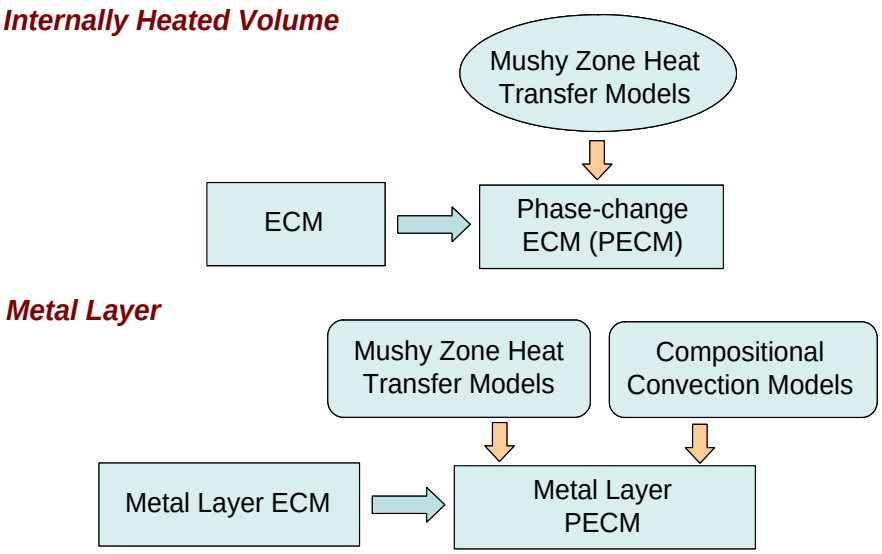

Figure 4.1: Outline of developed models.

For an internally heated volume, the mushy zone heat transfer model is implemented in the PECM platform. For a molten metal layer which is characterized by Rayleigh-Benard convection or mixed natural convection (i.e. Rayleigh-Benard convection in the presence of side cooling), the PECM is augmented by the mushy zone heat transfer model and the compositional convection model. The compositional convection model is implemented in the PECM platform to take into account possible natural convection caused by concentration gradients.

4.2. The ECM for simulation of internally heated fluid volume

A short introduction of the ECM is provided here, more detailed descriptions of the ECM are presented in Appendix B. The main idea of the ECM is to use directional characteristic velocities, instead of instantaneous fluid velocities, to remove the heat to the cooled boundaries while solving the energy conservation equation. The heat transfer characteristic velocities are defined through empirical heat transfer correlations (Nusselt number), thus the ECM is a correlation-based model.

Selection of the directional heat transfer coefficients to be implemented in the ECM is supported by the CFD study. Turbulent natural convection in an internally heated

volume is described by several heat transfer correlations, which although are close in value and trend (Figure 4.2). The CFD study helps to scrutiny the applicability of the selected heat transfer coefficients for implementation in the ECM.

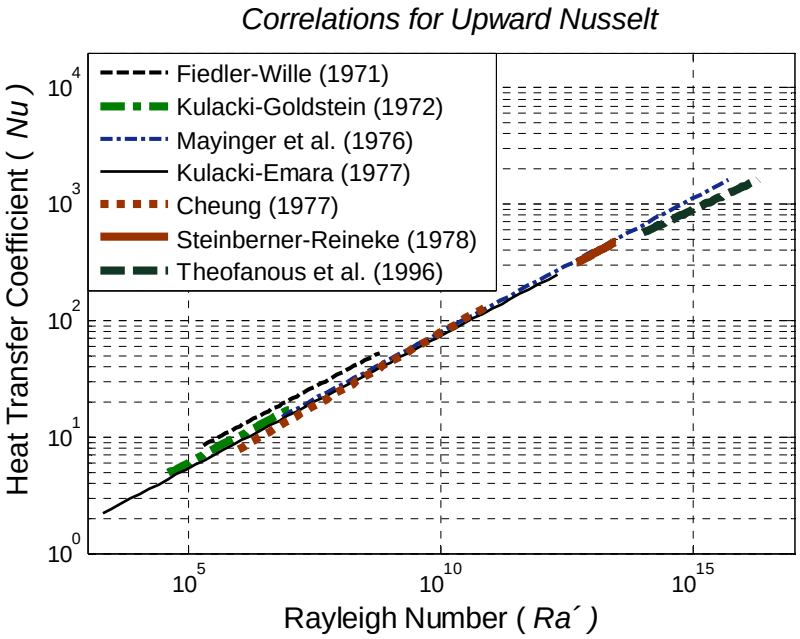

Figure 4.2: Upward heat transfer correlations in a wide range of Rayleigh number.

In the ECM, the average directional Steinberner-Reineke correlations, i.e. the upward, sideward and downward Nusselt number described by Eqs.(2.6-2.9) are used. The profile of the sideward heat transfer coefficient is described by the boundary layer model, i.e. Eq.(2.17) validity of which was confirmed by CFD simulations (Appendix A, Appendix B).

The ECM is implemented in the commercial **Fluent** code (see Appendix B), this allows to take all advantages of a commercial CFD code and use all the available pre- and post processing tools, as well as the advanced tool like the Adaptive Mesh Refinement (AMR) technique.

4.3. Phase-change ECM (PECM) and mushy-zone heat transfer models

The ECM was extended to phase-change problems (PECM) enabling simulations of melt pool formation heat transfer during the long transient accident progression in a LWR lower plenum.

In the PECM, a formulation based on the enthalpy conservation equation is employed, thus the phase change interface can be treated using a fixed grid. The source-based method is used to model the solidification/melting process, assuming that the total enthalpy is a dependent variable along with temperature. The mushy zone is considered

as a fixed columnar zone, and the phase-change material is assumed to be mushy as its temperature falls in the range between the liquidus and solidus temperatures.

The main treatment of the PECM is modeling natural convection in a mushy zone. As natural convection in the bulk fluid is modeled using the heat transfer characteristic velocities (in the ECM), convection in a mushy zone can be modeled using reduced heat transfer characteristic velocities (or so-called mushy characteristic velocities). Therefore, to describe mushy zone heat transfer, the PECM employs the mushy characteristic velocity (U_M) which is a function of characteristic velocity ($U_{x,y,z}$) and liquid fraction (F_{LIQ}):

$$U_M = f\left(U_{x,y,z}, F_{LIQ}\right) \tag{4.1}$$

Liquid fraction dependency of the mushy characteristic velocity is still remained uncertain, depending on the mushy zone characteristics, fluid property and natural convection in the bulk fluid. Three different models of mushy characteristic velocity were implemented and their effects on pool heat transfer were compared. The linear model describing liquid fraction dependency of the mushy characteristic velocity was benchmarked against CFD ILES data. More detailed descriptions of the PECM are presented in Appendix D. Validation of the PECM for an internally heated volume can be found in Chapter 5, Appendix A, Appendix C and Appendix D.

4.4. Metal layer ECM/PECM

The approach adopted for development of metal layer ECM and PECM is similar to that of the ECM/PECM for an internally heated volume, and described in details in the previous section. The metal layer ECM and PECM and their implementation in the **Fluent** code are described in details in Appendix E, here a brief introduction is provided with focus on mushy characteristic velocity models.

The metal layer ECM and PECM are developed for simulation of heat transfer in a metal layer is which heated from below and cooled from the top (and side wall), and characterized by Rayleigh-Benard convection or mixed natural convection. The main purpose of the ECM and PECM is enabling heat transfer simulation of a molten metal layer which may be formed atop an oxidic pool in the reactor lower plenum during a hypothetical severe accident.

The metal layer ECM uses the same concept of effective convectivity which was employed in the ECM for an internally heated volume. The characteristic velocity is used to describe convective heat transfer from the heated lower surface to the top and/or side cooled surfaces. The characteristic velocities are described by empirical heat transfer coefficients. In the present work, the Globe-Dropkin correlation is used for determination of the upward characteristic velocity, and Churchill-Chu correlation incorporated with the boundary layer model [Eq.(2.17)] is used for determination of the sideward characteristic velocity, i.e. along the horizontal direction. The applicability of these correlations was

supported by the CFD study which employed ILES for simulation of molten metal fluid layer heat transfer in specific BWR geometries.

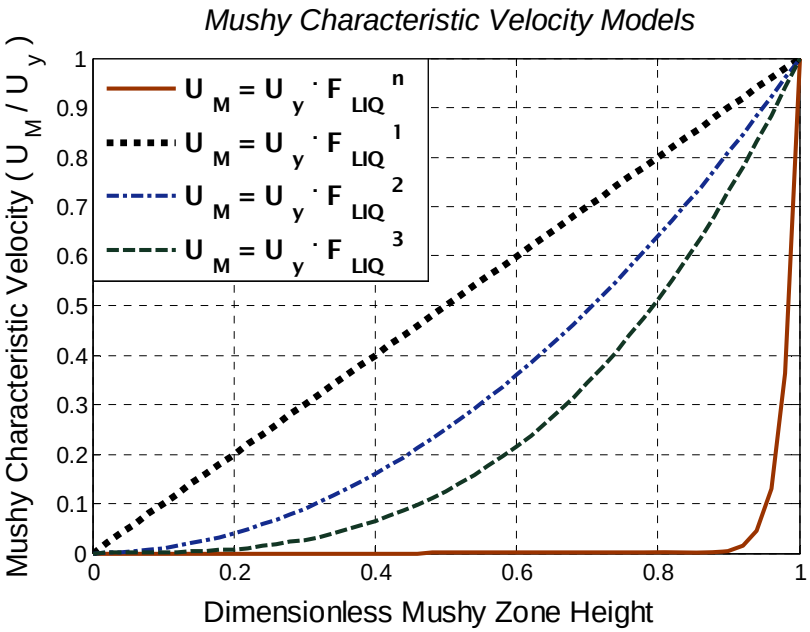

Figure 4.3: Different mushy characteristic velocity models (along the vertical direction).

To describe the transient phase change in a metal layer, the ECM was extended to phase-change problems (the metal layer PECM). The PECM implements different mushy characteristic velocity models (Figure 4.3) to describe convective heat transfer in a mushy zone. For a non-eutectic binary melt, it is possible that natural convection in the bulk fluid is due to not only the thermal gradient but also the compositional gradient (combined convection). Additionally, to take into account compositional convection, the PECM employs the compositional convection models using compositional Rayleigh number (Ra_C) along with the thermal convection Rayleigh number (Ra_T). Thermal Rayleigh number Ra_T is defined as follows (Worster, 1991):

$$Ra_T = \frac{g\beta_T \Delta T H^3}{\alpha \nu} \tag{4.2}$$

where ΔT is defined as $\Delta T = T_\infty - T_E$. Compositional Rayleigh number Ra_C can be determined as:

$$Ra_C = \frac{g\beta_C (r_C \times \Delta C) H^3}{\alpha \nu} \tag{4.3}$$

where ΔC is the concentration difference across the fluid (liquid) layer and r_C is defined as the rejectability coefficient. The presence of the rejectability coefficient in the compositional Rayleigh number expression is explained as follows.

According to the definition, the concentration difference is $\Delta C = C_\infty - C_E$. However, binary mixture solidification experiments (Wettlaufer and Worster, 1997; Trivedi et al., 2001) show that the value of ΔC remains uncertain due to rejectability of the higher concentration (compared with the bulk fluid) solute from a mushy zone to the bulk fluid. For one binary melt, the solute with higher concentration may easily be rejected from the mushy zone, while for another mixture, this higher concentration solute may be stuck in the mushy zone and be solidified. Depending on the mushy zone characteristics, the intensity of natural convection in the both mushy zone and bulk fluid, the fluid property, and the direction and rate of cooling, the rejectability of the solute from a mushy zone may be different. Thus in the present work, different models of rejectability are also examined.

It was found that different models of mushy characteristic velocity (U_M) and different models of compositional convection (r_C) result in different rates of crust formation and mushy zone thicknesses. Results of PECM validation against several experiments with transient phase change are presented in Chapter 5, and Appendix E.

Chapter 5: Validation of the ECM tools

5.1. Validation of the ECM/PECM for an internally heated volume

Validation of the ECM/PECM covers the whole spectrum of governing physical phenomena (Table V.1) involved in melt pool heat transfer, for a wide range of Rayleigh number and different geometries (Table V.2). Table V.2 lists all the experiments used for validation of the ECM/PECM. In Appendix A, ECM and PECM validation results are shown as representative for governing physical phenomena of melt pool heat transfer, while in the Appendix C, ECM/PECM validation is shown to cover various types of geometries of interest. Note that as the dual approach of validation is adopted in the developed method, the ECM/PECM is also validated against CFD-generated data where experimental data are not available.

Table V.1: BWR corium coolability and vessel thermal loading governing phenomena

Number	Physical phenomena	Effect
1	Natural convection (transient)	Integral
2	Natural convection (steady state)	Integral
3	Thermal stratification	Integral
4	Boundary layer development along an inclined cooled surface	Local
5	Impinging flow heat transfer on the lower cooled surface	Local
6	Phase change and crust formation on cooled surfaces	Local

Table V.2: Validation matrix of the ECM/PECM (internally heated volume)

No.	Experimental data and CFD generated data [validated models]	Geometry and BC	*Ra'* number range	Physical phenomena in Table V.1
1	Kulacki-Emara experiment (1977) [ECM]	Fluid layer cooled from top	1.18×10^{10}	1 (Appendix A)
2	Kulacki-Nagle experiment (1975) [ECM]	Fluid layer cooled from top	9.3×10^{7}	1 (Appendix C)
3	Cheung analytical model (1977) [ECM]	Fluid layer cooled from top	10^{9}-10^{11}	2 (Appendix C)
4	Kulacki-Goldstein	Fluid layer cooled	1.6×10^{4}	2, 3

	experiment (1972) [ECM]	from top and bottom	and 6.3×10^5	(Appendix A)
5	Steinberner-Reineke experiment (1978) [ECM]	Rectangular cavity cooled from all walls	3.52×10^{13}	2, 3, 4 (Appendix C)
6	Jahn-Reineke experiment (1974) [ECM]	Semi-circular cavity cooled at boundaries	9.16×10^{10}	2, 3, 4 (Appendix C)
7	CFD ILES data [ECM]	Semi-circular cavity cooled at boundaries	2×10^{11}	2, 3, 4 (Appendix A)
8	CFD ILES data [ECM]	Unit volume cooled from top, CRGT and bottom walls	2.9×10^{12}	2, 3, 4, 5 (Appendix A, Appendix C)
9	ACOPO transient cooldown experiment (Theofanous et al., 1997) [ECM]	Hemispherical pool cooled from top and lower boundary walls	10^{16}-10^{14}	1, 3, 4 (Appendix C)
10	COPO experiment (Kymalainen et al., 1994) [ECM]	Torospherical cavity cooled from top and lower boundary walls	1.24×10^{14} - 1.66×10^{15}	2, 3, 4 (Appendix C)
11	Asfia-Dhir experiment (1996) [ECM]	Hemispherical plenum (bell jar) cooled from top and lower boundary walls	3.03×10^{13} and 7.8×10^{13}	2, 3, 4 (Appendix C)
12	SIMECO eutectic experiment (Sehgal et al., 1998) [PECM]	Semi-circular cavity cooled at top and lower boundaries	8.49×10^{12}	2, 3, 4, 6 (Appendix C)
13	SIMECO non-eutectic experiment (Sehgal et al., 1998) [PECM]	Semi-circular cavity cooled at top and lower boundaries	1.39×10^{13}	2, 3, 4, 6 (Appendix A)
14	LIVE L1 experiment, non-eutectic mixture (Miassoedov et al., 2007) [PECM]	Hemi-spherical plenum cooled at top and lower boundaries	$<1.3 \times 10^{14}$	1, 2, 3, 4, 6 (Appendix C)

In this section, results of the ECM and PECM validation are shown to confirm that the ECM and PECM are capable to predict all important parameters of interest, that is energy splitting, the pool temperature profile (superheat), heat flux profiles along the pool boundaries, and crust thickness (by the PECM). Correct prediction by the ECM/PECM about these parameters ensures reliable prediction of thermal loads from a melt pool to the vessel wall and structures.

Energy splitting predicted by the ECM and Steinberner-Reineke correlations (1978) are reported in Table V.3. It can be seen that the predicted results are in good agreement with the correlations, especially for the upward and sideward coefficients. The downward heat transfer coefficient predicted by the ECM is slightly higher than that calculated by the correlation, however, the deviation is in the acceptable range.

Table V.3: ECM predicted and experimental heat transfer coefficients in rectangular cavity with all walls cooled ($Ra' = 3.52 \times 10^{13}$)

Prediction method	Nu_{up}	Nu_{side}	Nu_{down}
ECM simulation	505.8	288.7	35.8
Correlations (Steinberner-Reineke, 1978)	494.6	318.7	26.9

To compare the temperature profiles, the ECM is used to simulate an enveloped corium melt pool in unit volume geometry for which the CFD simulation (ILES method) was also performed (Section 3.2). The predicted profiles are qualitatively agreed, the difference in pool superheat is of a mere 5 K (Figure 5.1).

Figure 5.1 also exhibited that in the ECM simulation pool, the amount of cold liquid accumulated in the lower region is less than that of the CFD simulation pool. That can be explained that for a low *Pr* number fluid due to descending flow from the boundary layer, the cold liquid is more accumulated in the lower region.

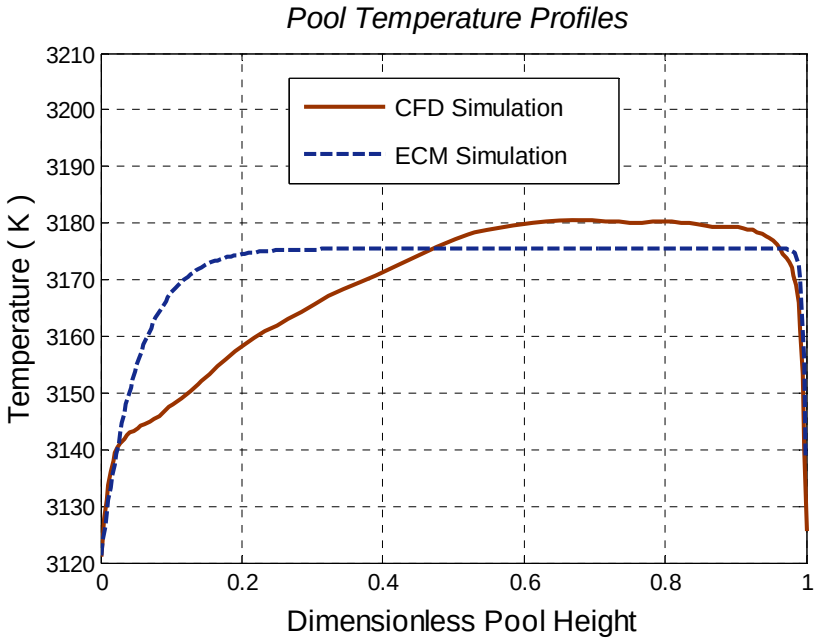

Figure 5.1: Temperature profile in a corium molten pool (CFD vs. PECM simulations).

Agreement of the pool temperatures was also achieved in the PECM and CFD simulations of an internally heated fluid layer cooled from the top in the presence of

phase change (Figure 5.2). Detailed information of these PECM and CFD simulations is reported in Appendix D.

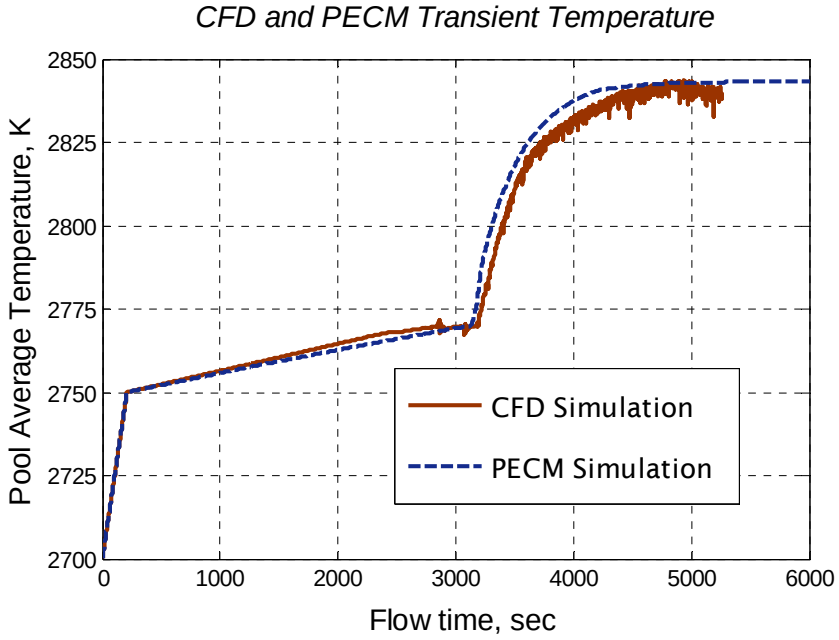

Figure 5.2: CFD and PECM transient melt pool temperatures.

In the experiments performed by Asfia and Dhir (1996), the fluid with heat generation was confined in a bell jar cooled from the top rigid surface and bell jar boundaries. Heat transfer coefficient profiles along the hemispherical plenum (bell jar) cooled wall were reported. Figure 5.3 shows plots of ECM and experimental heat transfer coefficient profiles along the vessel wall boundary. Apparently the profiles are well agreed. However, the peaked locations of the heat transfer coefficients predicted by the ECM are not coincided with the experimental.

The PECM heat flux profile was obtained in one simulation of the SIMECO experiment (Sehgal et al, 1998). In this experiment, eutectic KNO_3-$NaNO_3$ melt contained in a semicircular cavity was heated by electric coils while the cavity boundaries were kept at temperature lower than the melt solidus temperature. More detailed information of the experiment and PECM simulation results are presented in Appendix D. Figure 5.4 shows plots of heat flux profiles obtained in the experiment and PECM simulation. They are well corresponded, although in the lower region of the melt pool, the PECM heat flux is higher than the experimental. This effect can be explained by larger amount of cold liquid accumulated in the pool's lower region, this is consistent with the result discussed previously (Figure 5.1).

The PECM was used to predict the LIVE L1 experiment (Miassoedov et al., 2007). Description of the experiment and results of the PECM simulation are presented in Appendix C. Although the PECM crust thickness in the pool's lower part is less than

experimental (due to less amount of cold liquid accumulated), the results of the PECM simulation shows that the PECM is capable of predicting the crust thickness (Figure 5.5).

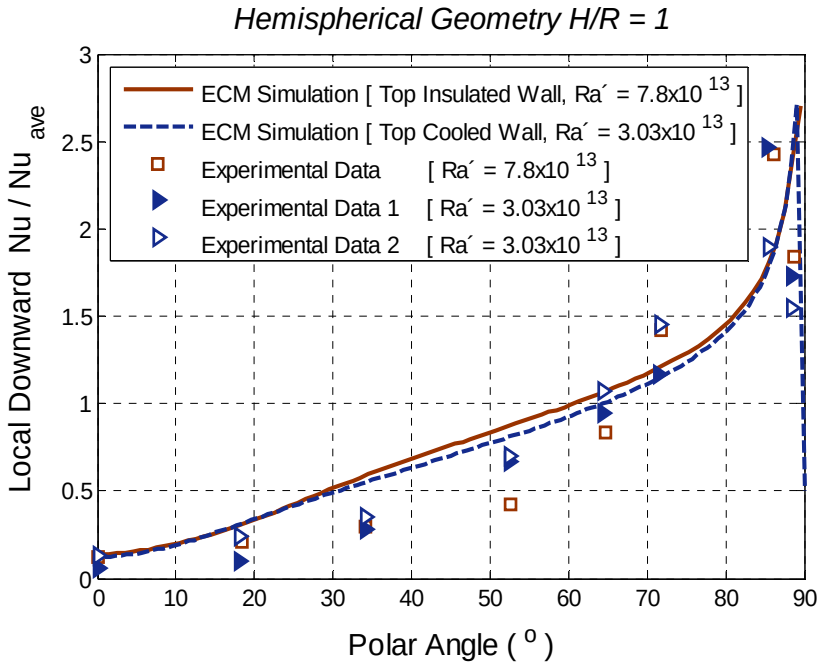

Figure 5.3: Heat flux distribution along the lower cooled wall (hemi-spherical cavity).

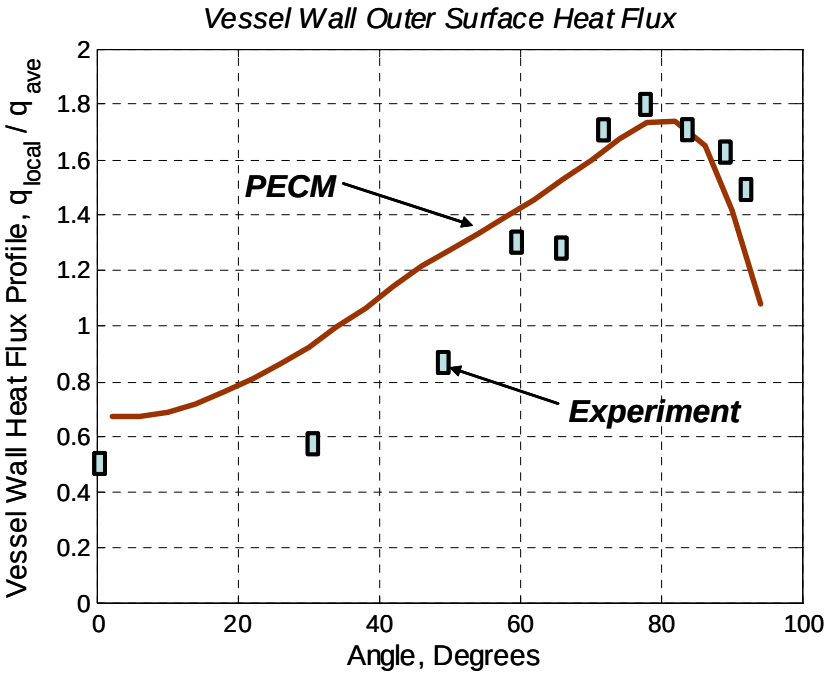

Figure 5.4: Heat flux profiles along the vessel wall surfaces (semi-circular cavity, SIMECO eutectic mixture experiment).

A conclusion which can be made is that for an internally heated volume characterized by turbulent natural convection, the ECM and PECM can be used to predict the energy splitting, the pool's temperature profiles and heat flux distributions along cooled walls. The ECM and PECM are suitable tools for prediction of thermal loads from a melt pool to the reactor vessel wall and structures.

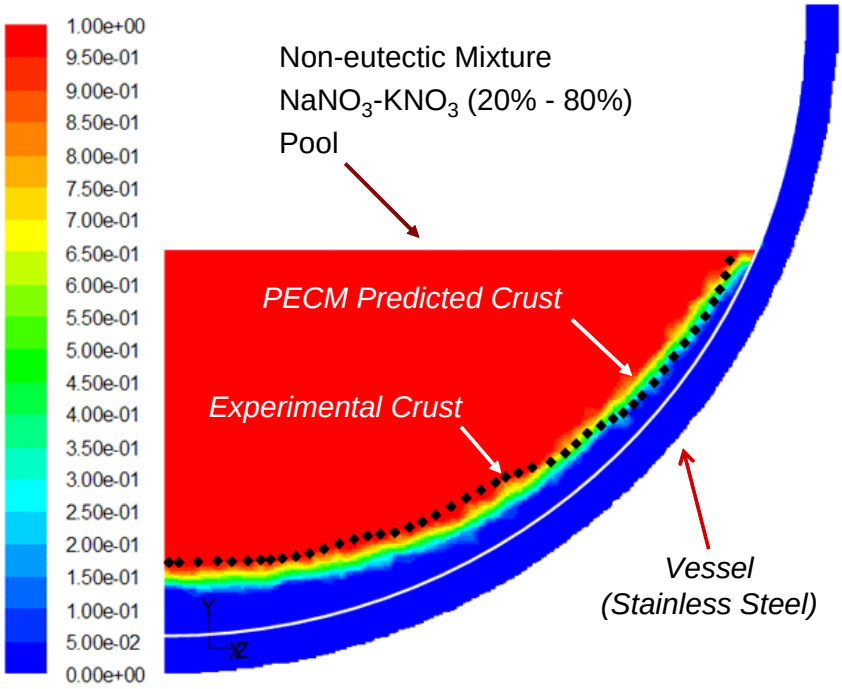

Figure 5.5: Crust thickness along the lower cooled boundary (LIVE L1 non-eutectic mixture experiment).

5.2. Metal layer ECM/PECM validation

The metal layer ECM and PECM are validated against various experiments. Validation of the metal layer ECM/PECM covers a wide range of governing physical phenomena (Table V.4) of fluid layer heat transfer: Rayleigh-Benard convection, mixed natural convection, boundary layer development along an inclined cooled wall, transient phase change, and crust formation for both eutectic and non-eutectic binary mixtures.

Table V.4: Physical phenomena involved in molten metal layer heat transfer

Number	Physical phenomena	Effect
1	Rayleigh-Benard natural convection	Integral
2	Mixed natural convection	Integral
3	Boundary layer development along an inclined cooled surface	Local
4	Transient phase change and crust formation on cooled surfaces	Local

Table V.5 shows the list of experiments used for validation of the metal layer ECM and PECM. Most of the experiments and ECM/PECM simulation results are described in Appendix E. In this section we present some results of the PECM simulations showing different crust thickness evolutions with different models of mushy characteristic velocity and compositional convection.

Table V.5: Validation matrix of the metal layer ECM/PECM

No.	**Experimental data and CFD generated data [validated models]**	**Rayleigh number range**	**Physical phenomena** in Table V.4
1	DNS data (Mohamad and Viskanta, 1993) [metal layer ECM]	$2.2\text{x}10^{7}$	1
2	DNS data (Otic et al., 2005) [metal layer ECM]	$6.3\text{x}10^{5}$	1
3	MELAD A1 experiment (Theofanous et al., 1994) [metal layer ECM]	$1.5\text{x}10^{9}$	2
4	CFD ILES data for a unit volume [metal layer ECM]	$1.46\text{x}10^{9}$	2, 3
5	Gau-Viskanta eutectic binary mixture experiment (1985) [metal layer PECM]	$< 1.2\text{x}10^{6}$	4
6	Kumar et al. non-eutectic binary mixture experiment (2003) [metal layer PECM]	$< 2.05\text{x}10^{5}$ (Ra_T)	4
7	Cao-Poulikakos non-eutectic binary mixture experiment (1990) [metal layer PECM]	$< 3.82\text{x}10^{8}$ (Ra_T)	4

The metal layer PECM with different models of mushy characteristic velocity and compositional convection is used to simulate two experiments of non-eutectic binary mixture solidification: the first is Kumar et al. experiment (2003), and the second is Cao and Poulikakos experiment (1990). The Globe-Dropkin correlation is used in the PECM.

In the first experiment, aqueous ammonium chloride (14.7% NH_4Cl-H_2O) in a rectangular cavity of (160 mm x 90 mm x 17 mm) was cooled from the top plate gradually to temperature below the melt solidus temperature (also 257.75 K). The crust thickness (solid crust and mushy thickness) was recorded during the experiment.

In the second experiment, 5% aqueous ammonium chloride in a rectangular cavity with sizes of (48.3 cm x 25.4 cm x 12.7 cm) is cooled from the top surface. Temperature of the top surface was gradually decreased to a value below the solidus temperature (257.75 K according to the phase diagram of mixture). Evolutions of crust thickness (solid and mushy) were recorded.

Figure 5.6 delineates crust thickness (total thickness of solid and mushy zone) evolution of the first experiment (Kumar et al, 2003), and PECM predicted crust evolutions for two different implemented mushy characteristic velocity models (under the same rejectability coefficient r_C, see Section 4.4. The predicted crust thickness evolutions are well agreed with the experimental data. However, different models of U_M result in slightly different crust thickness evolutions.

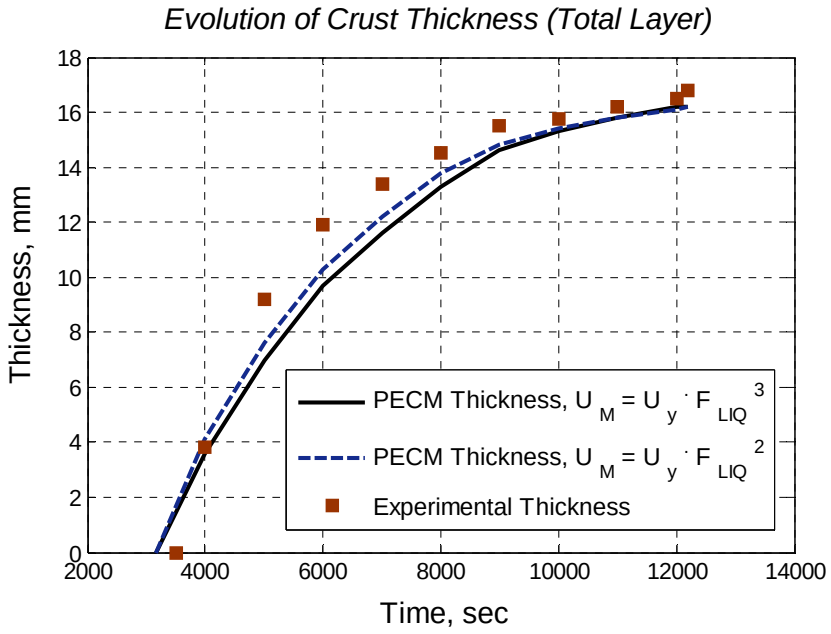

Figure 5.6: Evolution of PECM and experiment crust thickness for two mushy velocity models (combined convection with $r_C = 1$).

An analysis of mushy zone liquid fraction obtained in the PECM simulations of the Cao and Poulikakos experiment (1990) shows that different mushy characteristic velocity models implemented in the PECM result in significantly different liquid fraction curves across the mushy zone (Figure 5.7). With no mushy zone characteristic velocity (model $U_M = U_y \cdot F_{LIQ}^n$, $n \to \infty$), liquid fraction is linearly changed across the mushy zone (the lower curve). This reflects a realistic mushy zone where no convection is possible inside. The linear model ($U_M = U_y \cdot F_{LIQ}^1$) predicts more intensive convection, more liquid fraction is presented penetrating further into the mushy zone (the higher line).

To examine the effect of the rejectability model describing compositional convection, PECM simulations are performed for different r_C under the same mushy characteristic velocity model. Results of PECM simulations indicate that the rejectability model has a certain influence on the crust formation, especially the mushy layer thickness (Figure 5.8). Generally, convective heat transfer in a mushy zone and rejectability of one solute from the mushy zone to the bulk fluid remain highly uncertain. However, with appropriate selection of the mushy characteristic velocity model and rejectability model,

the PECM is capable to predict crust (solid and mushy layers) evolution during transient solidification of a non-eutectic binary melt (Figure 5.9).

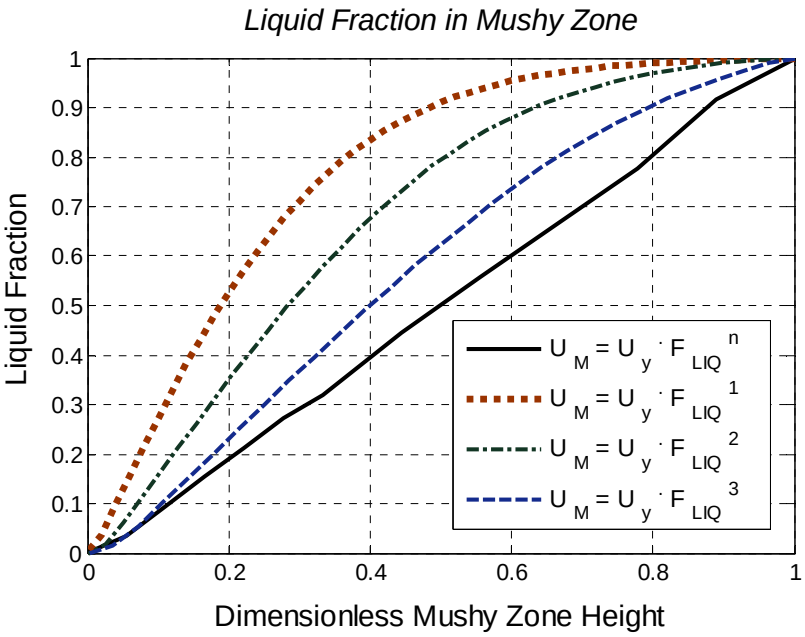

Figure 5.7: Resulted liquid fraction profiles across the mushy zone from different mushy velocity models (PECM simulation of Cao and Poulikakos experiment).

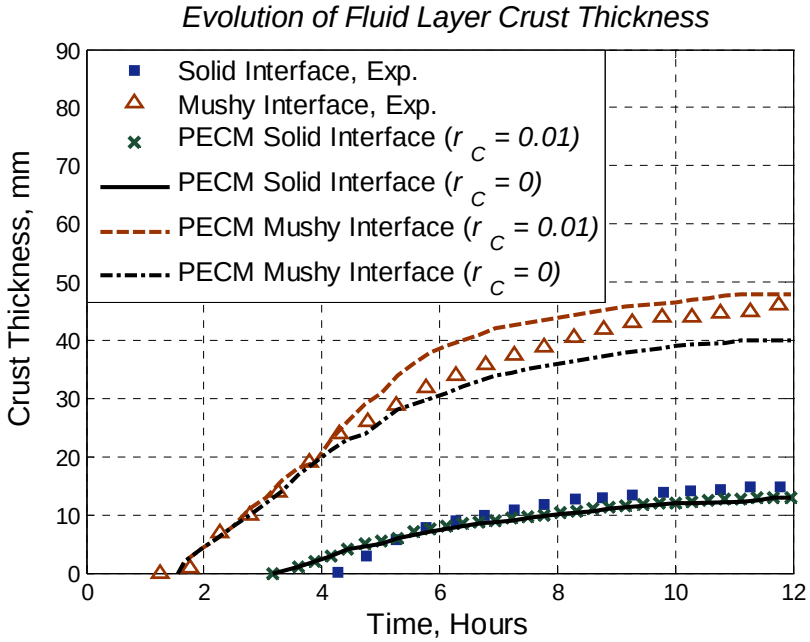

Figure 5.8: Evolution of PECM and experiment crust thickness for different r_C (mushy velocity model $U_M = U_y \cdot F_{LIQ}^3$).

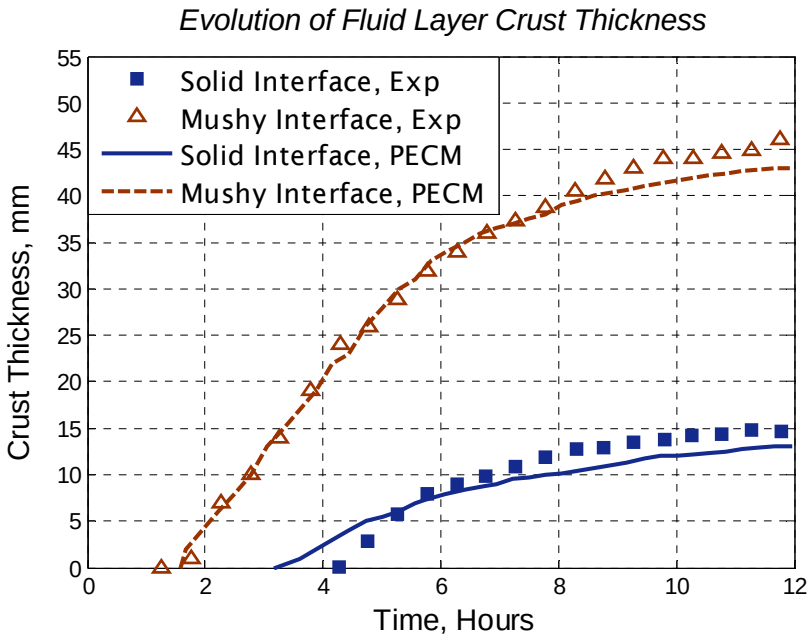

Figure 5.9: Evolution of PECM and experimental crust thickness (solid and mushy), mushy velocity model $U_M = U_y \cdot F_{LIQ}^3$, combined convection, $r_C = 0.07$.

5.3. Evaluation of the ECM and PECM efficiency

Validation results of the ECM and PECM for both internally heated volumes and molten metal layers have shown the capability of the ECM/PECM tools in reliable simulation of steady-state and transient melt pool heat transfer. The predicted results are sufficiently accurate, with less than 15% of errors.

The efficiency of the ECM and PECM can be evaluated comparing the calculation time of the ECM/PECM with that of the CFD method. The efficiency of the ECM and PECM is achieved due to larger time steps and coarser meshes compared to those of the CFD simulation. More importantly, solving only the energy conservation equation without the need to follow instantaneous fluid motion, the PECM requires a much smaller number of iterations to achieve solution convergence in each time step.

Table V.6 reports calculation times of the ECM/PECM simulations and CFD corresponding simulations for the same cases. As it is seen, the ECM/PECM simulation is about 2 orders of magnitude faster than the CFD simulation.

Table V.6: Comparison of ECM/CFD calculation times (Pentium IV ® 3GHz)

No.	Simulation cases	CFD calculation time, hours	ECM/PECM calculation time, hours
1	Unit volume simulation (case 8 in Table V.2)	400	2 (ECM)
2	3D semicircular cavity (Appendix A)	700	2 (ECM)
3	Fluid layer cooled from the top with phase change (Appendix D)	1224	10 (PECM)
4	2D Semicircular cavity cooled at boundaries with phase change (Appendix D)	1560	8 (PECM)
5	Metal layer heated from below and cooled from the top (Appendix E)	120	2 (Metal layer PECM)

Chapter 6: Application of the ECM and PECM

6.1. Homogeneous melt pool heat transfer in a BWR lower head

This section presents results of ECM and PECM melt pool heat transfer simulations performed for specific BWR lower plenum geometries. All simulations were performed with the presence of CRGT cooling, thus predicted thermal loads obtained in these simulations enable evaluation of CRGT cooling efficiency.

Two BWR lower plenum specific geometries are used for ECM/PECM heat transfer simulations. The specific geometries were defined based on the design of a reference ABB-Atom reactor. The first geometry is the unit volume which was defined in Section 3.1. The second geometry is a BWR slice which is a lower plenum segment full of corium and contains 6 CRGTs (Figure 6.1). Note that each CRGT is submerged in the segment only by a half part. For transient simulations with phase change, the slice is connected from below with a segment of the vessel wall.

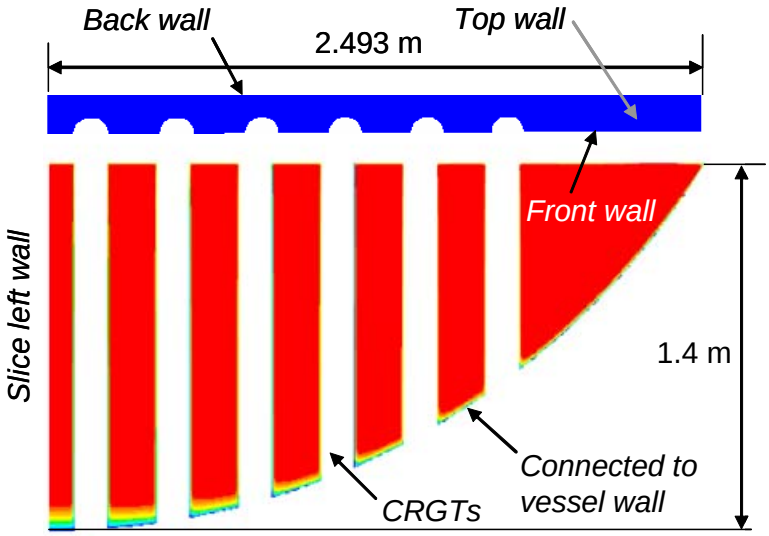

Figure 6.1: 3D slice geometry of the ABB-Atom BWR lower plenum.

Several calculations (by the analytical model) and simulations were performed with the unit volume and BWR slice by the CFD method, ECM and PECM (Table VI.1). Results of the ECM/PECM simulations are partly presented in Appendix A and Appendix C. In this section we focally present those results showing:

- Thermal loads on the CRGTs;
- Thermal loading on the vessel wall with different pool depth;
- The influence of the heat transfer local effect on vessel wall temperature;
- The efficiency of the CRGT cooling.

Table VI.1: Calculation matrix (analytical model, CFD method, ECM and PECM)

No.	Models\ Geometry	Unit volume geometry (with *H* of)				BWR slice geometry (with *H* of)		
		0.4 m	0.6 m	0.7 m	0.8 m	0.7 m	1.0 m	1.4 m
1	Analytical model	Yes	Yes	Yes	Yes	Yes	Yes	Yes
2	CFD ILES method	Yes	Yes	-	Yes	-	-	-
3	ECM	Yes	-	-	Yes	-	Yes	Yes
4	PECM	Yes	-	Yes	-	Yes	Yes	-

In Table VI.2 reports energy splitting in a unit volume (H = 0.4 m). It can be seen that results of the analytical model, CFD and ECM simulations are consistent. The PECM predicts a higher downward heat flux which is due to the presence of crust surrounded a melt pool (Tran and Dinh, 2007b). Basically, the heat flux to CRGT predicted by the CFD method, ECM and PECM tools are comparable or lower than that of the analytical. Results of the PECM simulations with the BWR slice also confirm that the PECM predicted heat fluxes to CRGTs are lower than those of the analytical model. Thus the heat flux calculated by the analytical model can be used for prediction of steam quality in the CRGT (Appendix F) and evaluation of the CRGT cooling efficiency. Note that the peaked value of the predicted CRGT heat flux is double of the average heat flux value. Therefore to define whether the CRGT heat flux exceeds the Critical Heat Flux (CHF) (Appendix F), the average CRGT heat flux should be multiplied by factor of 2.

Table VI.2: Energy splitting in a unit volume (H = 0.4 m)

No.	Models	Upward heat flux (q_{up}), W/m^2	Heat flux to CRGT (q_{CRGT}), W/m^2	Downward heat flux (q_{down}), W/m^2
1	Analytical	166141	120623	13254
2	CFD ILES method (Pr = 0.56)	161631	117641	24288
3	ECM	179900	108796	12263
4	PECM	118339	121419	57217

The PECM is used to simulation of a melt pool in BWR slice geometry. It is assumed that initially a debris bed (or debris cake) is formed in the lower plenum. Due to the decay heat and insufficient cooling, after dryout, the debris bed is heated up and remelted. It is also assumed that the IGTs are plugged and do not affect the pool formation process. The top surface temperature is assumed to be water boiling temperature, due to water injection to the debris bed top surface. Such a scenario is probable if the CRGT cooling has been activated. The water flow rate inside CRGTs is

supposed to be sufficient to avoid dryout on the CRGT internal surfaces, thus isothermal boundary conditions are also applied to the CRGT walls, which are submerged in the debris bed. Heat transfer across the thin gaps between the CRGTs and the vessel wall is by radiation and conduction. A heat flux of $20W/m^2$ is applied to the outer vessel wall surface to represent heat loss across thermal insulation. Prior to the transient simulation, the debris initial condition is 450K.

The simulation shows that in 2.8 hours to the initiation, remelting of the debris bed (cake) is started. First, small melt pools are formed in the midst of CRGTs (Figure 6.2). Afterward they are expanded and connected together to form a large common melt pool in the lower plenum. Maximum temperature of the vessel wall surface is steadily increased. Due to a high heat flux in the uppermost region of the pool, the vessel wall becomes remelted (Figure 6.3). Note that the vessel wall may fail prior to the vessel ablation (melting) due to thermal creep which is assumed to be as temperature of the vessel exceeds 1100 ^oC (Rempe et al, 1993).

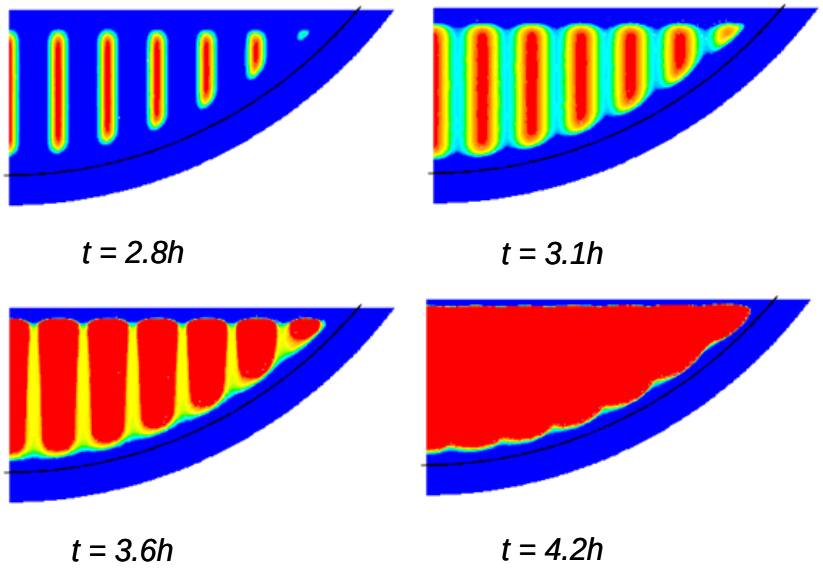

Figure 6.2: Melt pool formation in a BWR lower plenum (BWR slice geometry simulation, H = 1.0 m)

PECM simulations with a lower pool depth (H < 0.7 m) indicate that vessel wall surface temperature is well kept under the creep limit (Figure 6.4). The reason is that due to close contact with the cooled CRGTs, part of the heat from the vessel wall is transferred to CRGTs. More detailed results are presented in Appendix C. A conclusion which can be made is that the CRGT cooling can serve as an effective heat removal measure in the case of melt pool formation in the lower plenum, reducing the probability of vessel failure due to corium thermal attacks.

The PECM simulations which have been shown were performed with the built-in correlation-based downward heat transfer coefficient (Steinberner-Reineke, 1978). In Chapter 3, we have revealed the heat transfer local effect which is associated with the corium Prandtl number. To examine vessel wall temperature behavior upon the local

effect, the PECM is used to simulate transient melt pool heat transfer in unit volume geometry (H = 0.7 m) for two cases with modified heat transfer coefficients (peaked approaching the vertical cooled boundary). In case A, the peaked value is 5 times higher than the correlation-based value; in case B the peaked value is 7 times higher than the correlation-based value. The selected peaked values are based on the uncertainty quantification results which have been obtained in the CFD study (Chapter 3). In the peripheral areas, Nu is determined using the Steinberner-Reineke downward correlation.

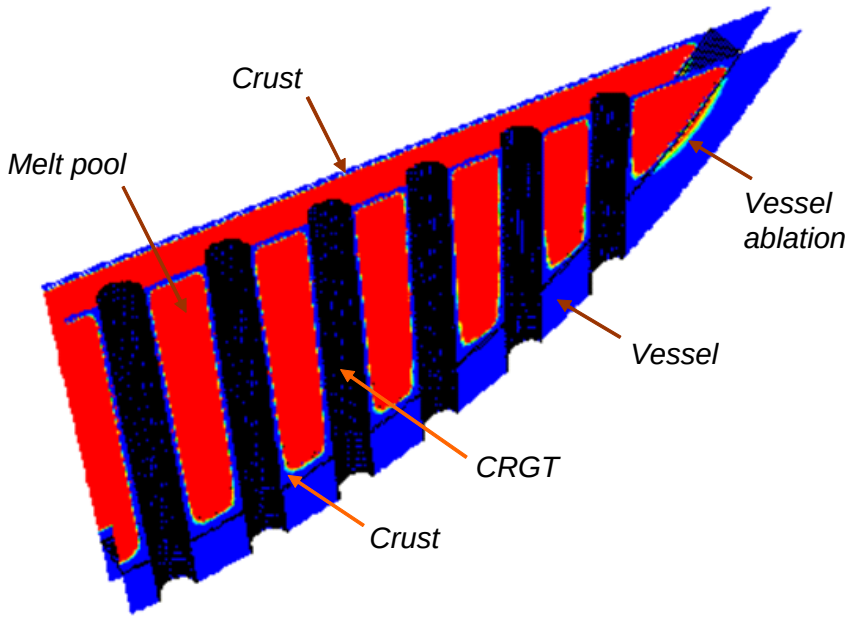

Figure 6.3: Melt pool configuration in the BWR lower plenum (t = 6.1 h).

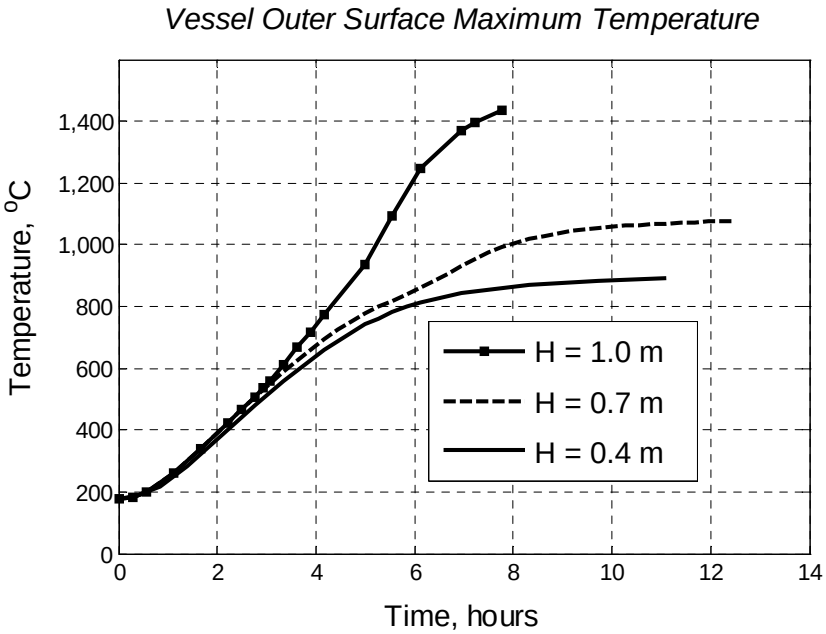

Figure 6.4: Evolution of vessel wall maximum temperature.

As it is shown in Figure 6.5, the local heat transfer effect apparently results in higher vessel wall temperature. Although the difference between case A and case B is not too large, the difference of case A and B compared with the base case (correlation-based *Nu*) is significant.

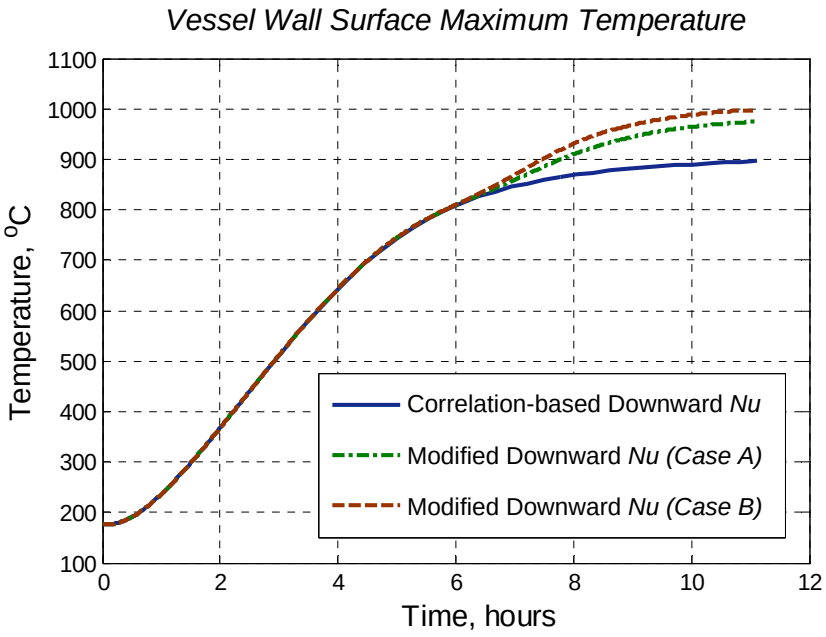

Figure 6.5: Evolutions of the maximum vessel wall temperature for different profiles of downward Nusselt number.

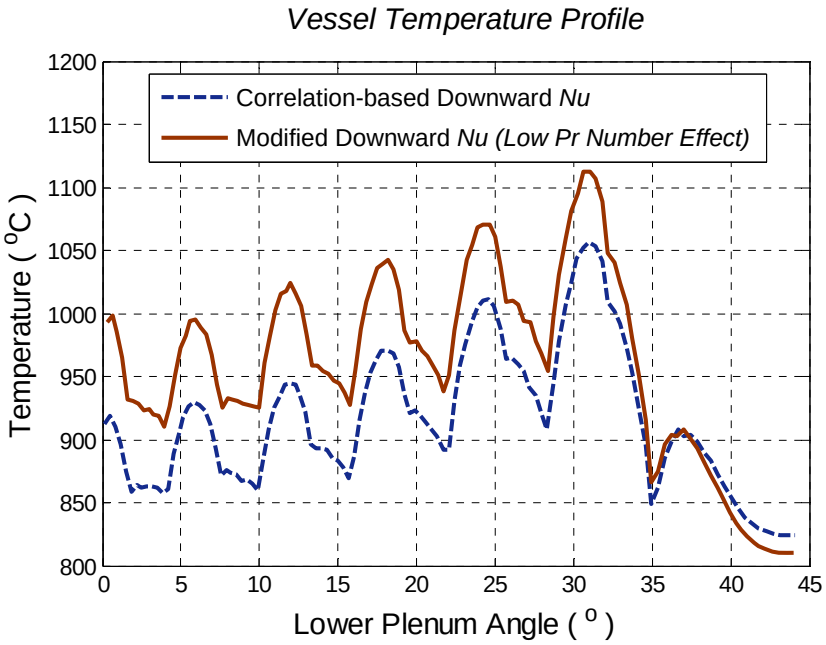

Figure 6.6: Steady-state vessel wall temperature profiles.

An additional PECM simulation performed for the BWR slice with H = 0.7 m shows that with the enhanced downward heat transfer coefficient (similar to case A), vessel wall does not hold the safe temperature level as previously for the correlation-based *Nu*. Maximum vessel wall temperature exceeds the creep limit in the vicinity of peripheral CRGTs (Figure 6.6). The local heat transfer effect (revealed by the CFD study) implemented in the accident analysis model (PECM) has shown a potential threat on the vessel integrity.

6.2. Simulation of stratified melt pool heat transfer

Detailed descriptions of the accident scenario, stratified melt pool formation in the lower plenum, and metal layer PECM application to transient simulation of stratified and uniform melt pool heat transfer are presented in Appendix E. Two scenarios considered are the stratified melt pool (with a metal layer of 0.2 m atop), and the uniform heterogeneous debris pool (molten metal in a matrix of solid oxidic particles). The total height of the melt pool (debris pool) is 1.0 m. The key findings are as follows.

It was found that in case of stratified melt pool formation in the BWR lower plenum, due to efficiency of the CRGT cooling, the decay heat is not focused to the vessel wall. Temperature of the vessel wall at the steady state is kept below 1100 ^{o}C (Figure 6.7). To compare different scenarios, a uniform heterogeneous debris pool (solid oxidic particles submerged in a liquid metal pool) is simulated. It is shown that in the case of uniform heterogeneous debris pool, i.e. without a metal layer atop, even with a less volumetric heat generation, temperature of the vessel wall is approaching 1200 ^{o}C.

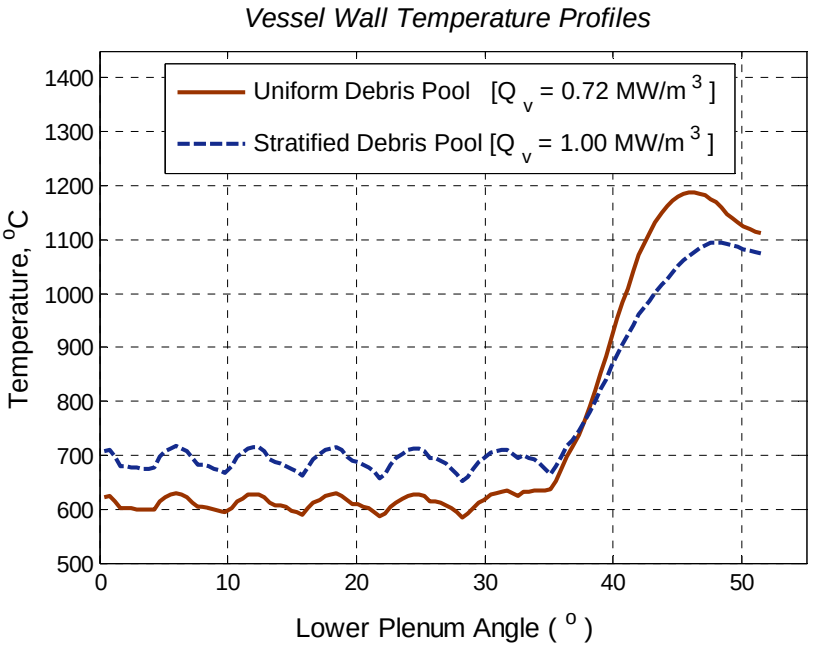

Figure 6.7: Temperature profiles of the vessel external surface.

However, the metal layer PECM simulation of stratified melt pool heat transfer exhibited a potential threat for the CRGT wall integrity. At the beginning of transient heatup, the transient heat flux to CRGT is high and in the range of 800 kW/m^2 (Figure 6.8). This high transient heat flux is due to latent heat released during fast solidification of the liquid metal surrounded the CRGTs (crust thickness evolution is shown in the figure). The transient heat flux is higher than the CHF of the CRGT nominal water flow rate that causes dryout of the CTGT wall, and consequently may lead to increase of the CRGT wall temperature higher than creep limit. An increase of the CRGT water flow rate is necessary to ensure efficient cooling of the CRGT wall, avoiding its failure.

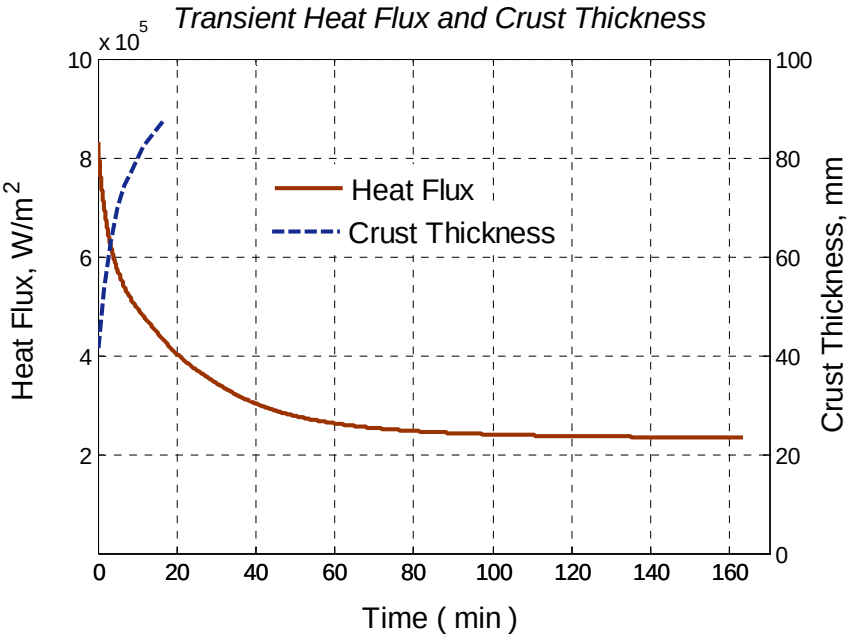

Figure 6.8: Transient crust thickness and heat flux to the CRGT section submerged in the metal layer.

6.3. Evaluation of the CRGT cooling efficiency

From the results of the analytical model calculations and CFD simulations, it is clear that in the case of homogeneous melt pool formation in the lower plenum, the average heat flux to a CRGT does not exceed 200 kW/m^2 (Figure 3.4). It is conservative to use the analytical model heat flux for calculation of steam quality along the CRGT. To evaluate the effectiveness of the CRGT cooling, the critical heat flux is needed. We use two methods to determine the critical heat flux along a CRGT: the Groeneveld-Kirillov look-up table (Groeneveld et al., 1996) and Katto's correlations (1979) for the forced convection boiling in vertical concentric annuli (water is flowing in the CRGTs through such annuli). The CHF calculation methods are presented in Appendix F.

The CHF is calculated for a wide range of water flow rate in the CRGTs, from 15kg/(m^2.sec) to 55kg/(m^2.sec). Note that the nominal water flow rate in the CRGTs, for the ABB-Atom reactor, is 15kg/m^2.s (equivalent to 62.5g/sec). In the present study, we

assume that the Automatic Depressurization System (ADS) has been initiated and pressure inside the reactor is not high during the accident progression. The calculations are performed for the pressure of 3 bars inside the CRGTs. The subcooling of inlet water is of 77 ^{o}C taken from ABB-Atom reactor data base.

Figure 6.9 presents the calculated CHF by the two methods and the heat flux imposed on the CRGT for different homogenous melt pool depth (height). It can be seen that predicted CHF by the look-up table and the Katto's correlations are well agreed. At the nominal water flow rate of 15 kg/(m^2.s), the thermal load from the melt pool imposed on the CRGT wall is predicted to be lower than the CHF for the corium pool with a height up to 0.9 m. The higher water flow rate, e.g. 20 kg/(m^2.s) can be sufficient to remove the heat from a pool of 1.2 m or higher. However, for a stratified melt pool considered previously (Section 6.2), the transient heat flux at the beginning (about 800 kW/m^2) seems to be exceeded the CHF for H = 1.0 m at the flow rate of 20 kg/(m^2.s). To ensure the CRGT cooling efficiency, it is necessary to increase the water flow rate to 30 kg/(m^2.s) or higher. Such an increase of water flow rate in the CRGTs is able to remove the decay heat from a melt pool (homogeneous or stratified) of 1.2 m height.

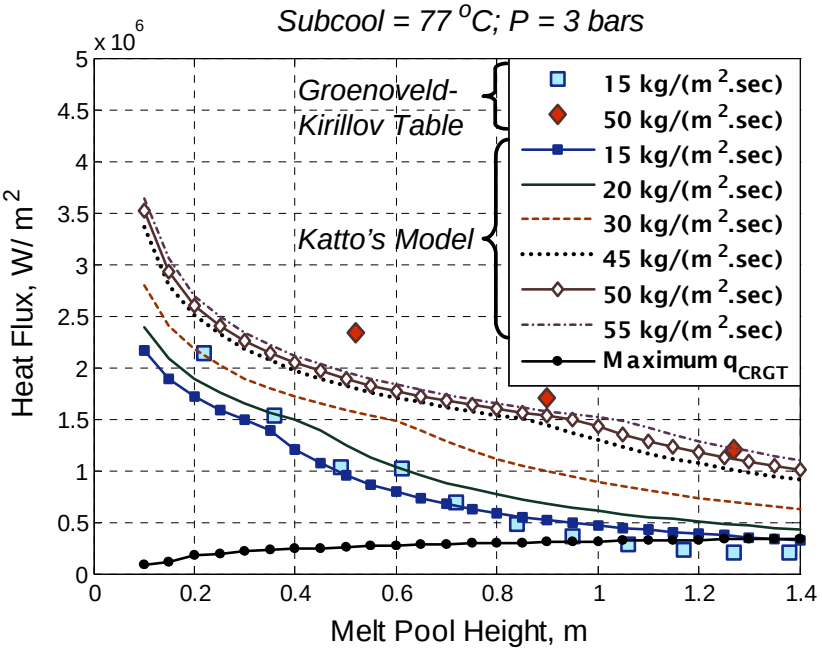

Figure 6.9: Imposed heat flux on a CRGT and Critical Heat Flux (CHF) in a CRGT annulus.

6.4. Discussion of uncertainty in heat transfer simulations

The heat transfer simulations and analysis which have been performed were based on several assumptions. In this section, the assumptions related to modeling and accident scenario uncertainty are discussed.

As previously mentioned, all the CFD, ECM and PECM melt pool heat transfer simulations are feasible if IGTs are intact or plugged (by penetrated material) during the heatup, melting and pool formation process of debris bed. However, failure mode of IGTs remain uncertain, as it depends on several factors, namely the accident scenario, debris bed configuration and thermal condition, on possibility of water access into the IGT wall surfaces from the top of debris bed (water is available on the top due to the CRGT cooling flow). In the case of IGT failure, there is likelihood that the resulted opening will be plugged by the melt solidified passing through the cooled thick vessel wall. IGT failure mode (plugged/failed) depends on the melt property, melt superheat and flow rate, IGT sizes and configuration, and the thermal condition of lower section of the IGT. Further study is necessary to quantify the uncertainties related to IGT failure modes.

Uncertainty in corium properties can be significant, but can be reduced with the availability of relevant data. Furthermore, this uncertainty is evaluated and found to be far less important than the uncertainties in an accident scenario, namely the rate of chemical reactions (oxidation of Zr, etc.), physicochemical interaction of melt materials with vessel wall, melt relocation modes, and conditions of the lower plenum prior to relocations etc. In the present work, the decay heat generation rate is assumed to be uniform over the corium debris bed and melt pool. In fact, the rate of heat generation can be different over the heated volume, depending on the debris bed (melt pool) configuration (e.g. the presence of suboxidized materials in the debris bed, melt pool). It is recognized that the debris bed (melt pool) configuration is a potential constituent to the uncertainty in debris bed (melt pool) heat transfer prediction. As it was mentioned earlier, the physicochemical phenomena involved in the accident progression are not fully understood, future experiments are needed to identify the material effects on melt pool formation and stratification.

The metal layer PECM heat transfer simulation of a stratified melt pool exhibited uncertainty in failure of the CRGT wall under a high transient heat flux from a metal layer atop of oxidic pool (Appendix E). This question is concerned with assessment of the CRGT cooling efficiency. Further study is needed to clarify the temperature behavior of the CRGT wall under the transient heat flux, and to quantify the necessary CRGT water flow rate to overcome the dryout.

Simulations also were made without taking into account the possibility of water ingression into narrow gaps formed between the CRGT wall (and the vessel wall) and the formed debris bed (cake). In reality it is possible, due to porous nature of the initial debris bed, or due to formation of crevices caused by thermal stresses in a debris cake (Rempe et al., 2008). Water ingression into the gaps may increase coolability of the debris bed (cake) or melt pool, decrease vessel wall temperature due to boiling. However, water ingression into such narrow gaps remains questionable therefore it was not taken into account in the present work.

6.5. An outlook to further study

The previous section provides a basis to discuss outlook to further study. Towards the assessment of the in-vessel coolability and CRGT cooling efficiency, the following

aspects need to be analyzed: IGT failure modes; debris bed thermal behavior under different corium thermal properties; CRGT cooled wall temperature variation under a high transient heat flux; and the coupled thermo-mechanical creep analysis.

To evaluate BWR vessel failure modes and timing due to IGT penetrations, study of IGT failure modes is necessary. The main task of the study is examining the thermo-mechanical behavior of IGT during the debris bed formation, heatup, remelting, and analysis of corium melt (or liquid metal) dynamics inside an IGT opening under different boundary conditions applied to the external surface of IGT.

It is clear that corium thermal property is changed with different fraction of presented metallic components. Most importantly, the fraction of metallic components in the corium (debris bed) defines the corium thermal conductivity which in turn may affect significantly on thermal state of the debris bed in the presence of CRGT cooling. The debris bed may remain its solid state, or matrix of solid and liquid phases (Appendix E), or will be remelted, it depends on the thermal conductivity. Therefore, parametric study on the debris bed behavior depending on thermal conductivity is useful for evaluation of in-vessel coolability.

In the next topic, it is needed to examine the water cooled CRGT wall thermal behavior under a variable heat flux which may exceeds the CHF. The metal layer PECM can be coupled with a system code (e.g. RELAP, MELCOR) to examine the efficiency of CRGT cooling at different water flow rates. In this task, the metal layer PECM simulation provides the spatial distribution of heat flux along the CRGTs to the system code. In turn, the system code predicts flow regimes inside the CRGTs and provides the heat transfer coefficient profile along the CRGTs to the PECM as the boundary conditions.

Predicted by the PECM thermal behavior of the vessel wall can be coupled with the mechanical analysis in ANSYS code, to examine creep of the vessel wall under transient thermal loads and pressure during severe accident progression (Willschuetz et al., 2006). Material property of the vessel steel (temperature dependence of the steel ultimate strength) can be imported to ANSYS as input data. The coupled thermo-mechanical creep analysis is necessary for detailed prediction of vessel failure mode and timing.

Preliminary evaluation of levels of uncertainty in the research tasks is shown in Table VI.3. These tasks are included in the APRI-7 program at KTH-NPS (2009-2011).

Table VI.3: Relative levels of uncertainty in the identified research tasks

No.	Description of the task	Level of uncertainty (research priority)
1	Instrumentation guide tube plug and failure modes	Large
2	Debris bed state in the presence of CRGT cooling	Significant
3	CRGT wall temperature variation under a high heat flux	Significant
4	Thermo-mechanical coupled creep analysis	Small

Chapter 7: Summary

The thesis work summarizes the research dedicated to development, validation and application of the Effective Convectivity Model (ECM) and Phase-change ECM (PECM) for simulation of melt pool heat transfer during a postulated severe accident in a Boiling Water Reactor (BWR).

To support the development of the accident analysis models for engineering analysis, an approach to make use of the Computational Fluid Dynamics (CFD) method was proposed and demonstrated. Application of the CFD method for examining flow physics, and generating data for validation of the accident analysis model is found to be particularly effective in nuclear reactor safety problems where experiments using reactor materials and under prototypic conditions are often unfeasible. In Chapter 3, the Implicit Large Eddy Simulation (ILES) CFD method was used for simulation of melt pool heat transfer in specific BWR geometries. The ILES method was validated against both integral and locally distributed data from available experiments. CFD simulations revealed the heat transfer local effect associated with the low Prandtl number property of corium melt. The downward heat flux to the vessel wall is enhanced in the vicinity of CRGT cooled wall. An uncertainty analysis was performed to quantify the local heat flux peaking which is further implemented in the accident analysis model to examine the potential effect of transient thermal loads on the vessel wall.

Chapter 4 presents development of the ECM which was based on the concept of effective convectivity pioneered in the Effective Convectivity Conductivity Model (ECCM). Development of the ECM was supported by the insights gained from CFD study. Augmented with the mushy zone heat transfer models, the ECM was extended to simulation of transient phase change, enabling simulation of melt pool formation heat transfer in a BWR lower plenum. Followed the guidelines proposed in the developed approach, the metal layer ECM and PECM were developed for heat transfer simulation of a molten metal layer heated from below and cooled from the top and side surfaces. In the metal layer PECM, beside the mushy zone heat transfer models, the compositional convection model was implemented using the compositional (concentration) Rayleigh number. The metal layer PECM enables simulation of solidification/melting of eutectic and non-eutectic binary mixtures. The resulting PECM for corium pool and metal layer present the required capability for simulation and engineering analysis of heat transfer in a BWR lower plenum.

In Chapter 5, validation of the ECM, PECM and metal layer ECM/PECM is performed within a dual-tier approach, using heat transfer experiments available in the open literature, and the CFD generated data for specific geometries and conditions of importance but relevant experimental data do not exist. The results show that the ECM and PECM tools are sufficiently-accurate and computationally-efficient for heat transfer simulation and prediction of transient thermal loads from a formed melt pool to the reactor internal structures and vessel wall during a hypothetical severe accident in a BWR lower plenum.

Chapter 6 presents applications of the ECM/PECM to simulation and analysis of heat transfer in a BWR lower head. The simulation results show that for a debris bed (melt pool) of less than 0.7 m thick formed in the lower plenum, the CRGT cooling at the nominal water flow rate is sufficient for removing the decay heat and thus likely adequate to ensure the reactor pressure vessel integrity. With a thicker debris bed, the vessel wall is predicted to fail in the section close to the uppermost region of debris bed (melt pool). The metal layer PECM simulation shows that in a stratified melt pool (0.2 m metal layer in 1.0 m total thickness), due to the CRGT cooling, the focusing effect is ameliorated. However, upon formation of the stratified melt pool, the transient heat flux to CRGTs submerged in the metal layer may be high enough to cause dryout inside the CRGT, leading to potential failure due to its high temperature. Increase of flow rate in the CRGT cooling is necessary to ensure the CRGT integrity and debris coolability.

The local heat transfer effect associated with the low *Pr* number property of corium melt on the vessel wall transient heatup was examined using the accident analysis PECM. The PECM simulation results show that an additional increase (about 100 K) of the vessel wall temperature takes place in the vicinity of the peripheral CRGTs, due to the local heat transfer effect. This increase in the vessel wall temperature potentially changes the failure mode of the BWR lower plenum during a postulated severe accident.

Results of ECM, PECM calculations in the present thesis work have shown that the CRGT cooling not only can reduce core materials heatup and melting in the early phase of accident scenario, but also can be an effective measure for heat removal from a melt pool formed in the BWR lower head in the late phase of in-vessel accident progression, thus increasing the likelihood of cooling and retaining corium in-vessel.

As a whole the present thesis work has demonstrated a close connection between modeling, experimentation (including the real experiments and “numerical experiments”, i.e. CFD simulations) and validation, leveraging the predictive capability in the nuclear engineering analysis tasks.

Bibliography

F.J. ASFIA, B. FRANTZ and V.K. DHIR, Experimental Investigation of Natural Convection in Volumetrically Heated Spherical Segments, *J. Heat Transfer*, **Vol.118**, pp.31-37, 1996.

V. ASMOLOV, N. N. PONOMAREV-STEPNOY, V. STRIZHOV, B. R. SEHGAL, Challenges Left in the Area of In-Vessel Melt Retention, *J. Nuclear Engineering and Design*, **Vol.209**, pp.87-96, 2001.

V. G. ASMOLOV, S. V. BECHTA, V. B. KHABENSKY et al., Partitioning of U, Zr and Fe between Molten Oxidic and Metallic Corium, *Proceeding of MASCA Seminar 2004*, Aix-en-Provence, France, 2004.

S.V. BECHTA, V.S. GRANOVSKY, V.B. KHABENSKY, V.V. GUSAROV, V.I. ALMIASHEV, L.P. MEZENTSEVA, E.V. KRUSHINOV, S.Yu. KOTOVA, R.A. KOSAREVSKY, M. BARRACHIN, D. BOTTOMLEY, F. FICHOT, M. FISCHER, Corium Phase Equilibria Based on MASCA, METCOR and CORPHAD Results, *J. Nuclear Engineering and Design*, **Vol.238**, pp.2761-2771, 2008a.

S.V. BECHTA, V.S. GRANOVSKY, V.B. KHABENSKY, E.V. KRUSHINOV, S.A. Vitol, A.A. SULATSKY, V.V. GUSAROV, V.I. ALMIASHEV, D.B. LOPUKH, D. BOTTOMLEY, M. FISCHER, P. PILUSO, A. MIASSOEDOV, W. TROMM, E. ALSTADT, F. FICHOT, O. KYMALAINEN, Interaction between Molten Corium UO_{2+X}-ZrO_2-FeO_Y and VVER Vessel Steel, *Proceedings of 2008 International Congress on Advances in Nuclear Power Plants (ICAPP ´08)*, Anaheim, CA, USA, June 8-12, 2008b.

C. BECKERMANN and R. VISKANTA, Natural Convection Solid/Liquid Phase Change in Porous Media, *Int. J. Heat Mass Transfer*, **Vol.31 (1)**, pp.35-46, 1988.

C. BECKERMANN and R. VISKANTA, Double-Diffusive Convection due to Melting, *Int. Journal of Heat Mass Transfer*, **Vol.31 (10)**, pp.2077-2089, 1988.

C. BECKERMANN, H.-J. DIEPERS, I. STEINBACH, A. KARMA, X. TONG, Modeling Melt Convection in Phase-field Simulations of Solidification, *J. Comput. Phys.*, **Vol.154**, pp.468-496, 1999.

W.D. BENNON and F.P. INCROPERA, A Continuum Model for Momentum, Heat and Species Transport in Binary Solid-Liquid Phase Change Systems – I. Model Formulation, *Int. J. Heat Mass Transfer*, **Vol.30 (10)**, pp.2161-2170, 1987a.

W.D. BENNON and F.P. INCROPERA, A Continuum Model for Momentum, Heat and Species Transport in Binary Solid-Liquid Phase Change Systems – II. Application to Solidification in a Rectangular Cavity, *Int. J. Heat Mass Transfer*, **Vol.30 (10)**, pp.2171-2187, 1987b.

L. BERNAZ, J.- M. BONNET, B. SPINDLER, C. VILLERMAUX, Thermal Hydraulic Phenomena in Corium Pools: Numerical Simulation with TOLBIAC and Experimental Validation with BALI, *Proceedings of In-Vessel Core Debris Retention and Coolability Workshop*, Garching, Germany, March 3-6, pp.185-193, 1998.

J.P. BORIS, F.F. GRINSTEIN, E.S. ORAN and R.L. KOLBE, New Insights into Large Eddy Simulation, *J. Fluid Dynamics Research*, **Vol.10**, pp.199-228, 1992.

B.E. BOYACK, I. CATTON, R.B. DUFFEY, P. GRIFFITH, K.R. KATSMA, G.S. LELLOUCHE, S. LEVY, U.S. ROHATGI, G.E. WILSON, W. WULFF and N. ZUBER, Quantifying Reactor Safety Margins. Part 1: An Overview of the Code Scaling, Applicability, and Uncertainty Evaluation Methodology, *J. Nuclear Engineering and Design*, **Vol.119**, pp.1-15, 1990.

V.A. BUI and T.N. DINH, Modeling of Heat Transfer in Heated-Generating Liquid Pools by an Effective Diffusivity-Convectivity Approach, *Proceedings of 2nd European Thermal-Sciences Conference*, Rome, Italy, pp.1365-1372, 1996.

W.-Z. CAO, D. POULIKAKOS, Solidification of an Alloy in Cavity Cooled through its Top Surface, *Int. J. Heat Mass Transfer*, **Vol.33 (3)**, pp.427-434, 1990.

B. CASTAING, G. GUNARATNE, F. HESLOT, L. KADANOFF, A. LIBCHABER, S. THOMAE, X.Z. WU, S. ZALESKI and G. ZANETTI, Scaling of Hard Thermal Turbulence in Rayleigh-Benard Convection, *J. Fluid Mech.*, **Vol.204**, pp.1-30, 1989.

L. CHANDRA, G. GROTZBACH, Analysis and Modelling of the Turbulent Diffusion of Turbulent Heat Fluxes in Natural Convection, *Int. J. Heat and Fluid Flow*, **Vol.29**, pp.743-751, 2008.

D. CHATTERJEE, S. CHAKRABORTY, A Hybrid Lattice Boltzmann Model for Solid–Liquid Phase Transition in Presence of Fluid Flow, *Phys. Lett.*, **A 351**, pp.359-367, 2006.

X. CHAVANNE, F. CHILLA, B. CHABAUD, B. CASTAING, and B. HEBRAL, Turbulent Rayleigh-Benard Convection in gaseous and Liquid He, *Physics of Fluids*, **Vol.13 (5)**, pp.1300-1320, 2001.

S. CHEN, B. MERRIMAN, S. OSHER, P. SMEREKA, A Simple Level Set Method for Solving Stefan Problems, *J. Comp. Phys.*, **Vol.135**, pp.8-29, 1997.

F.B. CHEUNG, S.W. SHIAH, D.H. CHO and M.J. TAN, Modeling of Heat Transfer in A Horizontal Heat-Generating Layer by An Effective Diffusivity Approach, *ASME HTD*, **Vol.192**, pp.55-62, 1992.

M.S. CHRISTENSON and F. INCROPERA, Solidification of an Aqueous Ammonium Chloride Solution in a Rectangular Cavity – I. Experimental Study, *Int. Journal of Heat Mass Transfer*, **Vol.32 (1)**, pp.47-68, 1989.

S.W. CHURCHILL and H.S. CHU, Correlating Equations for Laminar and Turbulent Free Convection from a Vertical Plate, *Int. J. Heat Mass Transfer*, **Vol.18**, pp.1323-1329, 1975.

S. CIONI, S. CILIBERTO, J. SOMMERIA, Experimental Study of High-Rayleigh-Number Convection in Mercury and Water, *Dynamics of Atmospheres and Oceans*, **Vol.24**, pp.117-127, 1996.

S. CIONI, S. CILIBERTO and J. SOMMERIA, Strongly Turbulent Rayleigh-Benard Convection in Mercury: Comparison with Results at Moderate Prandtl Number, *J. Fluid Mechanics*, **Vol.335**, pp.111-140, 1997.

T.N. DINH, Melt-Structure-Water Interactions (MSWI) during Severe Accidents, *Proceedings of the 23nd Meeting of Advisory Group for Research Project*, AlbaNova University Center, Stockholm, November 15, 2006.

T.N. DINH and R.R. NOURGALIEV, Turbulence Modeling for Large Volumetrically Heated Liquid Pools, *J. Nuclear Engineering and Design*, **Vol.169**, pp.131-150, 1997.

T.N. DINH, Y.Z. YANG, J.P. TU, R.R. NOURGALIEV, and T.G. THEOFANOUS, Rayleigh-Benard Natural Convection Heat Transfer: Pattern Formation, Complexity and Predictability, *Proceedings of ICAPP' 04*, Pittsburgh, PA, USA, June 13-17, 2004.

L.A. DOMBROVSKII, L.I. ZAICHIK and Y.A. ZEIGARNIK, Numerical Simulation of The Stratified-Corium Temperature Field and Melting of The Reactor Vessel for A Severe Accident in A Nuclear Power Station, *Thermal Engineering*, **Volume 45 (9)**, pp.755-765, 1998.

E.R.G. ECKERT and T.W. JACKSON, Analysis of Turbulent Free Convection Boundary Layer on Flat Plate, NACA TN 2207, 1950.

FLUENT Inc., Fluent 6.3 User's Guide, September, 2006.

J.D. GABOR, P.G. ELLISON, and J.C. CASSULO, Heat Transfer from Internally Heated Hemispherical Pools, *Presented at 19th National Heat Transfer Conference*, Orlando, Florida, July 27-30, 1980.

C. GAU, R. VISKANTA, Effect of Natural Convection on Solidification from above and Melting from below of a Pure Metal, *Int. J. Heat Mass Transfer*, **Vol.28 (3)**, pp.573-587, 1985.

R.O. GAUNTT, J.E. CASH, R.K. COLE, C.M. ERICKSON, L.L. HUMPHRIES, S.B. RODRIGUEZ and M.F. YOUNG, MELCOR Computer Code Manual, Core (COR) Package Reference Manuals, *NUREG/CR-6119*, 2 (2), 2005.

S. GLOBE and D. DROPKIN, Natural-Convection Heat Transfer in Liquid Confined by Two Horizontal Plates and Heated from Below, *J. Heat Transfer*, **Vol.81**, pp.24-28, 1959.

R. J. GOLDSTEIN, H. D. CHIANG and D. L. SEE, High Rayleigh-Number Convection in a Horizontal Enclosure, *J. Fluid Mech.*, **Vol.213**, pp.111-126, 1990.

D.C. GROENEVELD, L.K.H. LEUNG, P.L. KIRILLOV, V.P. BOBKOV, I.P. SMOGALIEV, V.N. VINOGRADOV, X.C. HUANG, E. ROYER, The 1995 look-up table for critical heat flux in tubes, *J. Nuclear Engineering and Design*, **Vol.163**, pp.1-23, 1996.

S. GROSSMANN and D. LOHSE, Scaling in Thermal Convection: a Unifying Theory, *J. Fluid Mech.*, **Vol.407**, pp.27-56, 2000.

G. GROTZBACH, Direct Numerical Simulation of the Turbulent Momentum and Heat Transfer in an Internally Heated Fluid Layer, *Heat Transfer*, Hemisphere, pp.141-146, 1982.

G. GROTZBACH, Direct Numerical and Large Eddy Simulation of Turbulent Channel Flows, *Encyclopedia of Fluid Mech.*, **Vol.6**, pp.1337-1391, 1987.

G. GROTZBACH, M. WORNER, Direct Numerical and Large Eddy Simulations in Nuclear Applications, *Int. J. Heat and Fluid Flow*, **Vol.20**, pp.222-240, 1999.

M. HELLE, O. KYMALAINEN and H. TUOMISTO, Experimental Data on Heat Flux Distribution from a Volumetrically Heated Pool with Frozen Boundaries, *Proceedings of In-Vessel Core Debris Retention and Coolability Workshop*, Garching, Germany, March 3-6, pp.173-183, 1998.

C.E. HENRY, V. LANDGREN, MAAP4 Modular Accident Analysis Program for LWR Power Plants, Computer Code User's Manual, *Electric Power Research Institute*, January, 2003.

H.E. HUPPERT, J.S. TURNER, Double-Diffusive Convection, *J. Fluid Mech.*, **Vol.106**, pp.299-329, 1981.

M. JAHN and H. H. REINEKE, Free Convection Heat Transfer with Internal Heat Sources: Calculations and measurements, *Proceedings of the 5th Int. Heat Transfer Conference*, Tokyo, Japan, Vol.3, Paper NC-2.8, 1974.

D. JURIC, G. TRYGGVASON, A Front Tracking Method for Dendritic Solidification, *J. Comp. Phys.*, **Vol.123**, pp.127-148, 1996.

A. KARBOJIAN, W.M. MA, P. KUDINOV, T.N. DINH, A Scoping Study of Debris Bed Formation in the DEFOR Test facility, *J. Nuclear Engineering and Design*, 2009.

Y. KATTO, Generalized Correlations of Critical Heat Flux for the Forced Convection Boiling in Vertical Uniformly Heated Annuli, *Int. J. Heat Mass Transfer*, **Vol.22**, pp.575-584, 1979.

V. KEK and U. MULLER, Low Prandtl Number Convection in Layers Heated from Below, *Int. Journal of Heat Mass Transfer*, **Vol.36 (11)**, pp.2795-2804, 1993.

R. KERR, Rayleigh Number Scaling in Numerical Convection, *J. Fluid Mech.*, **Vol.310**, pp.139-179, 1996.

R.M. KERR and J.R. HERRING, Prandtl Number Dependence of Nusselt Number in Direct Numerical Simulations, *J. Fluid Mech.*, **Vol.419**, pp.325-344, 2000.

J. KIM, Investigation of Heat and Momentum Transport in Turbulent Flows via Numerical Simulations, *Transport Phenomena in Turbulent Flows*, Hemisphere, pp.715-730, 1988.

Y.-T. KIM, N. GOLDENFELD, J. DANTZIG, Computation of Dendritic Microstructures Using a Level Set Method, *Phys. Rev. E*, **Vol.62**, pp.2471-2474, 2000.

A.T. KIRKPATRICK and M. BOHN, An Experimental Investigation of Mixed Cavity Natural Convection in the High Rayleigh Number Regime, *Int. J. Heat Mass Transfer*, **Vol.29 (1)**, pp.69-82, 1986.

P. KUDINOV, A. KARBOJIAN, W.M. MA, and T.N. DINH, An Experimental Study on Debris Formation with Corium Stimulant Materials, *Proceedings of ICAPP'08*, Anaheim, CA, USA, 2008.

F.A. KULACKI and A.A. EMARA, Steady and Transient Thermal Convection in a Fluid Layer with Uniform Volumetric Energy Sources, *J. Fluid Mech.*, **Vol.83 (2)**, pp.375-395, 1977.

F.A. KULACKI and R.J. GOLDSTEIN, Thermal Convection in a Horizontal Fluid Layer with Uniform Volumetric Energy Sources, *J. Fluid Mech*. **Vol.55 (2)**, pp.271-287, 1972.

F.A. KULACKI and M.E. NAGLE, Natural Convection in a Horizontal Fluid Layer with Volumetric Energy Sources, Transactions of the ASME, *Journal of Heat Transfer*, **Vol.97**, pp.204-211, 1975.

P. KUMAR, S. CHAKRABORTY, K. SRINIVASAN, and P. DUTTA, Studies on Transport Phenomena during Directional Solidification of a Noneutectic Binary Solution Cooled from the Top, *Metallurgical and Materials Transactions B*, **Vol.34B**, pp.899-909, 2003.

O. KYMALAINEN, H. TUOMISTO, O. HONGISTO, T.G. THEOFANOUS, Heat Flux Distribution from a Volumetrically Heated Pool with High Rayleigh Number, *J. Nuclear Engineering and Design*, **Vol.149**, pp.401-408, 1994.

F.B. LIPPS, Numerical Simulation of Three-dimensional Benard Convection in Air, *J. Fluid Mech.*, **Vol.75**, pp.113-148, 1976.

J. MAHAFFY et al., Best Practice Guidelines for the Use of CFD in Nuclear Reactor Safety Applications, *Nuclear Energy Agency Report*, NEA/CSNI/R(2007)5, 2007.

L.G. MARGOLIN, W.J. RIDER, F.F. GRINSTEIN, Modeling Turbulent Flow with Implicit LES, *Journal of Turbulence*, **Vol.7 (15)**, pp.1-27, 2006.

F. MAYINGER, M. JAHN, H. REINEKE, and U. STEINBERNER, Examination of Thermalhydraulic Processes and Heat Transfer in a Core Melt, *Final Report BMFT RS 48/1*, Hanover Technical University, 1976.

A. MIASSOEDOV, T. CRON, J. FIOT, S. SCHMIDT-STIEFEL, T. WENZ, I. IVANOV, D. POPOV, Results of the LIVE-L1 Experiment on Melt Behavior in RPV Lower Head Performed within the LACOMERA Project at the Forschungszentrum Karlsruhe, *Proceedings of 15th International Conference on Nuclear Engineering Nagoya (ICONE)*, Japan, April 22-26, 2007.

A.A. MOHAMAD and R. VISKANTA, Modeling of Turbulent Buoyant Flow and Heat Transfer in Liquid Metals, *Int. J. Heat Mass Transfer*, **Vol.36 (11)**, pp.2815-2826, 1993.

J. NI, C. BECKERMANN, A Volume-Average Two-Phase Model for Transport Phenomena during Solidification, *Metall. Trans. B*, **Vol.22**, pp.349-361, 1991.

R.R. NOURGALIEV, T.N. DINH and B.R. SEHGAL, Effect of fluid Prandtl Number on Heat Transfer Characteristics in Internally Heated Liquid Pools with Rayleigh Numbers up to 10^{12}, *J. Nuclear Engineering and Design*, **Vol.169**, pp.165-184, 1997a.

R.R. NOURGALIEV, T.N. DINH, B.R. SEHGAL, Simulation an Analysis of Transient Cooldown Natural Convection Experiments, *J. Nuclear Engineering and Design*, **Vol.178**, pp.13-27, 1997b.

R.R. NOURGALIEV and T.N. DINH, An Investigation of Turbulence Characteristics in an Internally-Heated Unstably-Stratified Fluid Layer, *J. Nuclear Engineering and Design*, **Vol.178**, pp.235-258, 1997.

S.A. ORSZAG, G.S. PATTERSON Jr., Numerical Simulation of Turbulence, Statistical Models and Turbulence, *Lecture Notes in Physics*, Springer-V, Berlin, pp.127-147, 1972.

I. OTIC, G. GROTZBACH and M. WORNER, Analysis and Modelling of the Temperature Variance Equation in Turbulent Natural Convection for low-Prandtl Fluids, *J. Fluid Mech.*, **Vol.525**, pp.237-261, 2005.

J.L. O'TOOLE and P.L. SILVESTON, Correlations of Convective Heat Transfer in Confined Horizontal Layers, *AIChE. Chemical Engineering. Progr. Symp. Ser.*, 57 (32), pp.81-86, 1961.

R. PARDESHI, V.R. VOLLER, A.K. SINGH, P. DUTTA, An Explicit-Implicit Time Stepping Scheme for Solidification Models, *Int. J. Heat and Mass Transfer*, **Vol.51**, pp.3399-3409, 2008.

H. PARK and V. DHIR, Effect of Outside Cooling on the Thermal Behavior of a Pressurized Water Reactor Vessel Lower Head, *J. Nuclear Technology*, **Vol.100**, 331-346, 1992.

S.S.L. PEPPIN, H.E. HUPPERT and M.G. WORSTER, Steady-state Solidification of Aqueous Ammonium Chloride, *J. Fluid Mech.*, **Vol.599**, pp.465-476, 2008.

J. L. REMPE, S. A. CHAVEZ, G. L. THINNES, C. M. ALLISON, G. E. KORTH, R. J. WITT, J. J. SIENICKI, S. K. WANG, L. A. STICKLER, C. H. HEATH, S. D. SNOW, Light Water Reactor Lower Head Failure Analysis, *NUREG/CR-5642, EGG-2618*, Idaho National Engineering Laboratory, USA, 1993.

J.L. REMPE, K.Y. SUH, F.B. CHEUNG and S.B. KIM, In-vessel Retention of Molten Corium: Lessons Learned and Outstanding Issues, *J. Nuclear Technology*, **Vol.161**, pp.210-267, 2008.

P.-E. ROCHE, B. CASTAING, B. CHABAUD and B. HEBRAL, Prandtl and Rayleigh Numbers Dependences in Rayleigh-Benard Convection, *Europhys.Lett.*, **Vol.58 (5)**, pp.693-698, 2002.

SCDAP/RELAP5-3D Code Development Team, SCDAP/RELAP5-3D© Code manual, *Report INEEL/EXT-02-00589*, Revision 2.2, Idaho National Engineering and Environmental Laboratory, USA, October, 2003.

B.R. SEHGAL, Stabilization and Termination of Severe Accidents in LWRs, *J. Nuclear Engineering and Design*, **Vol.236**, pp.1941-1952, 2006.

B.R. SEHGAL, V.A. BUI, T.N. DINH, J.A. GREEN, G. KOLB, SIMECO Experiments on In-Vessel Melt Pool Formation and Heat Transfer with and without a Metallic Layer, *Proceedings of In-Vessel Core Debris Retention and Coolability Workshop*, Garching, Germany, March 3-6, pp.205-213, 1998.

J.-M. SEILER, A. LATROBE, B.R. SEHGAL, H. ALSMEYER, O. KYMALAINEN, B. TURLAND, J.-L. GRANGE, M. FISCHER, G. AZARIAN, M. BURGER, C.J. CIRAUQUI, A. ZURITA, Analysis of corium recovery concepts by the EUROCORE group, *J. Nuclear Engineering and Design*, **Vol.221**, pp.119-136, 2003.

J.-M SEILER, B. TOURNIAIRE, F. DEFOORT, K. FROMENT, Consequences of Material Effects on In-Vessel Retention, *J. Nuclear Engineering and Design*, **Vol.237**, pp.1752-1758, 2007.

B.I. SHRAIMAN, E.D. SIGGIA, Heat Transport in High-Rayleigh-Number Convection, *Physical Review A*, **Vol.42 (6)**, pp.3650-3653, 1990.

U. STEINBERNER and H.H. REINEKE, Turbulent Buoyancy Convection Heat Transfer with Internal Heat Sources, *Proceedings of the 6th Int. Heat Transfer Conference*, Toronto, Canada, Vol.2, pp.305-310, 1978.

V. STRIZHOV, V. ASMOLOV, Major Outcomes of the RASPLAV Project, *RASPLAV Seminar 2000*, Munich, November, 2000.

J.M. SULLIVAN Jr., D.R. LYNCH, Finite Element Simulation of Planar Instabilities during Solidification of an Undercooled Melt, *J. Comput. Phys.*, **Vol.69**, pp.81-111, 1987.

Y. SUN, C. BECKERMANN, Sharp Interface Tracking Using the Phase-field Equation, *J. Comput. Phys.*, **Vol.220**, pp.626-653, 2006.

T.G. THEOFANOUS, C. LIU, S. ADDITON, S. ANGELINI, O. KYMALAINEN, T. SALMASSI, In-vessel Coolability and Retention of a Core Melt, *DOE/ID-10460*, Volume 1, October 1996.

T.G. THEOFANOUS, M. MAGUIRE, S. ANGELINI, T. SALMASSI, The First Results from the ACOPO Experiment, *J. Nuclear Engineering and Design*, **Vol.169**, pp.49-57, 1997.

D.C. THRELFALL, Free Convection in Low-Temperature Gaseous Helium, *J. Fluid Mech.*, **Vol.67 (1)**, pp.17-28, 1975.

K. TRAMBAUER, B. SCHWINGES, Evaluation of Research Priorities in the Frame of SARNET, *EC-SARNET: FI60-CT-2004-509065*, 2007.

C.T. TRAN and T.N. DINH, An Effective Convectivity Model for Simulation of In-vessel Core Melt Progression in Boiling Water Reactor, *Proceedings of ICAPP'07*, Nice Acropolis, France, 2007a.

C.T. TRAN and T.N. DINH, Simulation of Core Melt Pool Formation in a Reactor Pressure Vessel Lower Head Using an Effective Convectivity Model, *Proceedings of NURETH-12*, Pittsburgh, Pennsylvania, USA, September 30 – October 04, 2007b.

R. TRIVEDI, H. MIYAHARA, P. MAZUMDER, E. SIMSEK, S.N. TEWARI, Directional Solidification Microstructures in Diffusive and Convective Regimes, *J. Crystal Growth*, **Vol.222**, pp.365-379, 2001.

H.S. UDAYKUMAR, S. MARELLA, S. KRISHNAN, Sharp-interface Simulation of Dendritic Growth with Convection: Benchmarks, *Int. J. Heat Mass Transfer*, **Vol.46**, pp.2615-2627, 2003.

J.S. WETTLAUFER, M.G. WORSTER and H.E. HUPPERT, Natural Convection during Solidification of an Alloy from above with Application to the Evolution of Sea Ice, *J. Fluid Mech.*, **Vol.344**, pp.291-316, 1997.

R. VERZICCO and R. CAMUSSI, Prandtl Number Effects in Convective Turbulence, *J. Fluid Mech.*, **Vol.383**, pp.55-73, 1999.

R. VISKANTA, D.M. KIM and C. GAU, Three-Dimensional Natural Convection Heat Transfer of a Liquid Metal in a Cavity, *Int. Journal of Heat Mass Transfer*, **Vol.29 (3)**, pp.475-485, 1986.

V.R. VOLLER and C. PRAKASH, A Fixed Grid Numerical Modelling Methodology for Convection-Diffusion Mushy Region Phase-Change Problems, *J. Heat Mass Transfer*, **Vol.30 (8)**, pp.1709-1719, 1987.

V.R. VOLLER, A.D. BRENT and C. PRAKASH, The Modelling of Heat, Mass and Solute Transport in Solidification Systems, *Int. J. Heat Mass Transfer*, **Vol.32 (9)**, pp.1719-1731, 1989.

V.R. VOLLER, An Enthalpy Method for Modeling Dendritic Growth in a Binary Alloy, *Int. Journal of Heat and Mass Transfer*, **Vol.51**, pp.823-834, 2008.

G.E. WILSON, B.E. BOYACK, I. CATTON, R.B. DUFFEY, P. GRIFFITH, K.R. KATSMA, G.S. LELLOUCHE, S. LEVY, U.S. ROHATGI, W. WULFF, and N. ZUBER, Quantifying Reactor Safety Margins. Part 2: Characterization of Important Contributors to Uncertainty, *J. Nuclear Engineering and Design*, **Vol.119**, pp.17-31, 1990.

M.G. WORSTER, Natural Convection in a Mushy Layer, *J. Fluid Mech.*, **Vol.224**, pp.335-359, 1991.

M.G. WORSTER, Convection in Mushy Layers, *Annu. Rev. Fluid Mech.*, **Vol.29**, pp.91-122, 1997.

H.-G. WILLSCHUETZ, E. ALTSTADT, B.R. SEHGAL, F.-P. WEISS, Recursively Coupled Thermal and Mechanical FEM-Analysis of Lower Plenum Creep Failure Experiments, *Annals of Nuclear Energy*, **Vol.33**, pp.126-148, 2006.

E.L. TOLMAN, P. KUAN and J.M. BROUGHTON, TMI-2 Accident Scenario Update, *J. Nuclear Engineering and Design*, **Vol.108**, pp.45-54, 1988.

W. WULFF, B.E. BOYACK, I. CATTON, R.B. DUFFEY, P. GRIFFITH, K.R. KATSMA, G.S. LELLOUCHE, S. LEVY, U.S. ROHATGI, G.E. WILSON, and N. ZUBER, Quantifying Reactor Safety Margins. Part 3: Assessment and Ranging of Parameters, *J. Nuclear Engineering and Design*, **Vol.119**, pp.17-31, 1990.

P. ZHAO, M. VENERE, J.C. HEINRICH, D.R. POIRIER, Modeling Dendritic Growth of a Binary Alloy, *J. Comput. Phys.,* **Vol.188**, pp.434-461, 2003.